PENTLANDITE-PYROXENE AND PENTLANDITE-FELDSPAR INTERACTIONS AND THEIR EFFECT ON SEPARATION BY FLOTATION

By

Vratislav Malysiak

A thesis submitted to the University of Cape Town in fulfillment of the requirements for the degree of Doctor of Philosophy

Faculty of Chemical Engineering and Built Environment

University of Cape Town

June 2003

ACKNOWLEDGEMENTS

The author would like to thank Anglo Platinum management for support during the study and permission to publish the thesis. He wishes to express his gratitude to Professor Cyril O'Connor for his guidance and valuable suggestions during the course of this study. My sincere thanks go the Professor John Ralston for his valuable advice. The author records his thanks to Mrs. Natalie Shackleton for assistance with ToF-SIMS analysis and for valuable comments as well as to Dr. Andrea Gerson and Mr. Leon Coetzer for their useful discussion. The author also thanks to Mr. J.R. Towell for his assistance with editing of the manuscript.

CERTIFICATION BY SUPERVISOR

In terms of paragraph GP 8 of "General rules for the degree of PhD", I Prof. C.T. O'Connor, as supervisor of the candidate, V. Malysiak, certify that I approve of the incorporation in this thesis of material that has been published.

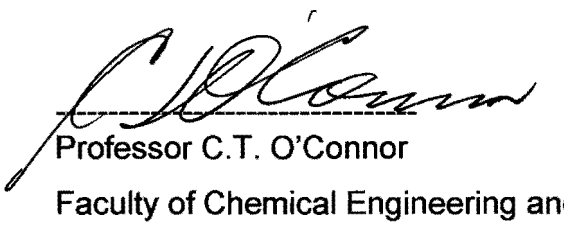

Professor C.T. O'Connor
Faculty of Chemical Engineering and Built Environment
University of Cape Town
Private Bag
Rondebosch
7700

TABLE OF CONTENTS

LIST OF APPENDICES

LIST OF FIGURES

LIST OF TABLES

PAGE NO

NOMENCLATURE

e	Ion charge
E°	Standard reduction potential
E_h	Oxidation/reduction potential
E_{kin}	Kinetic energy
ΔHo	Heat of formation
I	Ionic Strength
L_o	Effective length of spectrometer
m	Ion mass
m_o	Adjacent masses
Δm	Ion mass difference
t	Flight time
t_o	Length of primary ion pulse
Δt	Time difference
v	Ion velocity
V_o	Accelerating potential

GREEK LETTERS

ε	Fluid dielectric constant
η	Dynamic viscosity
κ	Debye-Huckel parameter
ζ	Zeta potential

LIST OF ABBREVIATIONS

a	Particle radius
ATR	Attenuated total internal reflection
COS	Complex oxidised sulphide
$CuSO_4$	Copper sulphate
DETA	Diethylenetriamine
e^-	Standard reducing agent
EDA	Ethylenediamine

EDTA	Ethylenediaminetetraacetic acid
FTIR	Fourier transform infrared spectroscopy
H^+	Concentration of standard acid
iep	Isoelectric point
IR	Infrared spectroscopy
LIMS	Laser ionisation mass spectrometry
Log(Conc.)	Logarithmic concentration
M	Molar concentration ($mol.dm^{-3}$)
M^+	Metal cation
MS	Metal sulphide
PAM	Polyacrylamide
pE	Equilibrium potential
PGM	Platinum group minerals
pH_{ie}	Isoeletric point pH
ppm	Concentration in parts per million
Rel Std Dev	Relative standard deviation
rpm	Revolutions per minute
SIBX	Sodium iso-butyl xanthate
$SIBX^-$	Xanthate anionic form
$(SIBX)_2$	Sodium iso-butyl dixanthogen
Std Dev	Standard deviation
ToF-SIMS	Time of flight secondary ion mass spectrometry
UV	Ultraviolet spectroscopy
wt.%	Weighted percent
X^-	Xanthate ion
XPS	X-ray photoelectron spectroscopy
IMP 4	Guar depressant
Dow 200	Glycol frother

SYNOPSIS

Flotation is used in the processing of the Bushveld Igneous Complex to separate the siliceous gangue from the platinum group minerals and sulphide minerals. The main base metal sulphide in Merensky ore is pentlandite. The predominant gangue minerals reporting to the flotation concentrate are pyroxene and feldspar. It is highly unlikely that xanthate collectors exhibit any affinity for siliceous gangue minerals to cause flotation. It was therefore postulated that the reason for these gangue minerals reporting to the concentrate was due to their inadvertent activation as a result of the presence of copper (II) from the copper sulphate added as an activator and nickel (II) ions emanating from the pentlandite. If these ions adsorb onto the surface of the siliceous gangue minerals it could result in subsequent xanthate adsorption, which would result in true flotation of these minerals. With respect to pentlandite, it was hypothesised that the difficulties in recovering pentlandite might be attributed to surface oxidation, valuable-gangue mineral aggregation and formation of passivating layers by the ions typically found in circuit water such as Ca(II) and Mg(II).

The present study has focused on exploring the extent to which metal ion activation occurs and influences flotation and how this can be managed so as to increase the separation of pentlandite from pyroxene and feldspar. The aim was to minimise the percentage pyroxene and feldspar reporting to the concentrate and simultaneously maximise the pentlandite recovery. The possible chemical reactions taking place on surfaces of synthetic pentlandite, natural pyroxene and feldspar were investigated at pH 4, 6 and 9 in di-sodium tetraborate solution and in synthetic process water in the case of zeta potential determinations, microflotation and ToF-SIMS (time of flight secondary ion mass spectrometry) analyses and in synthetic process water in the case of batch flotation tests.

The results obtained during the study have demonstrated that inadvertent activation of the siliceous gangue by heavy metal ions, Cu (II) and Ni (II), contributes significantly to the true flotation of these minerals. ToF-SIMS analysis and zeta potential determinations showed the presence of xanthate on copper (II) ion activated mineral surfaces of pyroxene and feldspar. In the absence of copper ions, no xanthate ion adsorption was observed. In di-sodium tetraborate solution as well as in the synthetic water, pyroxene was activated by the metal cations more significantly compared to feldspar. No true flotation of feldspar was observed in the synthetic water for any scenarios investigated.

In the case of pentlandite, the recovery was significantly enhanced in the presence of xanthate ions and even more so in the presence of copper (II) and xanthate ions. The microflotation results showed that the pentlandite recovery was higher at acidic pHs compared to alkaline pHs for all scenarios investigated. The higher recovery observed at pH 6 is attributed to the dissolution of hydroxide overlayers, which resulted in a sulphur enriched surface. Thus, in the presence of copper (II) ions, a higher degree of copper (II) ion adsorption onto the pentlandite sulphur sites occurred at pH 6 compared to 9, as seen from the copper ions removed in the presence of DETA at the different pHs. The pH range outside of hydroxide precipitation enhanced the formation of Cu(I)-X complexes and thus increased hydrophobicity and, ultimately, floatability.

The microflotation tests and ToF-SIMS analysis showed that pyroxene inadvertent activation was greatly reduced by the addition of diethylenetriamine (DETA) in combination with polyphosphate. However, the effectiveness was most noticeable at pH 6. The mechanism responsible for the observed selectivity is explained by the ability of DETA to form stable chelates with Ni(II) and Cu(II) ions. Furthermore, DETA reduced the level of surface oxidation products on pentlandite surfaces and also prevented xanthate ions adsorption onto the copper activated pyroxene surfaces. Polyphosphate introduced a more negative surface charge on the minerals studied and thus slime coating and aggregation between pentlandite and pyroxene particles was reduced.

In addition, the obtained results showed that the quality of process water plays an important role in flotation. The flotation recoveries for all minerals studied were lower in synthetic process water compared to those obtained in a simple electrolyte solution. The lower mineral floatability is attributed to the passivation of the mineral surfaces by the ions present in synthetic water, which adsorb onto the active sites of the minerals and thus interfere with the subsequent adsorption of copper (II), nickel (II) and xanthate ions. This process is non-selective and desirable only in terms of the gangue minerals.

The study has shown that the preferred conditions, in terms of pentlandite recovery and selectivity, were observed when a combination of polyphosphate, copper sulphate, DETA and SIBX were used at pH 6. For the system studied, the combination of DETA and polyphosphate represents a new approach to enhance pentlandite recovery and simultaneously improve selectivity between sulphide and gangue minerals.

CHAPTER 1

INTRODUCTION

The Merensky ore is found in a platinum group minerals (PGM) bearing reef in the Bushveld Igneous Complex in South Africa. The predominant sulphide minerals are pentlandite, chalcopyrite and pyrrhotite. Non-sulphide gangue minerals consist mainly of pyroxene and feldspar along with minor quantities of talc, chlorite and chromite. Flotation is used to separate the valuable minerals from the siliceous gangue, with selective separation achieved by the adsorption of a collector onto the surface of the PGM and sulphide minerals. The aim is to maximise recovery of PGM and sulphide minerals and minimise the amount of gangue minerals in concentrates, since the latter have an adverse effect on smelting.

The predominant gangue minerals reporting to the flotation concentrate are pyroxene and feldspar. They are characterised by a wide variation in chemical composition, crystal structure and content of isomorphous admixtures, which influence their behaviour in technological processes. It is believed that pyroxene and feldspar are naturally hydrophilic and thus when liberated they should report to the concentrate only by entrainment. Previous studies carried out by the author and colleagues at a PGM concentrator indicated that 61% of the total gangue in the concentrate was due to flotation and 34% due to entrainment. It is highly unlikely that xanthate collectors exhibit any affinity for siliceous gangue minerals to cause flotation. Therefore it is likely that activation of the mineral surface by metal ions is occurring, prior to xanthate adsorption. In terms of sulphide minerals, pentlandite is the most valuable base metal sulphide mineral in the Merensky Reef and it is the main source of nickel worldwide. There is scope for an improvement of pentlandite recovery at operating circuits treating Merensky Reef ore.

Due to a high percentage of gangue minerals reporting to the concentrate, the objective of the thesis was to evaluate what can be done to minimise the percentage pyroxene and feldspar reporting to the concentrate and simultaneously maximise pentlandite recovery.

It was postulated that activation of gangue minerals occurred as a result of the presence of copper (II) and nickel (II) ions followed by xanthate adsorption, which would result in true flotation of the siliceous gangue minerals. To test the hypothesis, pyroxene and feldspar

were conditioned and floated in the presence of xanthate as well as in the presence of copper ions (copper sulphate) followed by the addition of xanthate. It was further hypothesised that it would be possible to alleviate the inadvertent activation of gangue minerals by using a complexing agent such as diethylenetriamine (DETA). It was assumed that the mechanism responsible for an improved selectivity would involve the removal of copper ions, from the siliceous minerals as well as from the solution, through formation of stable DETA copper chelates.

In terms of pentlandite, it was hypothesised that the difficulties in recovering pentlandite might be attributed to surface oxidation, valuable-gangue mineral aggregation and formation of passivating layers by the metal ions present in the process water. To investigate the hypothesis, pentlandite mineral surface alteration and floatability were studied in a simple electrolyte as well as in synthetic process water at pH 4, 6 and pH 9. If the ions present in the synthetic water play a role in mineral surface passivation, the flotation response should be lower compared to that in the electrolyte. In terms of oxidation, it would be expected that sulphide mineral surfaces will oxidise less in acidic pHs and thus a higher flotation recovery should be obtained. The addition of a dispersant (sodium polyphosphate) was tested with the aim of introducing a more negative surface charge onto minerals investigated thus preventing the formation of valuable-gangue mineral aggregates.

This thesis presents the results of a study of pentlandite-pyroxene and pentlandite-feldspar systems with a view to exploring the extent to which metal ion activation occurs and influences flotation and how this can be managed so as to increase the separation of pentlandite from pyroxene and feldspar. The floatability of the minerals was studied in a simple electrolyte as well as in synthetic process water using microflotation techniques. The mineral surface alteration was investigated using zeta potential and ToF-SIMS (time of flight secondary ion mass spectrometry) techniques. Specifically, the effect of sodium isobutyl xanthate, copper sulphate, diethylenetriamine and sodium polyphosphate on pentlandite, pyroxene and feldspar surfaces was evaluated.

CHAPTER 2

LITERATURE REVIEW

For many years, flotation has been used for concentrating sulphide minerals that are a primary source of base metals. With the depletion of high-grade ore deposits it has become necessary to treat low-grade complex polymetallic ores. This often involves processing of fine particles that are more difficult to float. Better understanding of surface oxidation, collector adsorption and distribution as well as ionic activation of mineral surfaces is needed to maximise valuable minerals recovery.

Platinum-bearing ores were first discovered in South Africa in 1923. Today, the Bushveld Igneous Complex is the world's largest deposit of platinum group minerals. The Bushveld ore contains platinum, palladium, rhodium, ruthenium, iridium, osmium, gold, as well as copper, nickel and cobalt in economically recoverable quantities. The predominant PGM mineral types as well as the mineral association vary significantly across the ore body.

A typical process circuit used across the South African PGM industry consists of two or three stages of milling. Each comminution stage is followed by flotation (Figure 2.1). Autogenous mills can be used in primary milling circuits while ball mills are employed in secondary milling stages.

A large variety of flotation circuits are currently used across the industry in South Africa as the primary method for the upgrading of valuable minerals. The roughing and scavenging stages are complemented by a number of cleaning circuits. In the new flotation plants, trends have leaned towards using larger cells. Lately, tank cells have been used more extensively. Typically, flotation of platinum-bearing ores is carried out at a pH of about 8.7. Various collectors, depressants and frothers are being used. The most common collectors utilized by the PGM industry appear to be xanthates and dithiophosphates. In terms of depressants, carboxymethyl cellulose and guar based reagents have been found to be effective in improving the flotation efficiency of separating valuable minerals from siliceous gangue. In order to simplify the system studied and identify the effect of inadvertent activation on mineral floatability, depressants were only used during the batch tests and continuous flotation trials. In a number of operations, copper sulphate is used as an activator for pentlandite and pyrrhotite.

The major loss of PGM and base metal sulphides in the beneficiation of the Bushveld Igneous Complex occurs during the separation of the siliceous gangue from the PGM and sulphide minerals by selective flotation, therefore flotation remains the main metallurgical focus for the South African PGM producers.

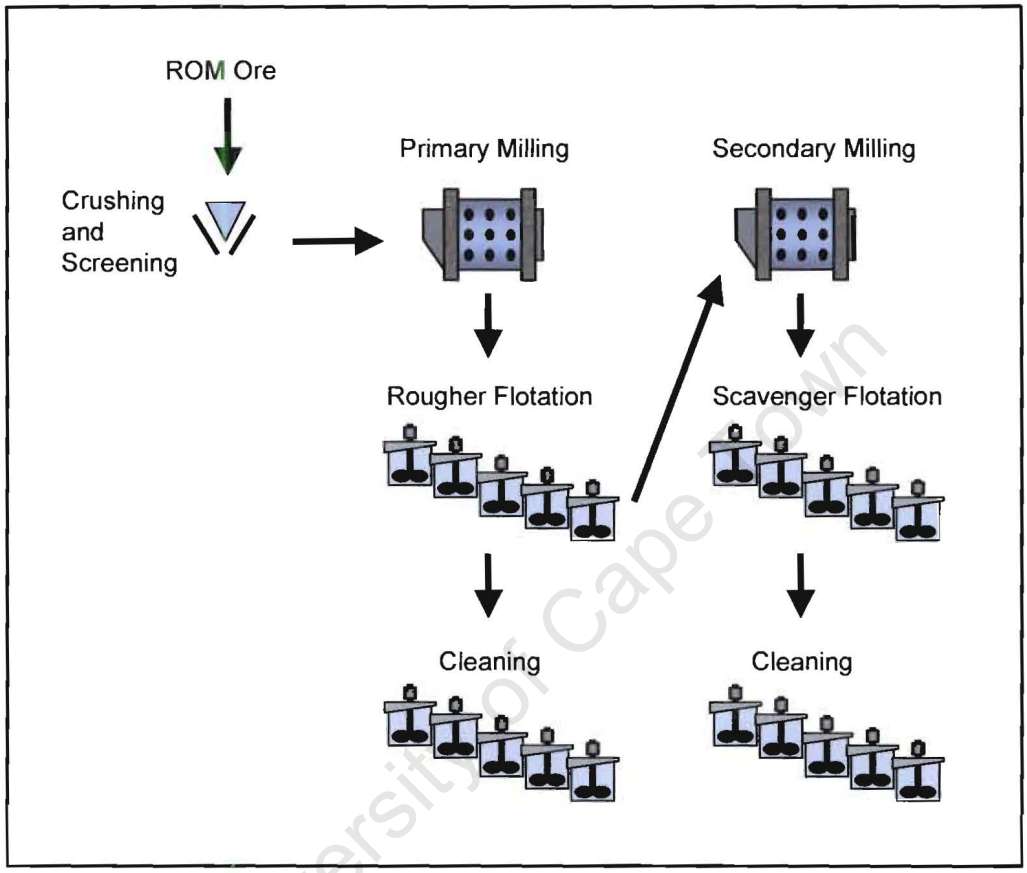

Figure 2.1: A Typical Concentrator Flowsheet

A review of the available literature mainly of pentlandite (which is nearly always associated with pyrrrhotite), pyroxene and feldspar with particular reference to the surface chemistry is discussed. The areas reviewed are on the existing knowledge of the mineralogy, flotation of ores, the chemistry of the reagents, as well as the speciation of the elements of interest.

2.1 Pentlandite

2.1.1 Mineralogy

Pentlandite is an iron nickel sulphide, which belongs to the sulphide mineral class. Most of the sulphide minerals are opaque with distinctive colours and characteristically coloured streaks. The general formula for the sulphides is given as X_mZ_n in which X represents the metallic elements and Z the non-metallic element. Pentlandite is an important ore of nickel and is commonly associated with other sulphides such as pyrite, chalcopyrite and pyrrhotite in basic igneous rock intrusions. Pentlandite's close association with the mineral pyrrhotite ($Fe_{1-x}S$) is believed to be the result of exsolution that occurs after magmatic segregation. Pyrrhotite is usually magnetic, although weakly so, and lacks the octahedral parting of pentlandite which provides the only good field tests for differentiation. Pentlandite's formula, $(Fe, Ni)_9S_8$, is believed to be composed of equal amounts of nickel and iron, but does show variation in tests. The structure of pentlandite is rather complex, with a face centered cubic arrangement and the metal ions in tetrahedral and octahedral coordination with the sulphurs. Coordination refers to the number and position of the sulphurs surrounding the metal ions. In the case of tetrahedral coordination, there are four sulphurs surrounding one metal ion and they are positioned at the four points of a tetrahedron. In the case of octahedral coordination, there are six sulphurs at the six points of an octahedron with a metal ion inside (Klein, C. and Hurlbut, Jr., C.S., 1985).

2.1.2 Surface and Flotation Studies

2.1.2.1 Self-induced (Collectorless) Flotation

The self-induced flotation of sulphide minerals has been known since the beginning of the last century. Pentlandite and pyrrhotite exhibit self-induced flotation, viz. flotation in the absence of collector, as a result of mild oxidation of the mineral itself. There have been many studies published in the literature confirming this observation. Ishihara and Kagami (1964) showed that pyrrhotite is highly susceptible to oxidation as compared to other sulphide minerals. However, mild oxidation enhanced flotation due to the formation of elemental sulphur and Trahar (1984) has reported that pyrrhotite and pentlandite are strongly floatable.

Trahar (1984) also pointed out that there are at least three types of floatability displayed by sulphide minerals: self-induced, sulphur induced and collector induced. The floatability for each type is considered to be dependent on the oxidation-reduction state of the pulp.

The effect of pulp potential was investigated further by Heyes and Trahar (1984). They suggested that the collectorless floatability of pyrrhotite is dependent on the pulp potential. They pointed out that flotation occurs in mildly oxidising but not in reducing conditions. It was suggested that elemental sulphur might be responsible for collectorless flotation. They demonstrated that pyrrhotite shows self-induced flotation upon mild oxidation. In alkaline solutions, however, metal hydroxides form and when their solubility products are exceeded, collectorless flotation is inhibited. Elemental sulphur oxidises to sulphur oxygen species and eventually to sulphate ions.

In 1987, Hayes summarised that sulphide minerals which are amenable to collectorless flotation form metal-deficient sulphides and/or elemental sulphur on the mineral surfaces.

Healy and Trahar (1989) found that the potential at which self-induced flotation occurs (50% in the first minute) is at E_h values of -0.15 and 0.0 V for pentlandite and pyrrhotite, respectively. Ralston (1991) also reported that collectorless flotation is possible only under specific oxidation-reduction or E_h conditions in the flotation pulp.

Heiskanen et al. (1991) studied collectorless flotation of noritic and serpentinic nickel ores using batch flotation techniques. Only pH was varied from 3-12 during the tests. Pyrrhotite (Noritic ore) floated markedly well at pH 3-5 but had a very low recovery at higher pH, which could be attributed to mechanical entrainment. Pentlandite gave a good recovery at low pH and a recovery of 40-60% at higher pH values. The results obtained showed that process iron had a marked effect on the collectorless flotation. Sulphides from samples ground in a ceramic mill floated better than those ground in a steel mill. The results demonstrated that either hydroxide and/or sulphate layers tend to build up during a long aeration time, thus hindering flotation. It was pointed out that the oxidation of pyrrhotite progressed more rapidly than that of pentlandite.

It can be deduced from the above observations that for collectorless flotation to take place the minerals should be exposed to some form of mild oxidation so that elemental sulphur, and/or metal deficient lattice, and/or polysulphide are present on the mineral surfaces, which would induce hydrophobicity. However, the identity and stability, both thermodynamic and kinetic, and the involvement of the hydrophobic species given above in collectorless flotation have been topics of considerable debate and there is still no single acceptable interpretation.

2.1.2.2 Collector Induced Flotation (Xanthates)

Xanthates are one of the major classes of collectors used in flotation of sulphide minerals. They have been successfully employed in the industry to separate sulphides from gangue minerals such as silicates.

Wang et al (1989a) carried out thermodynamic calculations for the Fe-EX-H_2O system to study the stability of iron-xanthates. They showed that the formation and stability of insoluble iron-xanthate compounds depended critically on the xanthate concentrations, and on the pH and redox potential of the solutions. Ferric xanthate could be formed and was stable in acidic pH and in xanthate concentration ranges used in conventional flotation. It improved or caused the recovery of iron-sulphide flotation in this pH range. Insoluble hydroxyl ferric xanthate could be obtained and remained stable at very low xanthate concentrations in the pH range of weakly acidic to alkaline and under a wide range of redox potentials. Ferric dihydroxo xanthate was only slightly hydrophobic. Dixanthogen was formed at high redox potentials and high xanthate concentrations. No dixanthogen could be obtained under conditions where ferric and hydroxyl ferric xanthates were formed. Ferrous xanthate could be obtained only with very high xanthate concentrations and under reducing conditions. Its role in the iron-sulphide flotation could be completely ignored.

Hodgson and Agar (1989) reported that xanthate adsorbs at pH 9 on the pyrrhotite surface forming an $Fe(OH)_2X$ product. Unlike chemisorption, no electron transfer was considered to arise through the adsorption of xanthate on the surface. The collector was adsorbed through coulombic attraction with cationic iron (III) site generated through oxidation of the mineral surface:

$$FeS + H_2O \rightarrow Fe(OH)[S]^+ + H^+ + 2e \quad (1)$$

$$Fe(OH)[S]^+ + X^- \rightarrow Fe(OH)[S]X \quad (2)$$

Xanthate then oxidised to dixanthogen through the reduction of oxygen at the pyrrhotite surface

$$2X^- \rightarrow X_2 + 2e \quad (3)$$

$$O_2 + 2H_2O + 4e \rightarrow 4OH^- \quad (4)$$

Dixanthogen formation was considered to take place adjacent to the oxidised pyrrhotite surface and be physisorbed via the alkyl groups of the Fe(OH)[S]X complex. Dixanthogen was the species that conferred hydrophobicity on the surface of pyrrhotite and oxygen was required to promote the bubble contact. In the case of pentlandite it was concluded that the collector chemisorbed directly on to the nickel sites (pH 9). The addition of xanthate reduced the degree of oxidation of the pentlandite surfaces. Dixanthogen is formed from chemisorbed xanthate on the pentlandite surface according to the following reactions

$$Ni + X^- \rightarrow NiX + e \quad (5)$$

$$NiX + X^- \rightarrow Ni(X)_2 \rightarrow NiX_2 + e \quad (6)$$

The formation of dixanthogen would occur concurrently with the adsorption of xanthate on the pentlandite during the oxidation process and enhances hydrophobicity.

The reaction of amyl xanthate in solution in the presence of pentlandite in a water-ethanol mixed solvent was studied by McNeil et al. (1994). Compared with water only, this solvent kept all products in solution while maintaining the same U.V. spectra, making it well suited to the study. Rapid oxidation of xanthate to dixanthogen was found, which appeared to be catalytic as no reaction products could be extracted from the pentlandite surface.

Bozkurt et al. (1997) investigated the effect Ni ions and pentlandite/pyrrhotite interaction has on adsorption of isobutyl xanthate using FTIR-ATR spectroscopy and open circuit potential measurements. Dixanthogen was the major surface product under all conditions on both minerals. From single mineral studies, dixanthogen concentration was greater on pentlandite than pyrrhotite and Ni ions always enhanced it. For mineral mixtures, dixanthogen concentration increased on pentlandite and decreased on pyrrhotite. The presence of Ni ions moderated this effect.

A year later, Bozkurt et al. (1998) reported on a similar study during which the interaction of isobutyl xanthate with pentlandite and pyrrhotite was investigated using ATR, FTIR and open circuit potential (rest potential) measurements. The study was performed with single and mixed mineral systems at pH 9.2. Mixing the minerals showed that dixanthogen formation on pentlandite was promoted while on pyrrhotite it was suppressed. A mixed potential model was used to explain this effect of mineral interaction on dixanthogen formation. At the potential of the mixed mineral system, the anodic reaction (xanthate oxidation to dixanthogen) occurred preferentially on pentlandite and the cathodic reaction (reduction of oxygen to hydroxyl ion) occurred on pyrrhotite.

2.1.2.3 Surface Oxidation

A number of researchers have studied the problem of pentlandite alteration due to oxidation.

Broomhead and Layers (1976) studied factors governing the dissolution of nickel and iron in pentlandite and pyrrhotite concentrates in aqueous solutions at normal temperatures and pressures. The direct reaction of oxygen in aerated water with pyrrhotite was much faster than with pentlandite and reaction rates were proportional to the dissolved oxygen concentration. The different reactivity can be explained by their different crystal structure. Pyrrhotite has vacancies and pentlandite does not. Divalent metal sulphates were produced initially for both minerals. The subsequent oxidation of iron (II) to iron (III) and its oxolation produced acid solutions, which rapidly attacked both minerals. Acidity increased with time.

The alteration in surface chemistry of pentlandite exposed to air was studied by Boyd (1979). If the mineral was cleaved in pure argon the only oxidation product formed was Fe_2O_3, if the mineral was cleaved in air, Fe_2O_3 and NiO were produced. Contacting the mineral with SIBX gave FeO, nickel xanthate, $Ni(IBX)_2$ and two unidentified species.

Thornber (1983) studied mineralogical and electrochemical stability of the nickel-iron sulphides - pentlandite and violarite. He pointed out that in a primary assemblage composed of pentlandite, pyrrhotite and pyrite, pentlandite reacted first at the lowest oxidation potential and it altered to violarite with nickel and iron released into solution according to the following reaction

$$Fe_{4.5}Ni_{4.5}S_8 \rightarrow 2FeNi_2S_4 + 0.5Ni^{2+}\ 2.5Fe^{2+} + 6e^- \qquad (7)$$

At the same time, the increased nickel activity caused the pyrrhotite to become unstable and it took up nickel from solution to form violarite

$$Fe_7S_8 + 4Ni^{2+} \rightarrow 2FeNi_2S_4 + 5Fe^{2+} + 2e^- \qquad (8)$$

Richardson and Vaughan (1989) used synthetic pentlandite to study the alteration of surfaces due to oxidation. The oxidants used were air, steam, ammonium hydroxide, hydrogen peroxide, and sulphuric acid. Electrochemical oxidation was also investigated. After oxidation the pentlandite surfaces were enriched in nickel in the subsurface. The subsurface is believed to restructure to violarite. The oxidised surfaces consisted of a range of iron oxides and hydroxides (Fe_3O_4, Fe_2O_3, FeOOH, $Fe(OH)_3$), nickel oxide (NiO) and iron sulphates ($FeSO_4$, $Fe_2(SO_4)_3$) of which the layer was approximately 10 Å in depth. The proportions of the phases present in the surface layer were dependent on the strength of the oxidant employed and the thermodynamic stability of the phases.

In 1991, Buckley and Woods used XPS and electrochemical techniques to investigate the surface oxidation of pentlandite. They found that on exposure to air, iron was removed from the pentlandite lattice to form a hydrated iron oxide overlayer, which left metal deficient pentlandite in addition to a restructured nickel-iron sulphide. Further oxidation resulted in some nickel being included in the oxide overlayer. The study in acetic acid

(pH 2.9) showed that the oxide layer was largely soluble. Oxidation in basic media (pH 9.2) indicated that virtually all the iron and most of the nickel within the outermost few nanometres were bonded to oxygen. The voltammetric studies carried out at pH 4.6, 9.2 and 13 showed that the major process in the oxidation of pentlandite is the selective removal of iron. At pH 4.6 the sulphur product of oxidation process was mainly sulphur. At pH 9.2 and 13, the sulphur was again the major oxidation product but some sulphate was also formed, with a fraction of the mineral being oxidised to sulphate (increasing with increasing potential). They pointed out that the oxidation products of pentlandite are similar to those of pyrrhotite.

Kelebek (1993) investigated the effect of oxidation on flotation behaviour of pyrrhotite and pentlandite using a nickel-copper ore sample of the Sudbury basin. In general, moderate oxidation promotes the floatability. Under oxidation deficient conditions the formation of hydrophobic surface species on pyrrhotite were restricted or at least retarded. Pyrrhotite requires higher redox potentials for reactions leading to its hydrophobisation. Pentlandite recoveries were practically the same in nitrogen and in air. Flotation selectivity increased in time towards higher pentlandite recovery. This indicates that pyrrhotite particles undergo a selective oxidation that renders the mineral more hydrophilic. He pointed out that an oxidation period of nearly six hours accounted for about 70% decrease in pyrrhotite recovery. The ferrous hydroxide that initially formed was subsequently converted to more stable ferric hydroxide and/or oxy-hydroxide thus contributing to the hydrophillic nature of pyrrhotite.

Smart (1994) pointed out that sulphide mineral surfaces undergo significant changes in the surface layers due to structural and chemical rearrangements after immersion in solutions. The iron-containing sulphide minerals are known to react in solution by the loss of iron ions from the sulphide lattice to form hydroxide overlayers. The removal of these hydroxide products from the surface during acid attack revealed a sulphur rich layer in which restructuring of $Fe_{1-x}S$ to a tetragonal Fe_2S_3 intermediate based on a defective pyrite lattice, is found. In this structure, the linear chains of Sn polysulphides have a S-S distance closely similar to that of elemental sulphur apparently conferring hydrophobicity on these surface layers.

Recently, near-pristine surfaces of natural pentlandite samples were studied by Legrand et al. (1997) using X-ray photoelectron spectroscopy. They found two major doublets in the S 2p spectrum, one with a S $2p_{3/2}$ binding energy of 161.44 eV and the other at 162.19 eV. These doublets were interpreted as being due to sulphur in a 4-coordinate and 5-coordinate environment, respectively. After exposure to de-ionised water for 1.5 hours, the results revealed that pentlandite surfaces were oxidised to give surfaces that were rich in iron oxyhydroxide species and depleted in nickel and sulphur.

In summary, surface oxidation is one of the most important factors that influence the flotation selectivity and recovery in the processing of complex sulphide ores. The degree of oxidation determines whether the surface film formed on a sulphide mineral will enhance hydrophobicity or hydrophilicity. The overall oxidation reaction suggested for pyrrhotite and pentlandite is

$$MS + xH_2O + 1/2xO_2 \rightarrow M_{1-x}S + xM(OH)_2 \qquad (9)$$

where MS represents a metal sulphide.

Oxidation arises from the dissolution of minerals and grinding media. Dissolved metal ions hydrolyse and sulphide ions oxidise. These ions can re-adsorb on the mineral surfaces or react with each other or the dissolved gas molecules before precipitation (Clarke et al. 1995). It is well established that the surface products of excessive oxidation have a profound effect on surface hydrophobicity. Mild oxidation however, appears to be necessary for the flotation of sulphide minerals and is often a requirement for self-induced flotation. On the other hand, excessive oxidation inhibits flotation. The rate of oxidation of sulphide minerals depends on the surface area available for reaction, the partial pressure of oxygen, the type and composition of the sulphide mineral, solution pH and temperature (Ralston, 1991).

2.1.2.4 Heavy Metal Activation

The presence of metal ions in solution can have a major influence on the flotation and separation of sulphide minerals. Metal ion contamination of surfaces is frequently suspected of playing a detrimental role in selective flotation.

Forssberg and Jonsson (1981) carried out experiments that have shown that relatively large amounts of heavy metal ions can adsorb on both synthetic and natural pyrrhotite in an acidic pH. The possible cause is the presence of iron vacancies in the crystal lattice, as indicated by the chemical formula of pyrrhotite, $Fe_{1-x}S$. The vacancies can be filled by metal ions of suitable size. Pyrrhotite releases fairly large quantities of Fe^{2+} and Fe^{3+} ions under oxidising conditions. This can adversely affect the adsorption of heavy metals. Synthetic samples showed a higher specific adsorption, probably due to pores, which give them a higher adsorption rate.

Yoon et al. (1995) also showed that pyrrhotite can be activated by heavy metal ions present in the plant water. The pyrrhotite activation by Cu^{2+}, Ni^{2+}, and Ag^{+} ions was confirmed by XPS and LIMS analyses of the mineral specimens immersed in simulated plant water of pH 9.5 for 15 minutes. These ions can form more insoluble sulphides than Fe^{2+} ions therefore pyrrhotite can be activated by these heavy metal ions. When pyrrhotite is activated thiol collectors can adsorb on the surface at lower collector concentrations and lower potentials.

The influence of sulphur containing ions (several hundred mg/l) in recycled water on selective flotation of chalcopyrite, cubanite, pyrrhotite and pentlandite was investigated by Barskii et al. (1986). A study of the effect of pH on the potential of a mineral electrode showed that in the pH range 7-12, the pentlandite electrode was positive, while the pyrrhotite electrode potentials were negative. If the aqueous phase was saturated with thiosulphate ions, the oxidation of pentlandite and pyrrhotite was increased. If the aqueous phase was saturated with sulphate ions, the potential rapidly increased. The value of the surface charge on the sulphides was determined by the sulphate and thiosulphate ion concentrations in the pulp, and a change in their ratio caused a shift in the potential. The sorption of aerofloat on pentlandite increased significantly with increase in the sulphate ion concentration in the pulp. On pyrrhotite the sorption curve showed a discontinuity at

SO_4^{2-} = 0.4 x 10^{-2}M, above which the sorption increased. The sorption of aerofloat was reduced with an increase in the thiosulphate ion concentration. Under highly reducing conditions, the collector was adsorbed physically on the surface of pentlandite and pyrrhotite. They concluded that there is a close correlation between the selectivity of flotation complex copper-nickel sulphide ores and the sulfoxide ion concentration in pulp.

Hodgson and Agar (1989) carried out electrochemical studies to determine a possible effect of Ca^{2+}, $S_2O_3^{2-}$ and SO_4^{2-} ions on pentlandite and pyrrhotite floatability and xanthate interactions. It was found that these ions were significantly surface active at the normal process pH. It was concluded that these ions would influence the extent of X^- adsorption by the sulphide minerals as well as control the onset of hydrophobicity. $S_2O_3^{2-}$ and Ca^{2+} ions competed with xanthate for adsorption on the surface sites of pentlandite, whereas only Ca^{2+} increased the xanthate dosage required rendering pyrrhotite hydrophobic. The calcium ions adsorbed onto the surface sulphur sites, sulphate also being adsorbed onto the Fe sites. The $S_2O_3^{2-}$ ion was considered to be coordinated onto surface via the oxidised Fe sites or the Ca (S_2) product. Iron and polysulphides were considered to be surface-active forms, which form part of the pyrrhotite surface. Ca^{2+} cations can chemisorb onto the pentlandite surface, replacing metal ions at the pentlandite surface. The initial oxidation reaction for pentlandite is pH independent and to be of the following form

$$Fe_{4.5}Ni_{4.5}S_8 \rightarrow (Fe_{4.5-x}Ni_{4.5-x}S_8)+xFe^{2+}+xNi^{2+} + 4xe \qquad (10)$$

Presence of Ca ions modifies this reaction by replacing the metal cation at the surface.

A similar trend was observed by Agar et al. (1982) during the bench-scale testwork performed on the feed to the separation flotation circuit at INCO Metals' Copper Cliff Mill. They showed that lime addition caused desorption of xanthate from pentlandite, which raised the concentration of xanthate in solution.

Rao and Finch (1991), however, found that the presence of cationic species in water appeared to enhance the pyrrhotite xanthate-dixanthogen uptake at pH 8.4. This was noted especially with calcium ions, which do not oxidise, decompose and precipitate xanthate, apparently due to the formation of $Ca(OH)^+$ species at the mineral surface

thereby providing a greater number of positive surface sites. In the presence of Cu^{2+} ions xanthate uptake is much greater and there is dixanthogen formed in the solution even in the presence of nitrogen. This is explained by the oxidising action of Cu^{2+}. There is no dixanthogen on the mineral surface observed in the presence of nitrogen. It shows that dixanthogen is formed on the mineral surface by oxidation of adsorbed xanthate. Fe^{3+} ions can also oxidised xanthate to dixanthogen in solution, but the oxidation at the mineral surface occurs only in the presence of air.

Liu et al. (1993) carried out batch flotation tests on copper-zinc ore from Kidd Creek using recycle water, tap and distilled water. The results showed that recycle water containing up to 500ppm thiosalts and 300ppm calcium was not detrimental to flotation and appeared to enhance the depression of pyrite in copper rougher flotation.

Moreover, Kirjavainen et al. (2002) concluded that calcium and thiosulphate ions improved floatability of nickel and copper sulphides at the normal process pH (pH 9) after grinding in a steel mill. They pointed out that galvanic interaction between sulphides and mill iron is of major importance. When the galvanic effect of mill iron was effective, calcium activated nickel and copper sulphides and increased the adsorption of ethyl xanthate on the sulphides. Thiosulphate ions decreased the adsorption of xanthate, and it was concluded that thiosulphate reduced the effect of hydrophilic compounds on sulphide particles and thus improved their flotation.

Copper activation has been reviewed a number of times over the last thirty years by inter alia Finkelstein and Allison (1976), Fuerstenau (1982) and Wang et al. (1989c). More recently Finkelstein (1997) gave an in depth review of current theories on copper activation. The main emphasis of the review is the effect on sphalerite, with a few references to pyrrhotite. It appears that there has been no significant study of copper activation of pentlandite.

Wang et al (1989b) carried out an investigation of the activation of natural pyrrhotite by Cu (II) in an acidic to neutral pH range. They deduced that the activation of pyrrhotite by Cu (II) ions involves a stochiometric replacement of iron in the lattice by Cu (II) from the solution. The reaction kinetics was characterised by two steps. The first very rapid step of the activation was controlled by the surface nucleation of copper sulphides. The second

step was slower and controlled by the diffusion of Cu (II) into the lattice. The solubility of pyrrhotite was reduced significantly in the presence of Cu (II) ions, probably due to the formation of a copper sulphide layer on the pyrrhotite surface. Copper adsorption increased with an increase in the solution pH. Although oxygen reduced the adsorption of copper on pyrrhotite, the effect increased with a decrease of solution pH. The oxidation product of a pyrrhotite surface is thought to inhibit the surface conversion of copper hydroxide into copper sulphides.

Finkelstein and Allison (1976) suggested that in addition to ion exchange for copper activation, there is an oxidation - reduction reaction in which Cu (II) is reduced to Cu (I) and the sulphide of the mineral is oxidised. It has been demonstrated that activation of sulphide minerals at acid pH can result in collectorless flotation, which is not the case for alkaline conditions.

Most of the observations and conclusions made to date have been based on classical chemical methods of measuring adsorption. Recently more studies have been conducted using instrumental techniques (Auger, XPS, ToF-SIMS) to identify surface species before and after copper activation. One of the major concerns related to information from these techniques is that they are ex-situ techniques and the surface can be significantly altered depending on the methods used to prepare the sample prior to analysis. In particular hydrolysis and oxidation products that are reversibly adsorbed on the surface can easily be removed by washing procedures prior to analysis, and are alternatively easily deposited on the surface from the solution when the samples are dried prior to analysis.

The difference is sample preparation, which can lead to different results as is demonstrated by seemingly contradictory results from similar XPS studies. The studies have shown that after the activation of sphalerite at pH 9 Cu (II) is converted to Cu (I) with time. Opinions are divided over whether Cu (II) and Cu (I) are present under alkaline conditions. Kartio et al. (1996) did not detect Cu (II) on the surface (sphalerite pH 9.2), while Perry et al., (1984) noted that in some cases there was Cu (II) and Cu (I) on the surfaces. Prestidge et al. (1997) reported evidence for Cu (II) on the surface in excess of a monolayer. The Cu (II) species had been attributed to cupric oxide and copper hydroxides. The one difference in the two studies has been the method used for preparing the samples. Perry et al. (1984) and Kartio et al. (1996) rinsed the samples in de-ionised

water, while Prestidge et al. (1997) rinsed the sample with an alkaline solution, transferred the sample as a slurry to the instrument and removed the water under vacuum. The first procedure may have removed the majority of the hydroxides. The second procedure while reducing dissolution could result in hydroxides being deposited from the solution onto the surface.

There is further controversy with regards to the form of the oxidised sulphide generally refered to as COS (complex oxidised sulphide) which is formed as a result of the oxidation – reduction reaction involved in copper activation. Is it a polysulphide or a metal deficient lattice? Finkelstein (1997) argues that the difference between the two forms is not merely about semantics, but rather about the difference between a localised increase in sulphur concentration (polysulphide) and a homogeneous distribution over an entire lattice. Finkelstein (1997) concludes that depending on the conditions either or both can be formed.

Ralston et al. (1981) found that as the pH of the solution increased, the amount of elemental sulphur on the surface of sphalerite decreased with no elemental sulphur being detected above pH 7.5. Under normal flotation conditions employed, which are alkaline, elemental sulphur species are not expected, and the oxidation of the sulphide surface would result in the formation of sulphoxy compounds.

Perry et al. (1984), using Auger spectroscopy, found for copper activation of sphalerite that patches of copper rich islands are formed only after a few monolayers of evenly distributed copper has been adsorbed. Prestidge et al. (1994) using XPS found that the copper is not evenly distributed for the same mineral.

Finkelstein (1997) discusses the kinetics and reaction mechanisms in depth. It is generally accepted that the reaction takes place in two stages, a rapid stage where a few monolayers are deposited on the surface and then a slower stage where the rate is controlled by diffusion into the sulphide lattice.

One of the findings highlighted by Finkelstein (1997) as being of importance for the application of metal activation to flotation is the extent to which the "lattice cations, the adsorbed cations and the induced acceptor states are mobile". Activation and oxidation of

the surfaces results in a surface layer that is significantly different in chemical composition from the bulk. The surface is described as being metastable and alters significantly with time. The implication of this is that the surface, which defines floatability, may change significantly during the passage through the flotation circuit. The time between activation and collector adsorption could therefore be used to improve the selectivity of flotation. With time the copper adsorbed on, say, pyrrhotite may diffuse into the bulk, leaving a surface without copper.

An important component in understanding copper activation is a thorough knowledge of the ionic species in the water used. The temperature, pH, E_h and ions present in the aqueous environment will dictate the chemistry of activation.

Wang et al. (1989c) reviewed the aqueous and surface chemistry in the flotation of sulphide minerals. It is well known that heavy metal ions undergo a series of pH-controlled hydrolysis reactions in a binary metal cation-water system. For example in the case of Cu (II), the following reactions occur spontaneously:

$$Cu^{2+} + OH \leftrightarrow Cu(OH)^{+} \quad \text{(initial hydrolysis)} \quad (11)$$

$$2Cu^{2+} + 2OH \leftrightarrow Cu_2(OH)_2^{2+} \quad \text{(dimer formation)} \quad (12)$$

$$Cu^{2+} + 2OH \leftrightarrow Cu(OH)_2(aq) \quad (13)$$

$$Cu^{2+} + 2OH \leftrightarrow Cu(OH)_2(s) \quad \text{(precipitation)} \quad (14)$$

$$Cu^{2+} + 3OH \leftrightarrow Cu(OH)_3^{-} \quad (15)$$

$$Cu^{2+} + 4OH \leftrightarrow Cu(OH)_4^{2-} \quad (16)$$

The distribution of these species at varying pH values can be calculated from their equilibrium constants. Numerous log concentration versus pH diagrams are available in the literature (Figure 2.2). The only concern is that most of this data is produced at 25°C rather than the higher temperatures often typical of flotation circuits.

Note that free metal ions dominate only at very acidic pH values. At highly alkaline pH, they will precipitate as metal hydroxides. In medium pH range, the systems are highly complicated by the formation of soluble hydroxyls and even dimers and polynucleas. Thus, different interactions between the mineral surface and metal ions should be expected, depending on the solution pH and total metal ion concentration.

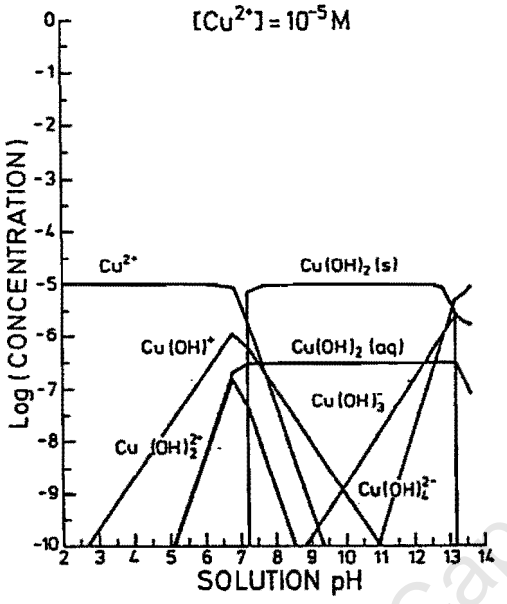

Figure 2.2: Log(Conc.)-pH Diagram for Metal-Water System of Cu (II) Activator at a Total Metal Concentration of 1 x 10^{-5}M

From Figure 2.2 it is evident that at the pH typical of Merensky ore flotation circuits, namely pH 9, the Cu species present in decreasing order are $Cu(OH)_2$ (s) >>$Cu(OH)_2$ (aq) > $Cu(OH)_3^-$> $Cu(OH)^+$> $Cu(OH)_4^{2-}$> $Cu_2(OH)_2^{2+}$. The addition of copper sulphate at pH 9 is therefore expected to produce a copper hydroxide precipitate.

Wang et al. (1989a) have studied the stability of the ternary Fe(III)-OH-EX complexes and have shown that the intermediate pH depression of pyrite in its flotation with xanthate is very strongly correlated with the presence of ternary compounds. They have also shown that these ternary compounds are not strongly hydrophobic, however, if excess collector is present, they will be associated on the mineral surfaces and make the mineral particle sufficiently hydrophobic for flotation. The stability of Cu(OH)EX(s) would be expected to lie between that of $Cu(EX)_2$(s) and that of $Cu(OH)_2$(s). The equilibrium potential (pE) vs. pH diagram of the Cu-EX-H_2O system at a total concentration of 1 x 10^{-4} M copper and ethyl xanthate is shown in Figure 2.3. Low pE values represent a reducing environment while

high pE values an oxidising environment. The pE scale is intended to represent the concentration of the standard reducing agent (the e^-) analogously to the pH scale representing the concentration of standard acid (H^+). The pE values are obtained from reduction potentials by dividing E° by 0.059. The stability constants were taken from Kakovskii (1957) and Kakovskii and Arashkevich (1968) and that of Cu(OH)EX(s) was estimated. From Figure 2.3 it can be seen that there is a large area of stability for Cu(OH)EX(s), thus if the redox potential of the system falls into this area flotation will be inhibited.

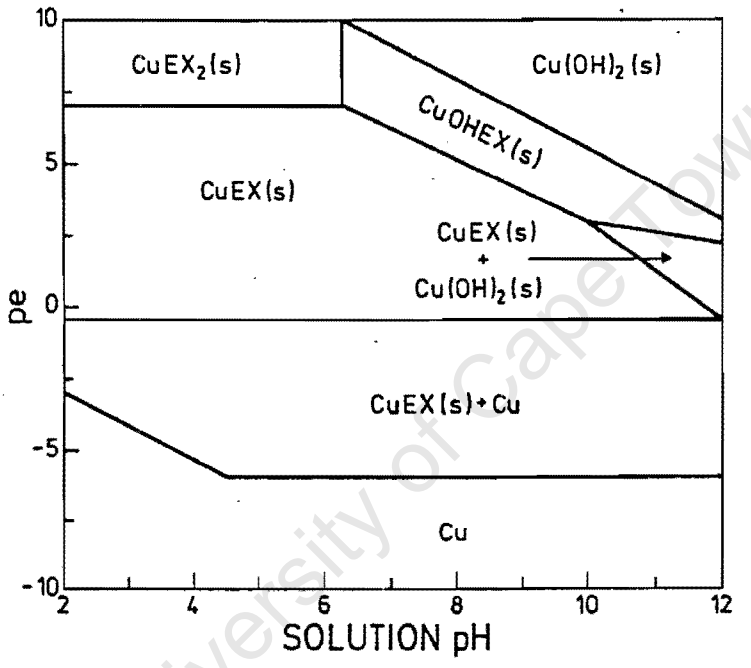

Figure 2.3: pE-pH Diagram for Cu-Ex System at a Total Concentration of Cu = 1 x 10^{-4}M and EX = 1 x 10^{-4}M, Showing Possible Stability Area of the Compound Cu(OH)EX.

Notwithstanding the literature review above, many questions remain regarding the issue of copper activation. In particular, little attention has been paid to pentlandite in terms of copper activation as well as the application of this knowledge to improve selectivity in flotation of Merensky Reef ore.

2.2 Pyroxene

2.2.1 Mineralogy

The pyroxene minerals belong to the silicate mineral class and approximately 30% of all minerals are silicates. With a few exceptions all the igneous rock-forming minerals are silicates, and they thus constitute well over 90% of the Earth's crust. The basic chemical unit of silicates is the SiO_4 tetrahedron shaped anionic group with a negative four charge. The central silicon ion has a charge of positive four while each oxygen has a charge of negative two and thus each silicon-oxygen bond is equal to one half the total bond energy of oxygen. This condition leaves the oxygen with the option of bonding to another silicon ion and therefore linking one SiO_4 tetrahedron to another and another, etc.. The silicate tetrahedrons can form as single units, double units, chains, sheets, rings and framework structures. A pyroxene structure is shown in Figure 2.4.

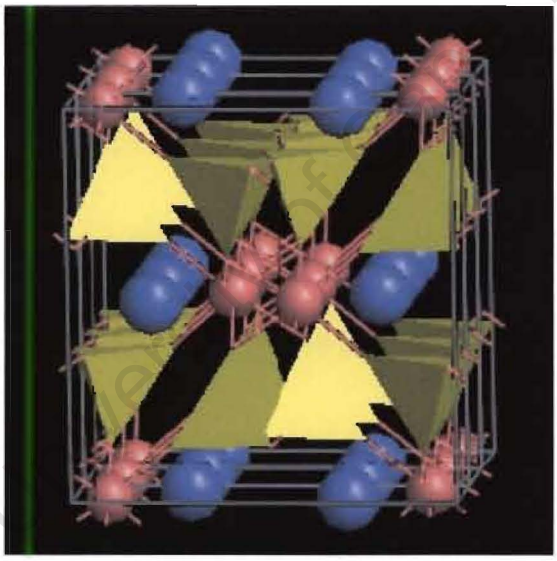

Figure 2.4: Pyroxene Structure, Viewed Obliquely along z. Yellow: SiO_4 Tetrahedra; Blue: Larger *X* Cation Sites; Red: Smaller *Y* Cation Sites

The pyroxene minerals are inosilicates of the general formula $XY(Si, Al)_2O_6$. The *X*, represents ions such as Ca^{2+}, Na^{1+}, Fe^{2+} and Mg^{2+} and more rarely zinc, manganese and lithium. The *Y*, represents ions of generally smaller sized such as Cr^{3+}, Al^{3+}, Fe^{3+}, Mn^{2+}, scandium, titanium, vanadium and even Fe^{2+}. Aluminium, while commonly substituting for silicon in other silicates, does not often substitute for silicon in a pyroxene. The typical pyroxene structure contains chains of SiO_3 tetrahedrons that every other one alternates

from the left side to the right side of the chain. Each of the tetrahedrons has one flat edge that lies on the "base" of the structure as if the entire chain were a chain of connected three sided pyramids on a flat desert. The orderliness of the tetrahedrons means that they repeat every three tetrahedrons, ie. left-right-left. The chain structure explains the general prismatic to fibrous character of the members of this group. The slope of the tetrahedral pyramids helps to determine the cleavage angle of the pyroxenes at nearly 90° degrees (actually 93° and 87°). The pyroxenes are closely related to a group of inosilicates called the pyroxenoids. The pyroxenes are an important group among the single chained inosilicates. They are common rock forming minerals and are represented in most igneous and many metamorphic rocks (Klein, C. and Hurlbut, Jr., C.S., 1985).

2.2.2 Surface and Flotation Studies

Deju and Bhappu (1965) studied surface properties of silicate minerals in terms of correlating the oxygen-silicon ratio for various silicate minerals to the adsorption of hydrogen ions. Upon the fracturing of a silicate mineral crystal, the oxygen-metal bond, which is almost entirely ionic in character, should break more easily than the oxygen-silicon bond, resulting in a negative charge on the surface. They concluded that the reaction between the silicate mineral particles and the acidified water involves mainly an exchange of metal ions for hydrogen ions on the surface of the solid, leading to an increase in pH of the aqueous phase. The degree of reaction depends directly on the oxygen-silicon ratio of the silicate structure and on the total surface area of the solid; i.e. on the number of exchange sites available. The reaction also seems to be greatly influenced by the amount of iron present on the solid, more iron increasing the degree of reaction.

In 1966, Deju and Bhappu reported that the point of zero charge of silicate minerals increases as the oxygen-silicon ratio increases. Also, since specific gravity is approximately directly proportional to the oxygen silicon ratio, it follows that point of zero charge is directly proportional to specific gravity for very pure silicate minerals. This relationship, however, will not be valid for impure minerals. If the silicate sample is leached and purified, a large number of the M^+ ions may leave the surface and an equivalent amount of H^+ ions will replace them. The number of M^+ ions present on the surface will then be substantially less than for the unleached sample and the amount of OH^- ion formed

as an end product will also be much less. For this reason, the point of zero charge of the leached and purified sample may be less than that of the impure sample.

Other published study worth mentioning is the investigation by Mackenzie and O'Brien (1969). They used zeta potential determinations to investigate the adsorption of nickel and cobalt ions from aqueous solution onto the quartz surface. They concluded that Ni^{2+} and Co^{2+} are only weakly adsorbed onto the quartz surface and that $NiOH^+$ and $CoOH^+$ were the main Ni (II) and Co (II) ionic species adsorbed. They suggested that the adsorption of these ions might involve a combination of Coulombic forces between the negative $Si\text{-}O^-$ sites at the quartz surface and the positive $NiOH^+$ and $CoOH^+$ ions as well as hydrogen bonding between the OH groups of the hydroxide complex and the Si-OH and $Si\text{-}O^-$ groups at the quartz surface; i.e. the latter being the dominant mechanism. They also pointed out that positively charged $Ni(OH)_2$ and $Co(OH)_2$ colloids could explain the positive zeta potential values at high pH values (less than 11).

Fuerstenau (1975) investigated the role of metal ion hydrolysis in oxide and silicate flotation systems. Electrophoretic data showed that a greater charge was left at the surface after hydroxy complex adsorption than was present prior to adsorption. Either of the two mechanisms could account for this phenomenon, namely, hydrogen bonding between the hydroxy complex and an oxide site, or water formation from the hydroxyl of the hydroxy complex and adsorbed hydrogen ions. In the case of water formation, he suggested that the hydrogen ion could adsorb onto oxide sites while hydroxyl ion could adsorb onto silicon sites. Adsorption of hydroxy complexes, such as $CuOH^+$, could occur by splitting out water. In the presence of collector, this could lead to collector adsorption onto this site.

Fuerstenau et al. (1977) also studied the mechanism of pyroxene (augite, diopside) flotation with potassium oleate. Electrophoretic data indicated that the hydroxy complexes $FeOH^+$, $MgOH^+$, and $CaOH^+$ were responsible for the flotation of these pyroxenes.

More recently, Nagaraj and Brinen (1995) have shown how SIMS and XPS were used to study copper ion adsorption, and its effect on subsequent sulphide collector adsorption, on pyrite and pyroxene minerals under flotation related conditions at pH 9. The analysis of pyroxene and pyrite treated with iso-butyl ethoxycarbonyl thionocarbamate indicated no evidence of collector adsorption in the absence of copper activation. Copper was found to

adsorb on both minerals, which caused sulphide collector adsorption. It was also found in this study that in the absence of collector, copper on pyroxene was in the Cu^{2+} form, whereas after collector treatment it was in the Cu^{1+} form suggesting the formation of a copper-collector complex. Unfortunately, they did not carry out flotation tests and thus link the surface coverage to floatability.

A year later, Nagaraj and Brinen (1996) reported on a similar study as described above. During this investigation, amyl xanthate in addition to iso-butyl ethoxycarbonyl thionocarbamate was used as a sulphide collector. SIMS and XPS techniques were employed to investigate the adsorption of sulphide collectors on pyroxene in the absence and presence of copper sulphate at pH 9. No collector adsorption could be detected on pyroxene. Once pyroxene was treated with Cu^{2+} ions, washed and then treated with collector, XPS measurements showed that Cu on pyroxene was reduced from cupric to cuprous upon collector adsorption. SIMS imaging suggests that collector adsorption occurs on copper sites on the surface. Once again, no flotation tests were carried out.

2.3 Feldspar

2.3.1 Mineralogy

Feldspar minerals are aluminosilicates whose structures are composed of corner-sharing AlO_4 and SiO_4 tetrahedra linked in an infinite three-dimensional array; charge balancing *M* cations with radius greater than 1.0 Å occupy large, irregular cavities in the tetrahedral framework. The general formula MT_4O_8 characterises their chemistry, where *T* is Al, Si and *M* is monovalent Na and/or K for $AlSi_3O_8$ alkali feldspars and divalent Ca, or Ba for $Al_2Si_2O_8$ frameworks. A complete range of compositions is observed in the plagioclase feldspar series, $Na_yCa_{1-y}Al_{2-y}Si_{2+y}O_8$ ($0 \leq y \leq 1$), and somewhat analogous K_xBa_{1-x} series. Minor or trace substituents in the irregular *M* polyhedral sites are Sr, Rb, Cs, Pb, Eu, other rare earths, and possibly Fe^{2+}, Mg, and hydronium (H_3O^+) (Ribbe, 1975). When feldspars are ground, the surfaces consisting of exposed silicon and aluminium atoms are unsaturated due to anionic tetrahedron breakage. In the presence of water, the surface atoms are saturated with hydroxyl groups. The dissociation of surface hydroxyl leads to a negatively charged surface of AlO^- and SiO^-. Hence, the point of zero charge of feldspar is low and occurs in the region of pH 2.

2.3.2 Surface and Flotation Studies

To the author's knowledge there does not appear to be any published research dealing with the effect of copper (II) and nickel (II) activation of feldspar surfaces in the separation of base metal sulphides from siliceous gangue minerals with xanthate collectors. Most of the studies related to feldspar flotation describe the mechanisms involved in the separation of feldspar and quartz. In a conventional process, feldspar is separated from quartz using a cationic amine collector and hydrofluoric acid as an activator for feldspar. Only a few studies are summarised below.

Buckenham and Rogers (1954) proposed that activation of feldspar by fluoride ion forms alumino-fluoride complexes at the feldspar surface, at which sites the dodecylammonium ion is adsorbed. However, Joy et al (1966) studied the dissolution of feldspar in perchloric acid and concluded that only aluminium ions were found in solution. While this depressed the mineral greatly, it did not affect dodecylamine adsorption or the response to fluoride atoms. It would appear that dodecylamine adsorption does not take place at aluminium atom sites and thus that fluoride ions do not activate by reaction at aluminium sites.

Warren and Kitchener (1972) concluded that the main effect of fluoride was to enhance the negative zeta-potential of feldspar and thus to favour adsorption of cationic surfactant. This observation is in line with the conclusions by Bolin (1983). He reported that hydrofluoric acid greatly enlarged the difference in zeta potential between feldspar and quartz by lowering the potential of feldspar surfaces.

The use of hydrofluoric acid is not acceptable due to the associated environmental and health problems, and a few new reagents schemes have been reported. For example, Shimoiizaka et al. (1978) described a new flotation process in which feldspar was floated from silica using n-alkyl trimethylene diamine acetate together with sodium petroleum sulfonate as collectors in an acidic circuit by hydrochloric or sulphuric acid at about pH 2. Basic studies showed that the simultaneous use of petroleum sulphonate promoted the floatability of feldspar by co-adsorption of it.

From other published literature, which is more closely related to the focus of this thesis, the following studies are worth mentioning.

An investigation by Shehu and Spaziarii (1999) showed that quartz could be separated from feldspar using a complexing agent (ethylenediaminetetraacetic acid) as modifier at pH 2. At this pH, EDTA reduced the zeta potential for feldspar and increased it for quartz.

The investigation by Wanxiong and Zhenghe (1986) focused on adsorption and flocculation behaviours of ilmenite and feldspar in the presence of sulphonated polyacrylamide (PAM). The results revealed that weak adsorption of PAMS on feldspar cause its dispersion to be more stable.

El-Salmawy et al (1993) pointed out in their study that according to the hydrated layer hypothesis, the surface of feldspar under acidic conditions is depleted in aluminium and alkali ions, but enriched in silicon, while under alkaline conditions the surface is depleted in silica and enriched in alkali ions. Their results of Ca^{2+} adsorption tests and zeta potential coincided with the hydrated layer hypothesis. The lower adsorption density of calcium ions onto feldspar surfaces, as compared to quartz, was attributed to the composition of a hydrated layer on the surface of feldspar, i.e. the presence of mobile cations such as aluminium and potassium may be exchanged with Na or NaOH competing with $CaOH^{+}$ in high alkaline medium.

2.4 Complexing Agents (Chelates)

2.4.1 Chemistry

Metal chelate compounds may be defined simply as complexes in which donor atoms are attached to each other as well as to the metal (Chaberek and Martell, 1959). A chelate has two or more donor atoms, with adjacent donors linked together by a short chain of atoms. These links are often carbon atoms but they could also be other non-metals, as in the oxyacids. The bound ligand and the metal ion form a 'ring' of atoms referred to as the 'chelate ring'. The optimal size for a chelate ring depends on the type of functional group(s) containing the donor atoms, and on the size and binding preference of the metal ion. For the majority of metal ions a 5-membered chelate ring is favoured: *i.e.* metal ion

plus two donor atoms plus two linking atoms. By sharing a common donor atom or a common atom in a chelate ring, ligands can have several donor atoms or donor functional groups linked together into a chain or cluster. The ligands formed are *poly*-dentate and will occupy 2 or more coordination sites on the metal ion. The linking together of two or more chelate rings introduces the possibility of ligands with rings of different size and/or different donor atoms.

An important example is polyamine: $NH_2(CH_2)_nNH(CH_2)_mNH_2$,

where n = 2 or 3 and m = 2, 3 or 4.

All properties of metal ions in aqueous solution become altered when they are combined with chelating agents. The solubility product determines whether the metal chelate will precipitate or remain in solution. If the metal chelate is quite stable, the reactivities of the metal toward various reagents may be greatly altered or completely blocked. Even when weak, highly dissociated metal chelates are formed, some of the common properties of the metal ion, such as colour, oxidation potential and solubility may be altered considerably.

Metal ions have characteristic coordination numbers, which indicate the number of groups that normally become associated with the metal ion through the formation of coordination bonds. The crystal structures of the Cu(II) compounds have been thoroughly investigated and show that only four donor atoms surround each copper ion. The stable complex ammines of Cu(II) have all been found to contain four basic nitrogen atoms per metal ion. In the presence of an excess of ammonia or amine, there is evidence for a relatively weak association between the complex and additional basic nitrogen atom. Therefore it is possible to conclude that, while the characteristic coordination number is 4, the coordination number may 5 or 6 be under special conditions.

Formation of single metal chelates, MA, occurs when a chelating agent contains a sufficient number of electron donor groups that the subsequent coordination with the given metal ion results in a saturation of its coordinating positions, a single stable chelate is generally formed. A good example is EDTA. Metal chelates may also combine with hydroxyl ions to form hydroxo-metal chelate compounds in which both the ligand and hydroxyl ion are coordinated with the metal ion. The tendency to form hydroxo species

would depend on the affinity of the metal for the donor atom of the ligand as well as the hydroxyl ion concentration and consequently the hydrolysis of relatively stable metal chelates occurs only in alkaline solutions if at all. The interaction of a metal ion with a chelating agent results in the successive formation of more than one stable chelate species in aqueous solution. Bidentate and in many cases terdentate ligands form stable complex compounds containing one, two and even three moles of chelating agent per mole of metal ion. A good example is the reaction of Cu(II) ions and ethylenediamine (EDA) as reported by Jonassen and Dexter (1949)

Selectivity, applied to ligands, refers to a ligand's ability to preferentially bind to one metal ion, or a group of metal ions, in the presence of others. This is thermodynamically driven and is expressed by the relative stability constants for complex formation. Selectivity could also be based on the relative rate constants for complex formation (kinetic selectivity). Selectivity is a key factor in ore enrichment, since the dissolution from minerals, grinding media and/or ions occurring in process water could alter the recovery and selectivity in the flotation process.

2.4.2 Applications of Complexing agents in the Mineral Processing Industry

Complexing agents have been recognised as potential reagents in mineral flotation for many decades. For example, complexing agents, in particular diethylenetriamine (DETA, NH_2-CH_2-CH_2-NH-CH_2-CH_2-NH_2), have been used in the selective flotation of pentlandite-pyrrhotite and copper-nickel ores. Investigations have mainly focused on the depressing mechanism of pyrrhotite by DETA. No investigations appear to have been reported on systems containing siliceous gangue minerals.

Marticorena et al. (1995) identified DETA as an effective pyrrhotite depressant, which has become a standard reagent in INCO's Sudbury area milling complex. DETA forms stable complexes with cuprous, nickelous and ferrous ions in mildly alkaline pH. DETA, as compared to EDTA, is a selective complexing agent and will readily complex with Cu^{2+} and Ni^{2+}, but not with Fe^{3+}, Ca^{2+} and Mg^{2+}. The complexing strength of DETA is sufficient to desorb copper and nickel species from pyrrhotite regardless of whether they are present as hydroxide or xanthate (Xu, et al., 1997).

Yoon et al. (1995) has also shown that DETA is a selective depressant for nickeliferous pyrrhotite during pentlandite flotation. The flotation of pyrrhotite was attributed to the inadvertent activation of the mineral by heavy metals ions, such as Ni^{2+}, Cu^{2+} and Ag^{+} that are present in process water. Pyrrhotite rejection was greatly improved by small additions of DETA, especially when the mineral was oxidised. It was also shown that both dixanthogen and iron xanthate are formed on the surface of pyrrhotite when contacted with amyl xanthate, the latter becoming more prominent at higher potentials. In the presence of DETA, only a small amount of xanthate is absorbed on the mineral at potentials ~200mV higher than is the case without DETA. It should also be noted that DETA is most effective when the process water is saturated with Ca^{2+} ions, the mechanism and role of the Ca^{2+} ions is not yet known.

Kelebek (1996) described collectorless flotation tests carried out in the absence and presence of DETA. Copper and nickel ions are known to adsorb onto pyrrhotite surfaces and promote flotation of this mineral whether a collector is present or not. DETA involves the sequestration of copper and nickel ions from surfaces under a wide range of redox conditions. Analysis of filtrate samples taken during the tests confirmed the sequestering action. Once deactivated (copper and nickel ions removed) pyrrhotite acquires a surface state characterised by a greater hydrophilic/hydrophobic ratio due to the formation of iron hydroxide(s) and/or the lack of kinetic capability to form elemental sulphur. The results also indicated that pentlandite recoveries were unaffected by the presence of DETA yet nickel grades were much higher in the presence of DETA. Thermodynamic calculations for the Ni-Fe-S-DETA-water, Cu-FE-S-DETA-water and Fe-DETA-water systems indicate that the action of DETA involves the sequestration of metal ions under a wide range of redox potentials. Thus it appears that DETA may enhance the self-hydrophobicity of chalcopyrite and pentlandite by exposing more of the sulphur-rich surface sites for bubble contact in flotation.

Kelebek et al. (1996) also describes similar findings as highlighted above for the differential flotation of chalcopyite, pentlandite and pyroxene in Ni-Cu sulphide ores. DETA controls the metal ions, which are responsible for inadvertent activation of pyrrhotite.

One possible function of DETA, the complexation and removal of potential activating ions, e.g. copper and nickel known to be present on the surface of pyrrhotite under plant

conditions, has also been explored by Xu et al. (1997). DETA was found to remove copper and nickel ions from the surface and leave hydrophilic ferric species on it. The metal: DETA molar ratio was 1:2. Copper was more readily removed than nickel. Certain combinations of nickel ions, xanthate, dithionite (S_2O_4) or dithionate (S_2O_6) and DETA produced hydrophilic precipitates. DETA adsorption on pentlandite surface was negligible indicating that DETA complexes readily with nickel when it is in the hydroxide and xanthate form. It does not, however, compete with the surface lattice Ni-S bond. Similar observations were reported by Rao et al. (1995) and Forward et al. (1960).

There are also reports of studies carried out on the effect DETA has on xanthate adsorption. Bozkurt et al. (1999) described the effect depressants have on xanthate adsorption on pentlandite and pyrrhotite. Xanthate interaction with pentlandite and pyrrhotite showed that dixanthogen was the main adsorption product on both minerals, but higher on pentlandite compared to pyrrhotite. The presence of DETA reduced the dixanthogen adsorption on both minerals. Similar observations were concluded for the study of the formation and charaterisation of nickel-DETA complexes related to flotation systems (Vreughenhil et al., 1997). These authors studied the soluble species and precipitates generated by mixtures of nickel ions with DETA and xanthate, in the presence of CO_3^{2-} or SO_3^{2-}, by IR and UV-visible spectroscopy. They found that DETA could coordinate metal ions with either two or three of its nitrogen atoms. In the case of two-fold coordination, the unattached nitrogen atom can replace one of the coordinated nitrogen ions. This process causes a flexible arrangement of the ligands around the metal atom. The complex formed depends on the relative molar ratio of nickel to DETA and the presence of other ligands. DETA is capable of rapidly dissolving many solid nickel salts, which suggests that, the formation of bis-DETA nickel or DETA-aquo nickel is an important mechanism by which nickel ions are removed from mineral systems. Ni-DETA in the presence of CO_3^{2-} or SO_3^{2-}, results in this case in a neutral complex, $[Ni(DETA)(L)]^{n+}$, where n depends on the charge of the ligand, L. The formation of this species indicates that the presence of other ligands could play a role in the action of DETA depression of pyrrhotite. The Ni-DETA-ethylxanthate precipitation formation indicates that xanthate is not coordinated to the nickel ion but is acting as a counter ion for the charged bis-DETA nickel complex. Ethylxanthate thus does not displace the DETA ligands to form the much less soluble xanthato-nickel complexes. The inhibition of xanthate nickel formation could also be an effective means by which DETA acts as a depressant. When half the amount of

ethylxanthate is added then ethylxanthate coordinates to nickel and the results suggest that when nickel is coordinated by only one DETA ligand, it is susceptible to attack by xanthate to form a metal complex containing both xanthate and DETA. This species is much less soluble than the species formed when nickel is coordinated with two molecules of DETA. It could, however, allow the formation of a hydrophobic coating on mineral surfaces.

2.5 Polyphosphates

2.5.1 Classification and Chemistry

The ability of phosphates to form soluble complexes with metal ions has long been recognised. The phosphate family of compounds was recently reviewed by Rashchi and Finch (2000). Polyphosphates are defined as compounds, which contain P-O linkages. The P-O bond has a length of 1.62 Å, with bond angles of 130° at the O atoms and 102° at P atoms. Rashchi and Finch reported that polyphosphates could be grouped into three types: orthophosphates, pyrophosphates and metaphosphates.

Orthophosphates are compounds containing discrete PO_4^{3-} ions. The pyrophosphates and metaphosphates (condensed phosphates) consist of chains of tetrahedral, each sharing the O atom at one or two corners of the PO_4 tetrahedron. Pyrophosphates, $P_2O_7^{4-}$ are the simplest condensed phosphate anion, formed by condensation of two orthophosphate anions. The term metaphosphates refer to cyclic anions with the composition of $(PO_3)_n^{n-}$. The condensed phosphates could be divided into three major categories: linear polyphosphates, cyclophosphates and ultraphosphates. In terms of complexing power, the chain polyphosphates form stable complexes, the ring polyphosphates are less effective, and the orthophosphates are the weakest of all. The chain polyphosphates are the only phosphates which show stable complexes with all ions except those of the alkali metals and quaternary salts.

Corbridge (1990) studied the hydrolysis of polyphosphates. Polyphosphates are stable in neutral solutions at room temperature, but hydrolysis occurs in an acidic aqueous medium. Soluble varieties of long chain polyphosphates give solutions, which are neutral or very slightly acidic, in contrast to the shorter chain compounds, which give an alkali reaction. The principal factors influencing the rate of hydrolysis of a condensed phosphate solution

are the number of corners shared by PO_4 tetrahedra in the structure, temperature, pH and concentration. The hydrolysis of polyphosphate chains could be catalysed by heavy metal cations, the effect being most pronounced with cations of high charge and small radius. The effect is believed to be connected with chelation of the cations by the oxygen atoms. There is a continuous transition in the physical properties of solutions of polyphosphates on passing from low to high molecular weight species. Apart from the initial few members of the series, they all exhibit typical properties of polyelectrolytes.

Sodium polyphosphates are used for water softening agents, detergents and for descaling boilers and pipes. They also protect metal surfaces in hard water by the formation of corrosion-inhibiting films. At higher concentrations of polyphosphate in hard water, formation of readily soluble complexes with Ca^{2+} and Mg^{2+} ions will occur. This results in water softening by the prevention of insoluble Ca^{2+} and Mg^{2+} soaps being formed. It is usually assumed that about five to ten times the amount of magnesium as compared to calcium will be sequestered by a given phosphate (Van Wazer and Callis, 1958).

2.5.2 Studies Related to Mineral Processing

In mineral processing, phosphates are used as depressants of gangues, dispersing agents of slimes, stabilisators of mineral suspensions, softening agents of hard water as well as for control of metal ions, which adsorb onto mineral surfaces and thus depress or inadvertently activate the mineral.

Serpentine minerals often interfere with the concentration of nickel sulphide ores. Edwards et al. (1980) investigated the effect of slime coating of chrysotile and lizardite on pentlandite flotation at pH 9. The recovery of negatively charged unoxidised pentlandite decreased with increasing concentration of positively charged lizardite and especially chrysotile. They concluded that slime coating on sulphide minerals was directly related to the surface charges. Chemical additives, which modified the slime surface charge, such as carboxymethyl cellulose, dextrin, sodium pyrophosphate and sodium silicate, were shown to be effective in reducing the adverse influence of the slime on the flotation of pentlandite.

In 1983, Changgen and Yongxin reported that depression of the calcium gangue minerals was related to the selective dissolution of calcium ions by the phosphates, and not to the

adhesion of the phosphates onto the mineral surfaces. The complexes formed were identified as $Na_2Ca_2(PO_3)_6$ and $Na_6Ca(P_2O_7)_2$. The mechanism of depressing calcium gangue minerals was attributed to several effects, namely the selective complexation of phosphates and dissolution of calcium ions from gangues, decrease of the number of active centers positively charged on their surfaces and the increase of their negative zeta potential as well as decrease of the adsorption of sodium oleate.

Fuliang and Fenglou (1997) found that floatability of galena increased by removing calcium and magnesium ions with sodium hexamethaphosphate.

A few researchers have studied adsorption and desorption of colloidal-sized particles in the system comprising titania surfaces and silica slimes particles. Feiler et al. (1999) reported that at pH4, adsorption of the negatively charged silica particles onto the oppositely charged titania surface occurred as a result of van der Waals and attractive electrostatic interactions. It was found that adsorption of polyphosphate onto the titania surfaces could significantly hinder the adsorption of slimes. Conversely, in a system where adsorption of the slimes to the titania surfaces has already occurred, addition of polyphosphate caused desorption of the slimes. Furthermore, the results showed that larger polyphosphates reduce the adhesive force between the silica and titania by a greater extent than the small one. The critical concentrations of polyphosphate for desorption to occur correlated with the concentration of polyphosphate at which the short-range interparticle forces changed from attractive to repulsive.

Michelmore et al. (1999) also investigated the influence of polyphosphates in modifying the surface behaviour and interactions of titanium dioxide and silica particles. They found that polyphosphates specifically adsorb onto titanium dioxide surfaces over a wide range of pH values. Their proposed mechanism involved the terminal PO_3 groups chemically adsorbing to the surface. The linking PO_2 groups did not chemically interact with the surface. Electrostatic attraction was also involved when polyphosphate and titanium dioxide surfaces were oppositely charged. The maximum amount of adsorbed polyphosphate observed was significantly higher at pH 4 (electrostatic attraction) compared to pH 9 (only chemical interaction). It was shown that polyphosphates did not interact with silica surfaces.

A fundamental investigation carried out by Huynh at el. (2000) showed that phosphate adsorbed on the titania particle surfaces gave rise to a change from an attractive to repulsive (electrostatic) force, an additional repulsive (steric) force, a reduction in adhesive forces and a decrease in frictional (shear) forces between the slime and valuable minerals. Bandini et al. (2000) reported that polyelectrolyte reagents, carboxymethylcellulose and polyphosphate, were highly effective at removing iron oxide slime coatings from galena surfaces.

A possibility of controlling inadvertent activation of sphalerite by lead ions through the formation of soluble lead-polyphosphate complexes was investigated by Rashchi and Finch (2002). They found that the minimum amount of linear polyphosphate (17 PO_3 groups) required to remove Pb as a soluble complex corresponds to a mole ratio of polyphosphate:lead = 1:2.

2.6 Comments Regarding the Literature Review

The mechanisms involved in pentlandite surface alteration due to oxidation in air and solution at various pH values have been studied extensively by many researches over the years. A range of iron oxides and hydroxides (Fe_3O_4, Fe_2O_3, FeOOH, $Fe(OH)_3$), nickel oxide (NiO) and iron sulphates ($FeSO_4$, $Fe_2(SO_4)_3$) were observed to form in the immediate oxidised surface. It was also found that the oxide and hydroxide layers were largely soluble in an acid environment. Pentlandite hydrophobicity in the absence and presence of collectors has also been studied at length. It was shown that xanthate chemisorbs directly onto the pentlandite nickel sites and, subsequently dixanthogen would form from the chemisorbed xanthate.

However, there is not much information available in the literature about pyroxene and feldspar in terms of inadvertent activation and subsequent flotation due to the adsorption of xanthate ions onto inadvertently activated silicate mineral surfaces. The mechanisms contributing to true flotation of pyroxene and feldspar are of primary interest at operating circuits treating Merensky Reef ore. The use of complexing agents and polyphosphates as well as the mechanisms involved have been described in the literature, however, to the author's knowledge, the application to deactivate siliceous gangue minerals has not been studied. The combination of DETA and polyphosphate, investigated in this thesis, is a new

approach to enhance recovery of pentlandite and simultaneously improve selectivity between the sulphide and gangue minerals.

CHAPTER 3

EXPERIMENTAL METHODS

3.1 Minerals

Natural pyroxene and feldspar from the Merensky Reef in the Northern Province, South Africa, were crushed to 2mm and selected by hand-picking. Pentlandite was synthesised at Anglo Platinum Research Centre using a method developed by Johnson Matthey, Sonning. After hydrogen desorption, which removed H_2 from the metal, reduced iron (11.0g) and reduced nickel (11.86g) were mixed with sulphur flake (11.41g) and transferred to a quartz ampoule. The evacuated, sealed ampoule was heated in a furnace to 1150°C then cooled to ambient temperature. Chemical composition of the minerals used during the study (Table 3.1) was determined by Inductively Coupled Plasma (ICP) Spectrometry.

Table 3.1: Chemical Composition (wt.%) of the Minerals Studied

MINERAL	SOURCE	ELEMENT Wt %						
		Mg	Al	Ca	Si	Fe	Ni	S
Pyroxene	Bushveld Complex	13.2	2.7	3.7	25.1	11.0	0	0
Feldspar	Bushveld Complex	0.3	15.7	9.4	22.1	0.5	0	0
Pentlandite	Synthetic	0	0	0	0	32.1	34.6	33.3

All mineral samples were stored under argon in a freezer and freshly ground in an agate mortar under argon in a glove box just prior to each experiment. The products were screened to obtain size fractions of –25µm for zeta potential determinations and +38 – 106µm for microflotation tests. Using the BET method, the surface area of the +38 – 106µm size fraction of pyroxene, feldspar and pentlandite was found to be 0.59m^2/g, 0.85m^2/g and 0.30m^2/g, respectively.

3.2 Reagents

During the study, water with a specific conductance of 0.7µS cm^{-1} and with a surface tension of 72.8 mN m^{-1} at 20°C, produced by a MILLI-RO PLUS apparatus, was used to prepare di-sodium tetraborate solution (Saarchem, background electrolyte, I = 3 x 10^{-3}) and synthetic water (I = 2 x 10^{-2}). All experiments were carried out in aerated solutions. High purity argon (Afrox) was used to minimise pentlandite oxidation during storage.

Purified collector, sodium isobutyl xanthate, was obtained from SENMIN and a commercial grade of depressant IMP 4 (guar) and frother DOW 200 (glycol) was received from Trohall and Cytec, respectively. Other chemicals were of analytical grade quality. Copper sulphate (Saarchem) was used as an activator. Diethylenetriamine (Riedel-de Haen) and sodium polyphosphate (Sigma Aldrich) were utilised as a complexing agent and dispersant, respectively. The desired concentration of calcium ions was maintained by the addition of calcium chloride (BDH Chemicals). Sodium carbonate (Saarchem) and hydrochloric acid (Riedel-de Haen) were used for pH adjustment.

The xanthate and copper ion mineral surface coverage calculations are provided in Appendix A.

3.3 Synthetic Water Composition

Water, with a specific conductance of 0.7μS cm^{-1}, was modified by the addition of various chemical salts of analytical grade quality (Table 3.2) to produce synthetic process water ($I = 2 \times 10^{-2}$). The synthetic water contained similar amounts of key ions typically found in circuit water (Ca^{2+} 80ppm, Mg^{2+} 80ppm, Na^{+}135ppm, Cl^{-} 270ppm, SO_4^{2-} 250ppm, NO_3^{-} 135ppm, NO_2^{-} 40ppm, CO_3^{2-} 40ppm, TDS 1030).

Table 3.2: Synthetic Water Composition

CHEMICAL COMPOUND	FORMULA	MASS (g) in 1 LITRE	Mol/l
Calcium chloride (BDH Chemicals)	$CaCl_2.2H_2O$	0.147	0.001
Calcium nitrate (BDH Chemicals)	$Ca(NO_3)_2.4H_2O$	0.236	0.001
Magnesium sulphate (Saarchem)	$MgSO_4.7H_2O$	0.615	0.0025
Magnesium nitrate (BDH Chemicals)	$Mg(NO_3)_2.6H_2O$	0.107	0.0004
Sodium chloride (Saarchem)	NaCl	0.356	0.0061
Sodium carbonate (Saarchem)	Na_2CO_3	0.058	0.0005

3.4 Zeta Potential Determinations

The use of electrokinetic studies in flotation is well established, especially for minerals and their interaction with collectors. The adsorption of collector onto the mineral surface can be controlled by the zeta potential of the particles.

3.4.1 Technique Description

Electrokinetic measurements are of considerable interest for the study of electrical double layers. The double layer model is used to visualise the ionic environment in the vicinity of a charged particle. The double layer is formed in order to neutralise the charged particle and, in turn, causes an electrokinetic potential between the surface of the particle and any point in the mass of the suspending liquid. It is customary to interpret electrokinetic data in terms of ζ-potential. This is the potential of the slipping plane between the moving and stationary phase, when the liquid far from the interface is considered to be at zero potential.

When an electrical field is applied across an electrolyte, charged particles suspended in the electrolyte are attracted towards the electrode of opposite charge. Viscous forces acting on the particles tend to oppose this movement. When equilibrium is reached between these two opposing forces, the particles move with constant velocity and this phenomenon is called electrophoretic mobility. The velocity of a particle is related to the dielectric constant and viscosity of the suspending liquid and to the electrical potential at the boundary between the moving particle and the liquid (Malvern Instruments Training Manual, 1996).

Zeta potential is related to the electrophoretic mobility by the Henry equation (Hunter, 1993):

$$u_E = \frac{\zeta\varepsilon}{1.5\,\eta} f(\kappa a) \qquad (17)$$

where u_E is the electrophoretic mobility, ε is the fluid dielectric constant, ζ is the zeta potential, η is the dynamic viscosity, κ is the Debye-Huckel parameter and a is the particle radius. For large particles in more concentrated electrolyte solutions $\kappa a >> 1$ and $f(\kappa a) = 1.5$. This transforms Henry's equation (17) into Smoluchowski's equation (18):

$$u_E = \frac{\zeta\varepsilon}{\eta} \qquad (18)$$

At 25°C this reduces to:

$$\zeta = 12.85 \times u_E \text{ (mV)} \qquad (19)$$

3.4.2 Experimental Testwork

During the study described in this thesis, the zeta potential determinations were carried out on dilute dispersions of the individual minerals studied using a Malvern Zetasizer 4. The instrument gives the electrophoretic mobility from which the zeta potential was calculated using the Smoluchowski equation 18. The zeta potential determinations were carried out at pH 4, 6, 8 and 10 at 25°C. During the experiments, the effect of SIBX (5×10^{-5}M), $CuSO_4$ (5×10^{-5}M), DETA (5×10^{-5}M), polyphosphate (3.1×10^{-6}M) and calcium ions (500 ppm) on the mineral surface alteration was investigated. A 0.075g mineral sample was dispersed in 60cm^3 of di-sodium tetraborate solution and/or synthetic water and the pH was adjusted to the desired value. Conditioning of the mineral for zeta potential determinations was carried out for 20 minutes. The pH was checked prior to taking the reading. The E_h was allowed to vary naturally. See Appendix B for a detailed procedure.

3.5 Microflotation Tests

A microflotation cell is a useful tool for the determination of the flotation response of pure minerals and mineral mixtures. A study of the effect of reagent adsorption on a specific mineral can be carried out, since the influence of a froth phase and cell dynamics in the pulp phase are not present.

3.5.1 Microflotation Cell Description

The cell consists of a conical tapered cylindrical tube with air introduced through a needle at the base of the cell. Mineral loaded bubbles rise through the cell and are deflected off the cone at the top of the cell, after which they burst, resulting in the minerals dropping into the concentrate launder. After a set time the needle is removed and the particles in the launder are collected as a concentrate. During the study, flotation was carried out by introducing air at a flowrate of 5 cm^3/min. The mean bubble size diameter was 0.957mm (Bradshaw and O'Connor, 1996). The peristaltic pump speed was kept constant and set to maintain an effective particle suspension. The microflotation apparatus used during the study is shown in Figure 3.1.

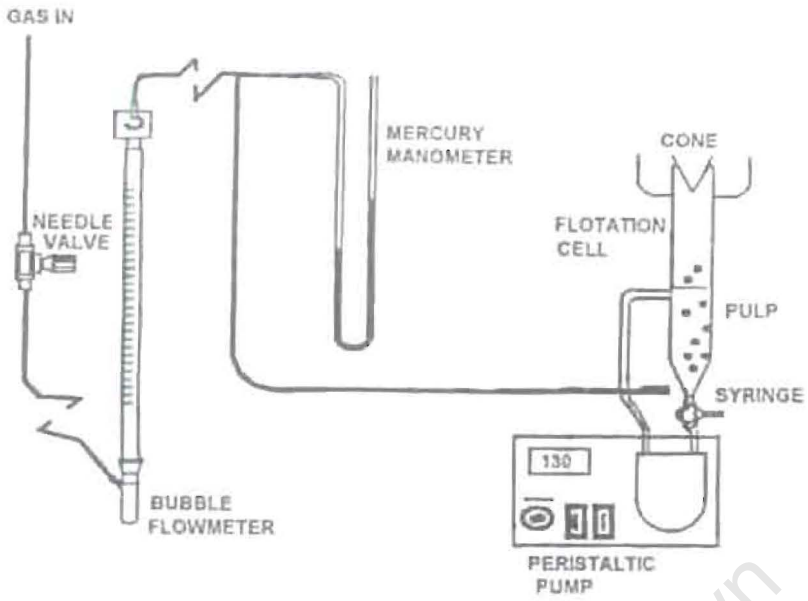

Figure 3.1: Microflotation Apparatus (Wesseldijk et al., 1999)

3.5.2 Experimental Testwork

Microflotation tests were conducted in di-sodium tetraborate solution and synthetic water. A 2g sample (1g of each mineral for mineral mixtures) was added to 250 cm^3 of solution, adjusted to the desired pH (4, 6, 9) and conditioned with desired reagents. A detailed microflotation test procedure is given in Appendix C. During the tests, various combinations of reagents were investigated. These were SIBX, [$CuSO_4$ + SIBX], [DETA + SIBX], [$CuSO_4$ + DETA + SIBX] and [sodium polyphosphate + $CuSO_4$ + DETA + SIBX]. The sequence of addition was as indicated by the sequence of reference in brackets. Concentrates were collected at time intervals of 2, 5, 10 and 20 minutes for a single mineral and 3 and 20 minutes for mixtures of minerals. The flotation time of 20 minutes was selected with the aim of simulating the residence time of a rougher flotation circuit. The floated and non-floated fractions were dried and weighed. In the case of mineral mixtures, microflotation products were analysed for sulphur using a LECO analyser, thus enabling the recovery of each individual mineral to be determined.

3.6 Time of Flight Secondary Ion Mass Spectrometry (ToF-SIMS)

ToF-SIMS analysis is known to be a technique used to determine the occurrence of atomic/molecular species on the surfaces of mineral samples.

3.6.1 Technique Description

The basic concept of time of flight secondary ion mass spectroscopy is fairly simple. A pulsed primary ion beam bombards the sample surface, causing the emission of atomic and molecular secondary ions. The term "secondary ions" is used to distinguish them from the primary bombarding ions. A small percentage of the secondary ions are charged and can therefore be extracted by an electric field (accelerating field) into a mass spectrometer. The kinetic energy of the ions can be expressed as

$$E_{kin} = eV_o = \frac{1}{2}mv^2 \qquad (20)$$

where V_o is the accelerating potential, m the mass of the ion and e its charge. Lighter ions have higher velocities than the heavier ions and will therefore arrive at the detector first. The mass separation is obtained by the flight time (t) from the sample to the detector. This can be determined using equation 21.

$$t = L_o/v = L_o\,(m/2eV_o)^{1/2} \qquad (21)$$

where L_o is the effective length of the spectrometer.

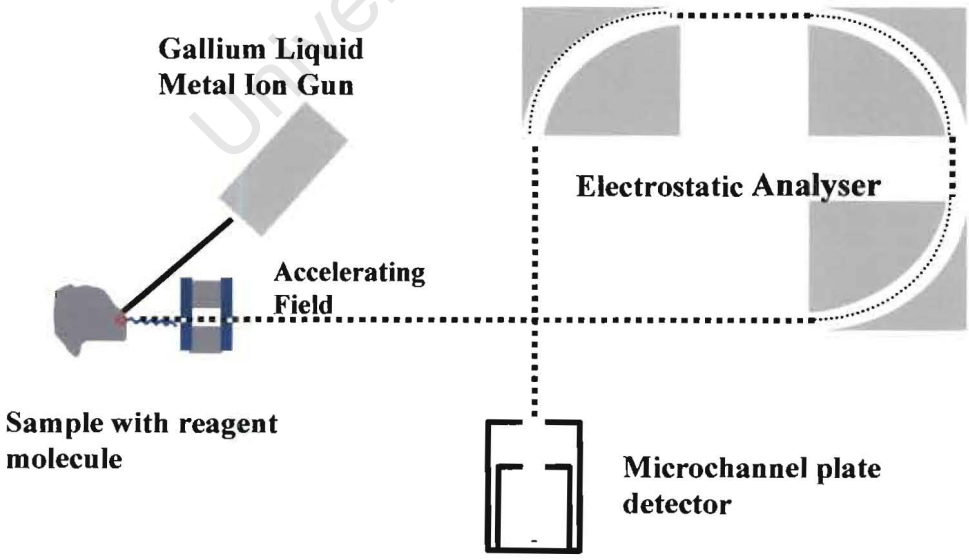

Figure 3.2: ToF-SIMS Layout (de Vaux, 1997)

The mass spectra are recorded by measuring the time difference between pulsing the primary ion gun and the arrival of secondary ions on a fast dual microchannelplate detector at the spectrometer by means of a multistop time-to-digital converter (TDC). Neighbouring masses m_o and $m_o+\Delta m$ can only be resolved if the relationship between time width and separation are correct. Using equation (21) it can be shown that for small mass differences the relationship between flight times and mass resolution is given by

$$m/\Delta m = t_o/2\Delta t \qquad (22)$$

From equation (22) it can be seen that in order to obtain high mass resolution, a short primary ion pulse (t_o) has to be used.

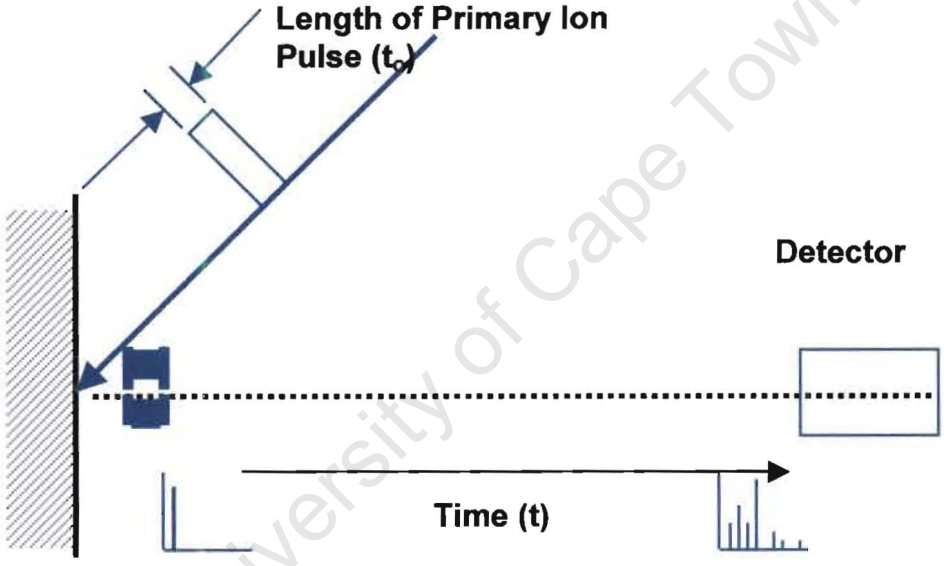

Figure 3.3: The Separation of Ions by Time of Flight (de Vaux, 1997)

The energy transferred when a primary ion impacts with the sample surface results in fragmentation of the original surface in the vicinity of the impact, resulting in the release of atomic species. Further away from the impact site, higher mass molecular species are released as a result of the energy transferred by the impact throughout the substrate. A heavy energetic primary ion cannot be stopped immediately by the first atoms it encounters and will therefore continue into the surface until it has lost all its energy due to elastic scattering off atomic cores and inelastic scattering off electronic shells and free electrons. The ions that are collided with will recoil and displace other atoms, which will in turn collide with other atoms, setting up a complex sequence of collisions. Some atoms will

be permanently displaced from their positions while others will return elastically to their original lattice positions. The collision cascade will eventually result in the surface atoms being displaced (Schueler, 1992, Reich, 1997).

The PHI TRIFT II^{NT} instrument operates in the static SIMS regime. The term static refers to the number of primary ions impacting on the surface per unit area. The static SIMS regime is accepted to be about 10^{12}–10^{13} primary ions/cm^2. The density of a silicon surface is approximately 10^{15} atoms/cm^2. The PHI TRIFT II^{NT} ToF-SIMS features state of the art primary ion gun technology, including a focused liquid metal ion gun with three orders of magnitude range of beam current, from 20 nA (fast spectroscopy) to 20 pA (high lateral resolution, 0.1 μm analytical probe). The ToF-SIMS is capable of analysing small features of interest on both conducting and insulating samples due to an automatic electron charge compensation (Reich, 1997).

3.6.2 Experimental Testwork

During the study, microflotation products as well as single minerals and mineral mixtures conditioned in borate solution and synthetic water in the presence of the desired reagents for 20 minutes, were analysed using ToF-SIMS instrument operating in the static SIMS regime. The procedures for the preparation of the conditioned samples were identical to those used for the microflotation tests. The samples were filtered and washed with water (conductivity 0.7μmS cm^{-1}), adjusted to the desired pH, to remove any physically attached ions. All samples were dried in an argon atmosphere at ambient temperature. The 15 kV, 600pA gallium beam was used throughout the investigation. 30 grains or more of each mineral were imaged and analysed for Ca, Mg, Al, Si, Fe, Na, P, Cu and Ni during positive ion analysis and O, OH, S and xanthate during negative ion analysis. An example of ToF-SIMS analysis spreadsheet is shown in Appendix D. The set of data obtained was evaluated using Statistica. The intensities obtained are normalised for the elements of interest and presented as a relative percent surface coverage.

3.7 Batch and Small Scale Continuous Flotation Tests

Batch Flotation tests were carried out in a laboratory Denver flotation machine (4.5 litre cell) at an impeller speed of 1000 rpm. During the flotation tests conducted on a sample of

Merensky ore at pH 6 and pH 9, incremental concentrates were collected after 2, 8 and 20 minutes. The flotation pulp density was 35% solids by mass. The material was floated at a grind of 60% -75µm. The froth height was maintained at 2.5cm. The reagents added were sodium polyphosphate (4000 g/t), $CuSO_4$ (300 g/t), DETA (300 g/t) and SIBX (200 g/t) in various combinations in the sequence of addition as given above. IMP4 (200 g/t) and Dow 200 (20 g/t) were added to all experiments.

Continuous flotation trials were conducted using Flexi-Float. The system consists of an agitated stock tank and two identical flotation banks operated in parallel. This configuration enables a direct comparison between two flotation systems (pH 6 and pH 9). Each bank comprises eight cells (pulp volume 7.3l per cell). The flotation cell configuration simulated a rougher bank. During the testwork, the first two cells were used as a conditioner. The Merensky ore sample was milled to approximately 60% -75µm using a ball mill just prior to flotation. Flotation ore feed rate was 33kg/hr per bank at a pulp density of 33% solids by mass. The froth height was maintained at 2.5cm. The material was floated with the aim of comparing the mineral flotation response with and without DETA and polyphosphate in the presence of copper sulphate and xanthate using similar conditions as described for the batch tests. Each sampling campaign was carried out over a period of 30 minutes, during which a sample of feed, tailings and six concentrates were collected. The batch and continuous flotation tests samples were processed and assayed for Ni(S) and SiO_2.

3.8 SOLGAS Water Program

Speciation diagrams were calculated using the program SOLGAS Water (Eriksson, 1979) to determine the thermodynamically predicted species presented in equilibrium, both in solution and precipitated from the bulk solution onto the mineral surfaces. The aim of these calculations was to predict the solution conditions at which homogeneous (i.e. not mineral surface mediated) precipitation occurs, that may be reflected by the presence of colloidal particles on the mineral surfaces. Thermodynamic data have been taken from the literature. Equilibrium constants for Cu^{1+}, $(EtX)_2$, HetX, $CaOH^+$ liquid and the solid $(EtX)_2$, CuEtX, $Cu(EtX)_2$ and $Ca(OH)_2$ species were taken from Forssberg, et al. (1984). Equilibrium constants for $Cu(OH)^{1+}$, $Cu(OH)_2$, $Cu(OH)_3^-$, $Cu(OH)_4^{2-}$, $Cu_2(OH)^{2+}$ and the solid $Cu(OH)_2$ species were taken from Lindsay (1979).

CHAPTER 4

EXPERIMENTAL RESULTS

4.1 Single Minerals Study in Di-sodium Tetraborate Solution

The objective of the single mineral study was to investigate if copper (II) ion adsorption is non-selective and whether subsequent addition of xanthate ions could cause true flotation of feldspar and pyroxene. An electrolyte solution was selected in order to simplify the system studied. Di-sodium tetraborate solution was used as a background electrolyte for its buffer capacity, which simulates the buffering effect of pulp solution at operating circuits.

4.1.1 Zeta Potential Determinations

4.1.1.1 Reproducibility

The aim of the reproducibility tests was to establish the reliability of the zeta potential determination procedure used during the study. Any possible error includes the variability of the mineral samples, the consistency of the Malvern Zetasizer operation as well as the operator's ability to be consistent.

In order to determine the reproducibility and standard deviation, zeta potential determinations were carried out on a sample of pyroxene, without any reagent addition, in quadruplicate. The zeta potential determinations and standard deviations for each pH investigated are given in Table 4.1. Graphically the results obtained are summarised by zeta potential-pH curves in Figure 4.1.

Table 4.1: Zeta Potential Determinations and Standard Deviations for pH 4, 6, 8, and 10

pH	Zeta Potential Determinations [mV]					Std Dev	Rel Std Dev [%]
	Test 1	Test 2	Test 3	Test 4	Mean		
4	-24.1	-22.9	-23.7	-22.2	-23.2	0.8	3.7
6	-25.6	-27.4	-27.3	-25.1	-26.3	1.2	4.4
8	-28.9	-31.8	-31.2	-31.2	-30.8	1.3	4.2
10	-29.0	-30.4	-30.6	-30.7	-30.2	0.8	2.7

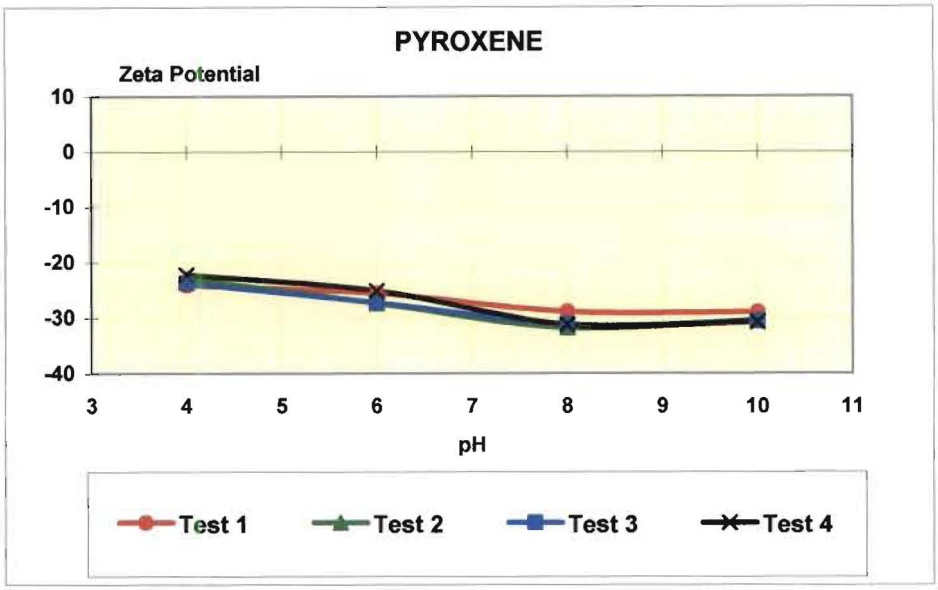

Figure 4.1: Zeta Potential Determination Reproducibility in $Na_2B_4O_7$ at 10^{-3}M, I = 3 x 10^{-3}

As demonstrated by the zeta potential-pH curves and the low standard deviation for each pH measured, the technique and the procedure used gave reproducible results.

The results obtained on pyroxene by the author in di-sodium tetraborate solution were compared to those achieved on pyroxene of a similar composition by Fuerstenau et al. (1977) in sodium chloride solution. As depicted in Figure 4.2, both researchers obtained similar zeta potential vs. pH curves, which is indicative of the consistency of the technique/method used.

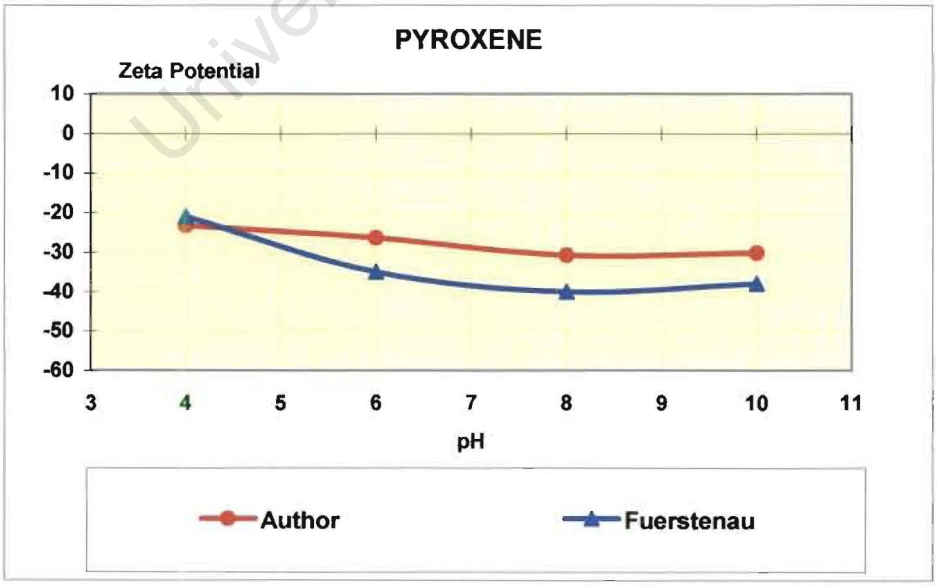

Figure 4.2: Zeta Potential of Pyroxene for the author's curve using 3 x 10^{-3}M di-sodium tetraborate solution and for Fuerstenau's curve using 3 x 10^{-3}M sodium chloride solution

4.1.1.2 Pentlandite

The zeta potential versus pH data for synthetic pentlandite (Figure 4.3) indicate that the mineral surfaces are highly oxidised, as would be expected after conditioning in an aerated solution for 30 minutes. Unoxidised sulphides in general have a pH_{iep} (isoelectric point pH) of about 2 (Acar and Somasundaran, 1992). As the mineral surfaces oxidise and become coated with impurities, a higher pH_{iep} is displayed. The results show that the synthetic pentlandite has a pH_{iep} of about 8.6, which is close to that of iron oxide (Acar and Somasundaran, 1992).

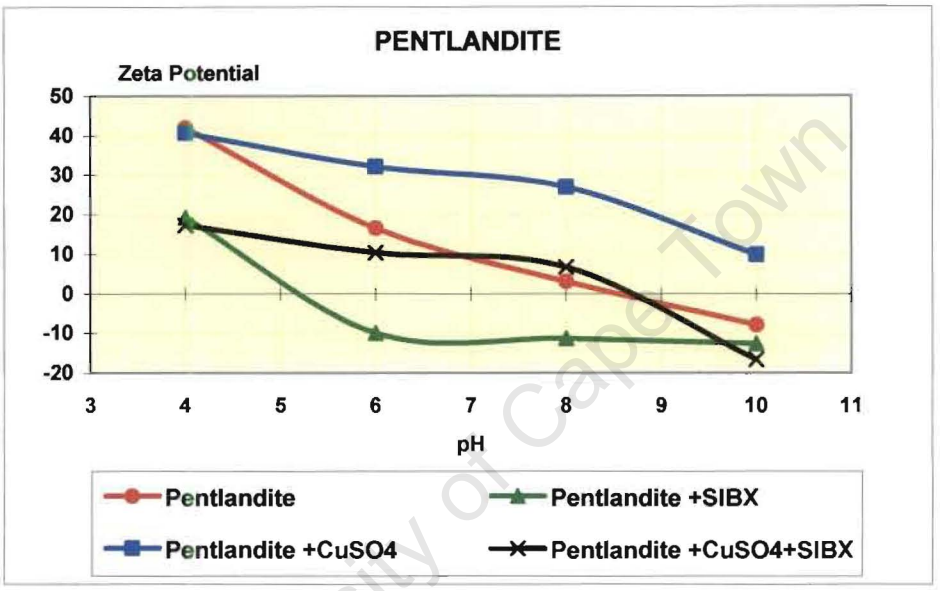

Figure 4.3: Zeta Potential of Pentlandite in $Na_2B_4O_7$ at 10^{-3}M, I = 3 x 10^{-3}, All reagent concentrations were 5 x 10^{-5} M

The addition of xanthate ions shifted the zeta potential versus pH curve to more negative values, indicating that adsorption of xanthate ions onto the pentlandite surfaces occurred. Furthermore, it is evident from these results that, in the presence of copper (II) ions, the pentlandite surfaces became more positively charged above pH 4. This indicates an adsorption of Cu^{2+} ions as well as various positively charged copper hydroxide species ($CuOH^+$, $Cu_2(OH)_2^{2+}$) which are predominant below pH 9.5 (Acar and Somasundaran, 1992). The concentrations of these species are pH dependent, as can be seen from the copper speciation diagram (Section 5.1) and they are known to specifically adsorb onto mineral surfaces (Fuerstenau, 1976, Wang et al., 1989). The iep value of copper oxide/hydroxide occurs at pH ~ 9.5 (Fullston et al., 1998). As expected, there was

adsorption of xanthate ions onto the copper activated pentlandite surfaces observed. The possible interactions between copper species and xanthate are discussed in detail in Section 5.1.

4.1.1.3 Pyroxene

The results obtained are plotted in Figure 4.4.

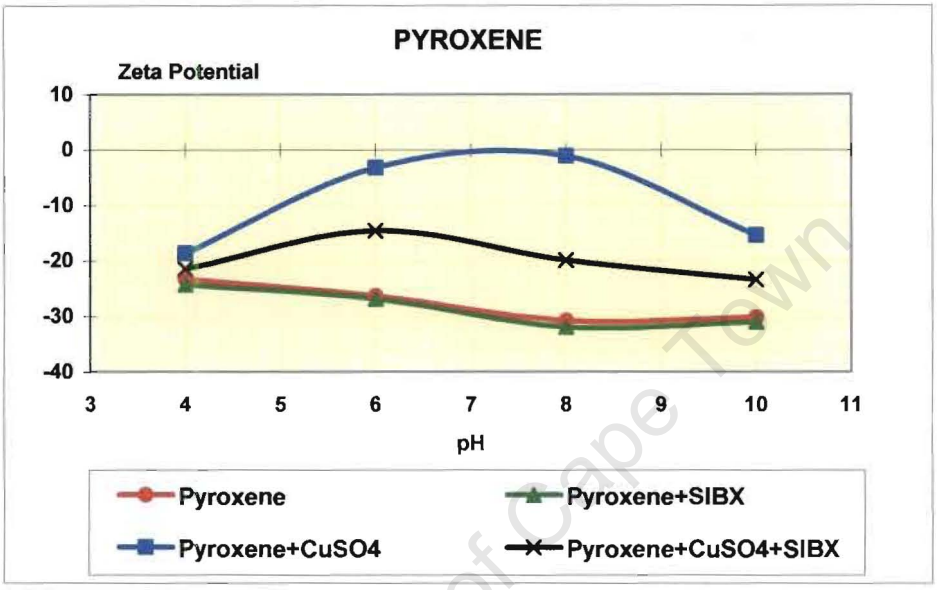

Figure 4.4: Zeta Potential of Pyroxene in $Na_2B_4O_7$ at 10^{-3}M, I = 3 x 10^{-3}, All reagent concentrations were 5 x 10^{-5} M

In the presence of SIBX, the zeta potential values are not significantly altered compared with those obtained without SIBX and thus it is concluded that xanthate ions do not adsorb onto the surface of pyroxene.

As observed for pentlandite, in the presence of copper (II) ions the zeta potential shifted to more positive values clearly demonstrating adsorption of positively charged copper species, as discussed for pentlandite, onto the pyroxene surfaces. In the presence of copper (II) ions subsequent introduction of xanthate ions shifted the zeta potential versus pH curve to more negative values, indicating that adsorption of xanthate ions onto the copper-activated pyroxene surfaces occurred. The interactions between copper species and xanthate are described in Section 5.1.

4.1.1.4 Feldspar

Figure 4.5 shows the zeta potentials for feldspar at various pH values, indicating that feldspar has a pH_{iep} (isoelectric point pH) of about 4. A pH of 2 is usually reported in the literature (Fuerstenau and Fuerstenau, 1982). The higher iep obtained could probably be attributed to the iron ions on the mineral surfaces, which originated from the mineral itself. A similar trend, in terms of the higher iep due to the iron impurities on the feldspar surfaces, was observed by Hudiburgh and Clifford (1976).

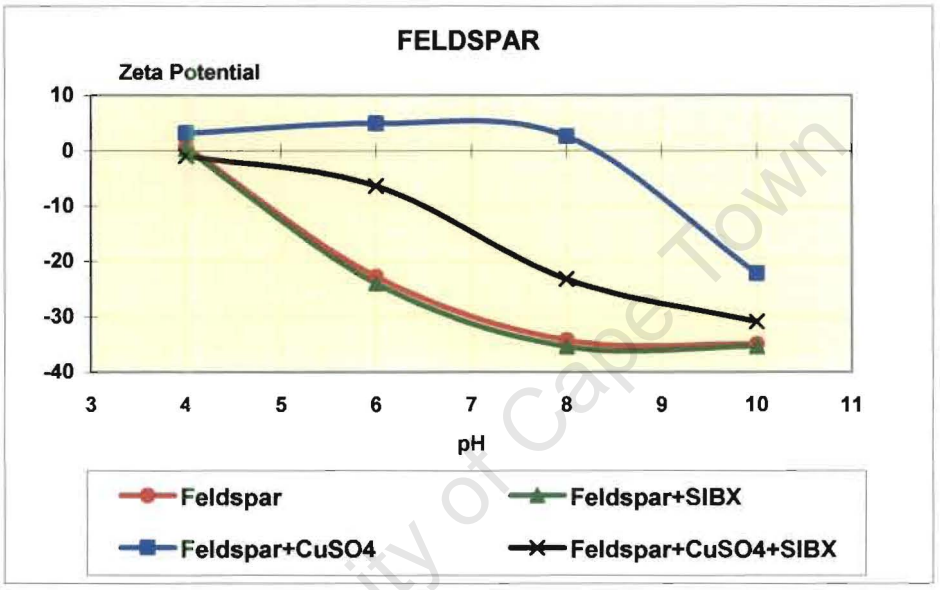

Figure 4.5: Zeta Potential of Feldspar in $Na_2B_4O_7$ at 10^{-3}M, I = 3 x 10^{-3}, All reagent concentrations were 5 x 10^{-5} M

When xanthate ions are added to the feldspar sample no adsorption is seen on the mineral surface. This has also been observed fro pyroxene. The zeta potential experiments revealed that unlike xanthate, copper (II) activation is non-selective. Silicate and sulphide minerals became more positively charged above pH 4 in the presence of copper (II) ions and subsequently xanthate ions adsorbed onto the copper (II) activated sulphide and silicate mineral surfaces (Section 5.1).

4.1.2 Microflotation Tests

Microflotation tests were carried out at pH 4 and pH 9 for all minerals studied with the aim of linking the trends observed from zeta potential determinations to floatability. In particular, the possible effect of subsequent adsorption of xanthate ions on copper (II) activated pentlandite, pyroxene and feldspar surfaces was investigated in terms of flotation response. To evaluate the contribution from entrainment and natural floatability, flotation tests were conducted without any reagent addition. In general, entrainment did not contribute significantly to the total recovery of the minerals studied.

4.1.2.1 Reproducibility

The objective of the reproducibility tests was to determine the reliability of the microflotation apparatus and the flotation procedure.

In order to establish the reproducibility and standard deviation, microflotation tests were conducted in quadruplicate at pH 9 on a sample of pentlandite. During the tests, xanthate was added at the concentration of 5 x 10^{-5}M. Concentrates were collected at time intervals of 2, 5, 10 and 20 minutes. The pentlandite recovery-time curves obtained from the four tests are plotted in Figure 4.6. The recoveries and standard deviation for the total concentrate collected over a period of 20 minutes are given in Table 4.2.

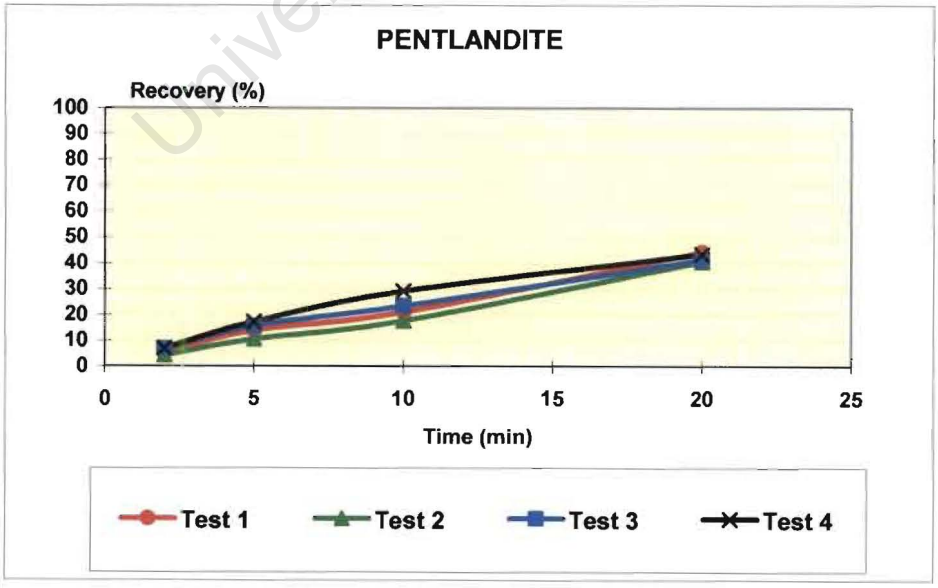

Figure 4.6: Microflotation Reproducibility (Single Mineral) in $Na_2B_4O_7$ at 10^{-3}M, I = 3 x 10^{-3}

Table 4.2: Pentlandite Recovery and Standard Deviation

Time [min]	Recovery [%]					Std Dev	Rel Std Dev [%]
	Test 1	Test 2	Test 3	Test 4	Mean		
20	44.3	40.6	41.1	43.4	42.4	1.8	4.2

The pentlandite recovery-time curves and the low standard deviation confirmed that reproducible results could be obtained using the microflotation apparatus and the flotation procedure.

4.1.2.2 Pentlandite

The pentlandite microflotation data summarised in Figure 4.7 showed that collectorless flotation, i.e. flotation in the absence of collector as a result of mild oxidation of the mineral itself, was low at pH 9 compared to pH 4. In the presence of xanthate ions, the recovery increased as expected, noticeably more for pH 9. The addition of copper sulphate and subsequent introduction of xanthate collector increased the recovery to 90% and 70% for pH 9 and 4, respectively. When copper sulphate was added after the SIBX addition the recoveries were virtually identical to those obtained using only SIBX thus indicating that copper sulphate was not able to induce desorption of xanthate.

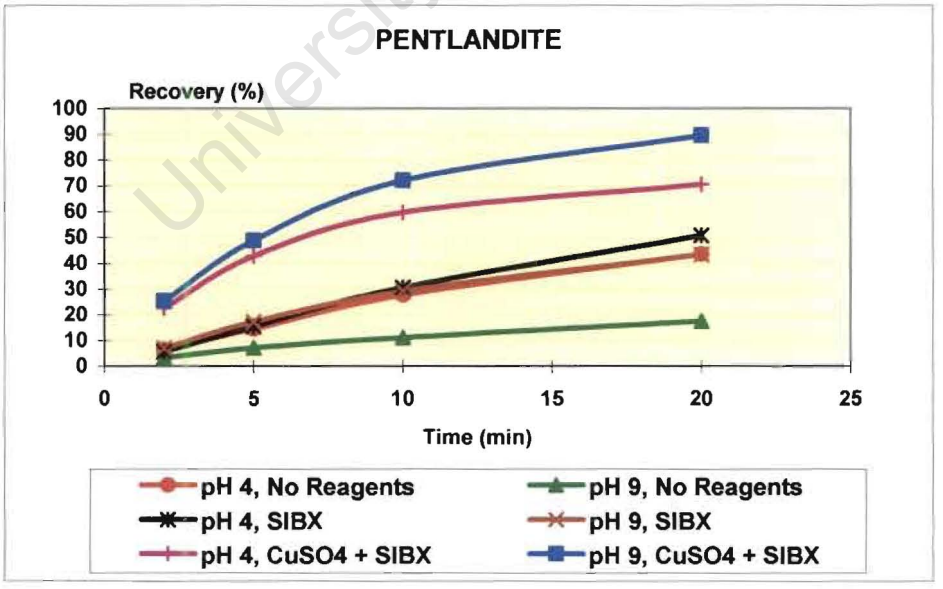

Figure 4.7: Pentlandite Recovery in $Na_2B_4O_7$ at 10^{-3}M, I = 3 x 10^{-3}, All reagent concentrations were 5 x 10^{-5} M

4.1.2.3 Pyroxene

The pyroxene recovery-time curves obtained are plotted in Figure 4.8. As zeta potential determinations suggested, the pyroxene flotation recoveries were not enhanced in the presence of xanthate ions compared to those without the collector added for both pHs studied. It would appear that for the conditions given above, the pyroxene floatability is not affected by the pHs tested. In addition, the results showed that in the presence of copper (II) ions on pyroxene surfaces the subsequent adsorption of xanthate ions caused pyroxene to float. The increase in floatability is more significant at pH 9 compared to pH 4. The possible cause of this observation is explained in Section 5.1 by means of the copper speciation diagram and interactions between various copper species and xanthate.

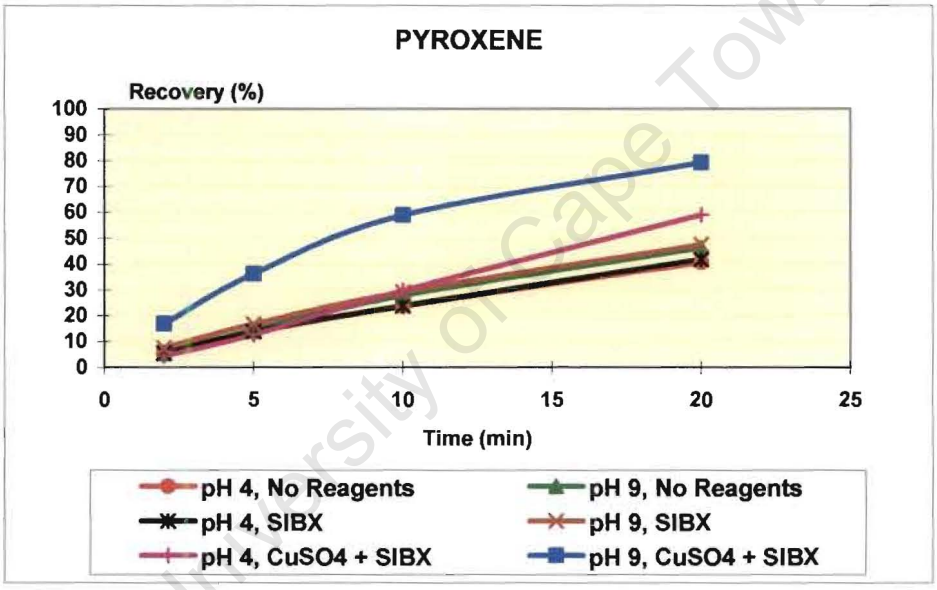

Figure 4.8: Pyroxene Recovery in $Na_2B_4O_7$ at 10^{-3}M, I = 3 x 10^{-3}, All reagent concentrations were 5 x 10^{-5} M

4.1.2.4 Feldspar

The feldspar results presented in Figure 4.9 showed that feldspar floatability is low compared to that observed on pyroxene (Figure 4.8) for all scenarios investigated. Xanthate on its own did not affect the floatability of feldspar at the pHs studied. A higher recovery of feldspar was only observed in the presence of copper and xanthate ions at pH 9, probably due to Cu (I) and/or Cu (II)-xanthate precipitants (Section 5.1).

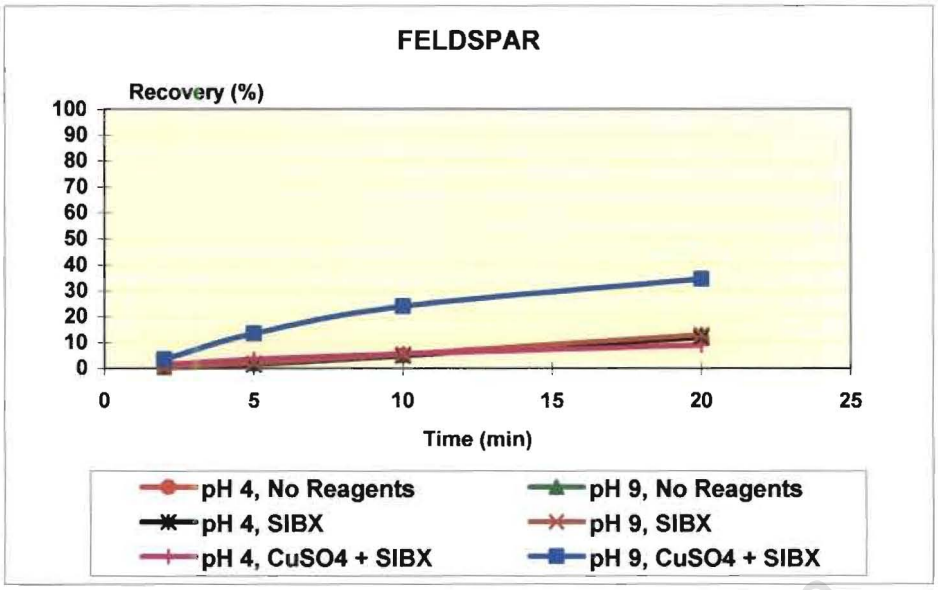

Figure 4.9: Feldspar Recovery in $Na_2B_4O_7$ at 10^{-3}M, I = 3 x 10^{-3}, All reagent concentrations were 5 x 10^{-5} M

4.1.3 ToF-SIMS Analyses

The mineral surfaces were studied using ToF-SIMS with the objective of investigating the mineral surface alteration in the presence of copper sulphate at pH 4 and pH 9. The supernatant solutions for each condition were also analysed using Inductively Coupled Plasma (ICP) Spectroscopy.

4.1.3.1 Pentlandite

Relative % abundance of nickel and iron ions at pH 4 and pH 9 without copper sulphate addition is displayed in Figure 4.10.

The data showed a higher pentlandite surface coverage of nickel ions at pH 9 compared to pH 4. Iron ions followed the opposite trend. The corresponding supernatant analysis (Figure 4.11) could explain this observation. The analysis indicates no presence of iron and nickel ions in solution at pH 9 due to low solubilities of the hydroxides. The pentlandite dissolution at pH 4 involved mostly the migration of nickel ions from pentlandite into solution. Thus the nickel ion surface concentration was lower at pH 4 compared to that at pH 9, while iron ion dissolution was very low for both pHs studied. The high surface charge

on pentlandite at pH 4 observed during the zeta potential experiments (Figure 4.3) could be attributed to the positively charged iron species.

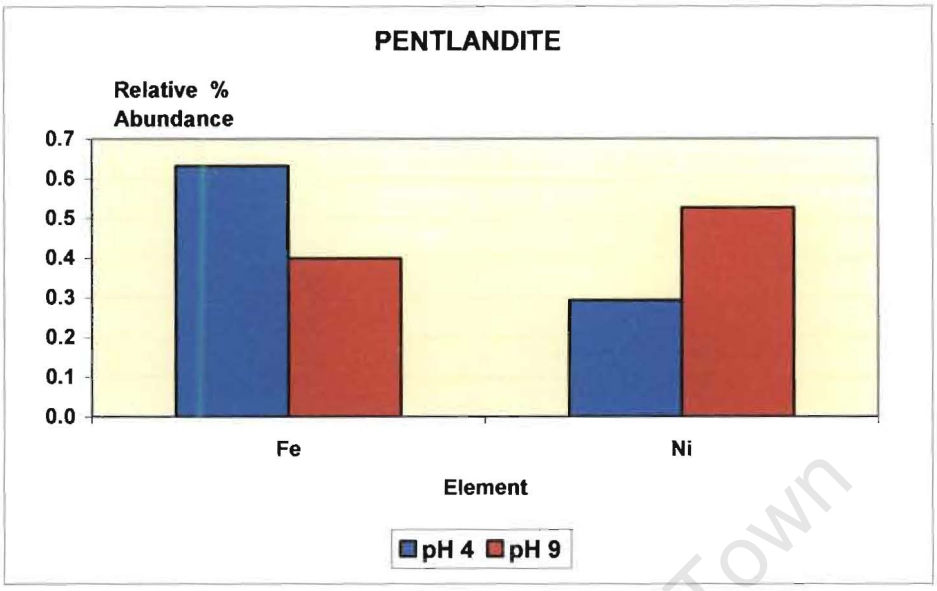

Figure 4.10: Relative % Abundance of Ni and Fe Ions on Pentlandite Surfaces without Copper Sulphate Addition

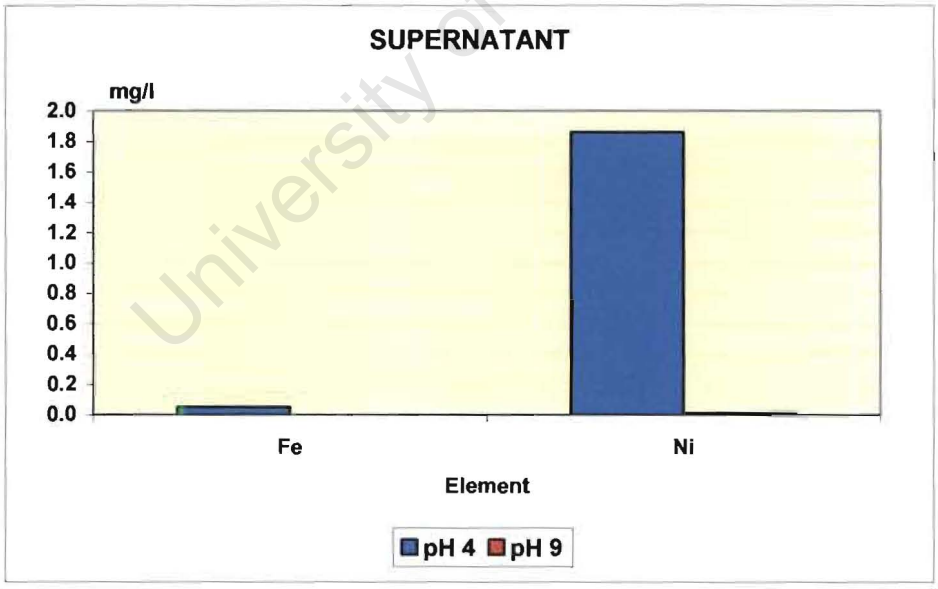

Figure 4.11: Supernatant Analysis for Pentlandite without Copper Sulphate Addition

In the presence of copper sulphate (Figure 4.12), a higher surface coverage of copper species on pentlandite was observed at pH 9 compared to pH 4, which is probably due to the precipitation of copper hydroxide species at the higher pH, as seen from the copper

speciation diagram (Section 5.1). The copper hydroxide thus reduced the surface coverage of iron ions and especially that of nickel ions at pH 9. The supernatant analysis (Figure 4.13) showed that copper ions stayed in solution at pH 4. In addition, the analysis showed that at pH 4, the dissolution of Ni ions from pentlandite was reduced with copper sulphate addition.

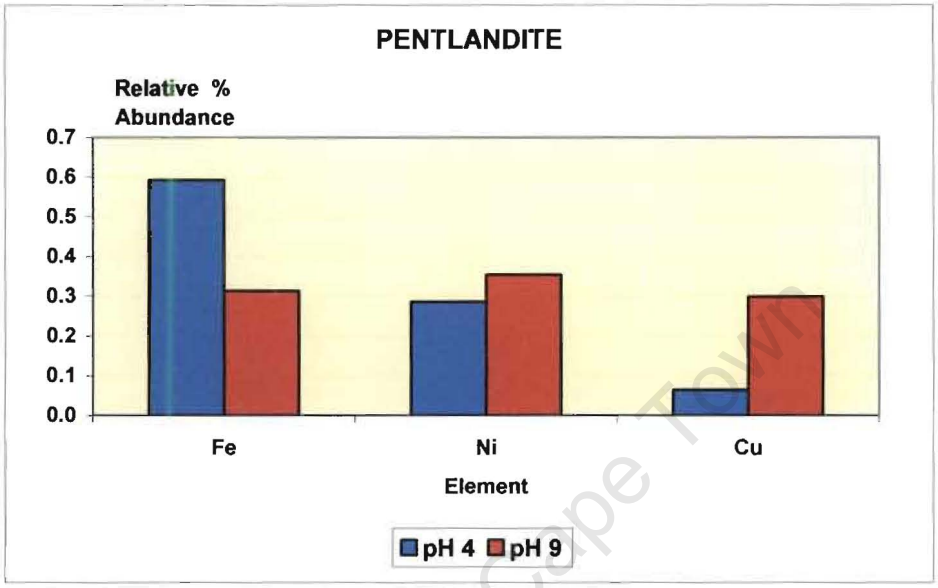

Figure 4.12: Relative % Abundance of Ni and Fe Ions on Pentlandite Surfaces with Copper Sulphate Addition

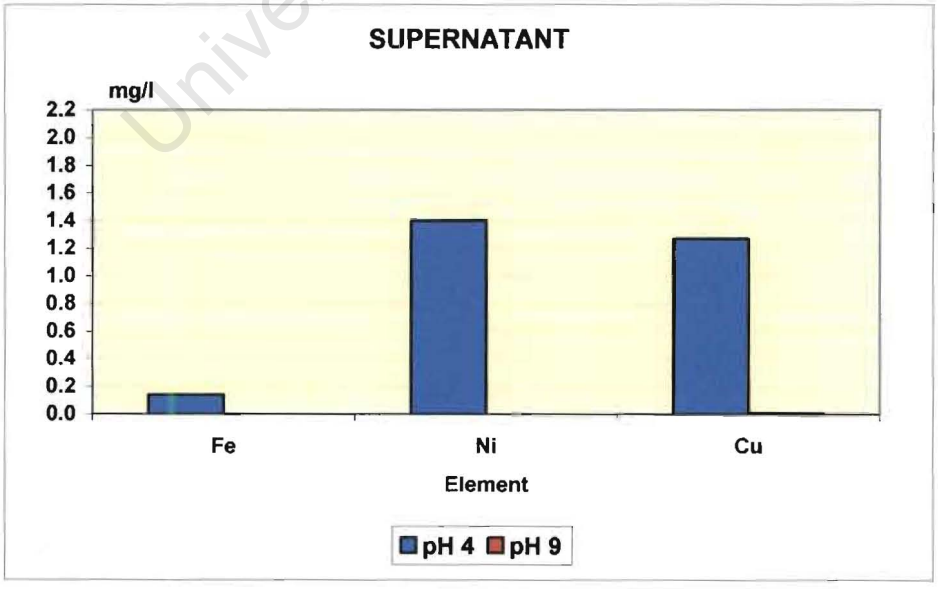

Figure 4.13: Supernatant Analysis for Pentlandite with Copper Sulphate Addition

4.1.3.2 Pyroxene

Pyroxene surface analyses with no copper (II) ions added and corresponding supernatant analyses are given in Figures 4.14 and 4.15, respectively.

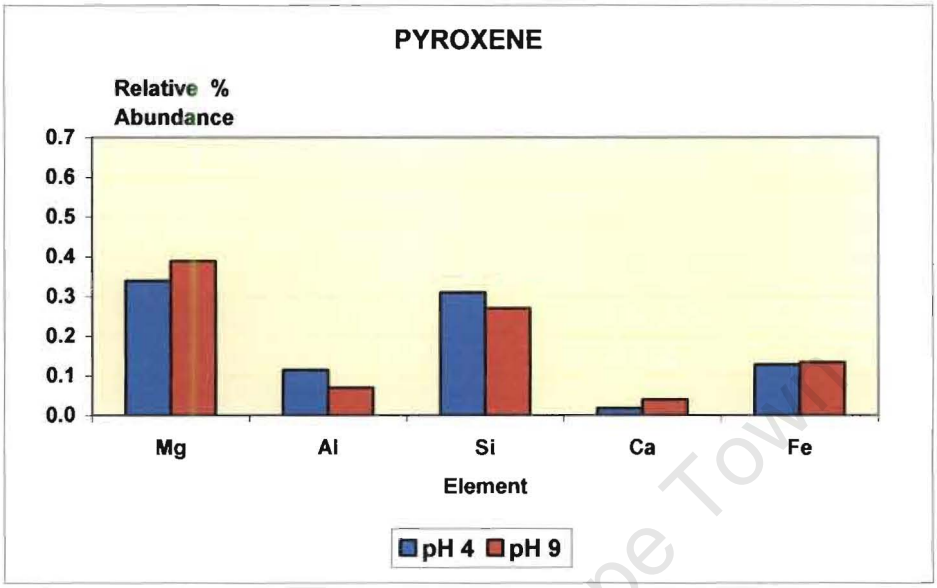

Figure 4.14: Relative % Abundance of Mg, Al, Si, Ca and Fe Ions on Pyroxene Surfaces without Copper Sulphate Addition

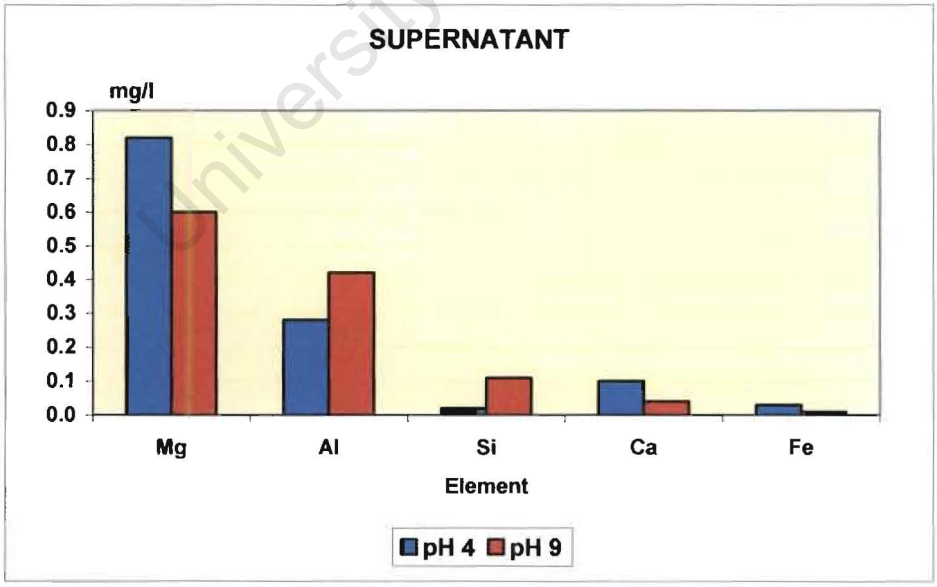

Figure 4.15: Supernatant Analysis for Pyroxene without Copper Sulphate Addition

The ToF-SIMS analyses revealed that the pyroxene surfaces mainly consist of magnesium and silicon ions at both pHs studied, despite the twice as high bulk concentration of silicon ions compared to magnesium ions (Table 3.1). Magnesium ion concentration was slightly higher at pH 9 compared to pH 4. Silicon ions followed the opposite trend. The supernatant analyses confirmed the ToF-SIMS data in terms of mineral surface alteration at the pHs tested. Aluminium ions appeared to dissolve readily.

The addition of copper sulphate resulted in adsorption and/or precipitation of copper ions (Section 5.1) onto the pyroxene surfaces, predominantly at pH 9 (Figure 4.16). Magnesium, silicon and iron ion concentrations are reduced in the presence of copper sulphate at pH 9. Magnesium and iron ion surface coverage was lower at pH 9 compared to pH 4, which is the opposite trend to that observed for pyroxene surfaces without copper sulphate addition.

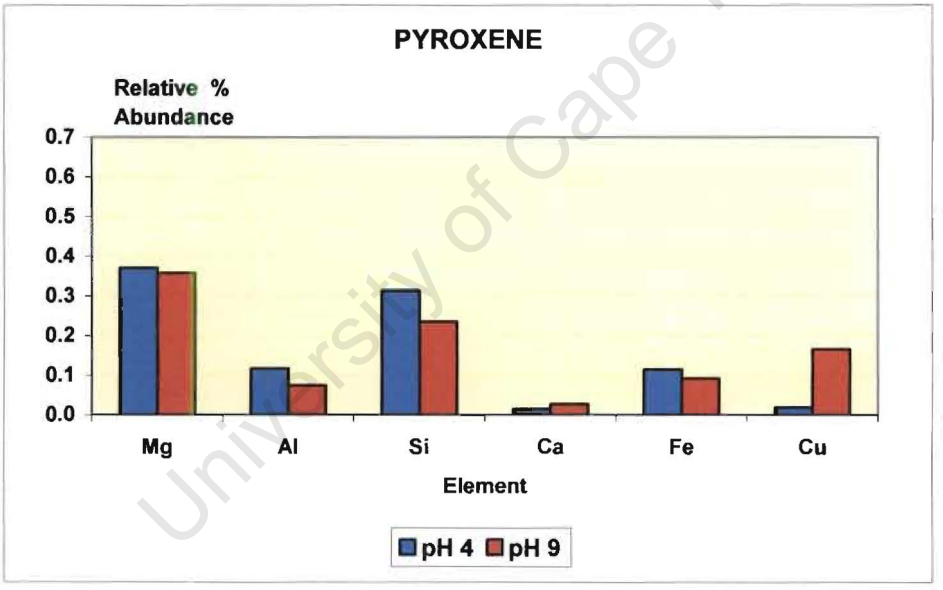

Figure 4.16: Relative % Abundance of Mg, Al, Si, Ca and Fe Ions on Pyroxene Surfaces with Copper Sulphate Addition

The supernatant analyses (Figure 4.17) showed very low adsorption of copper (II) ions onto the pyroxene surfaces at pH 4. Comparison between Figure 4.14 and Figure 4.16 suggests that the dissolution of magnesium ions at pH 9 and aluminium ions at both pHs was lessened in the presence of copper sulphate.

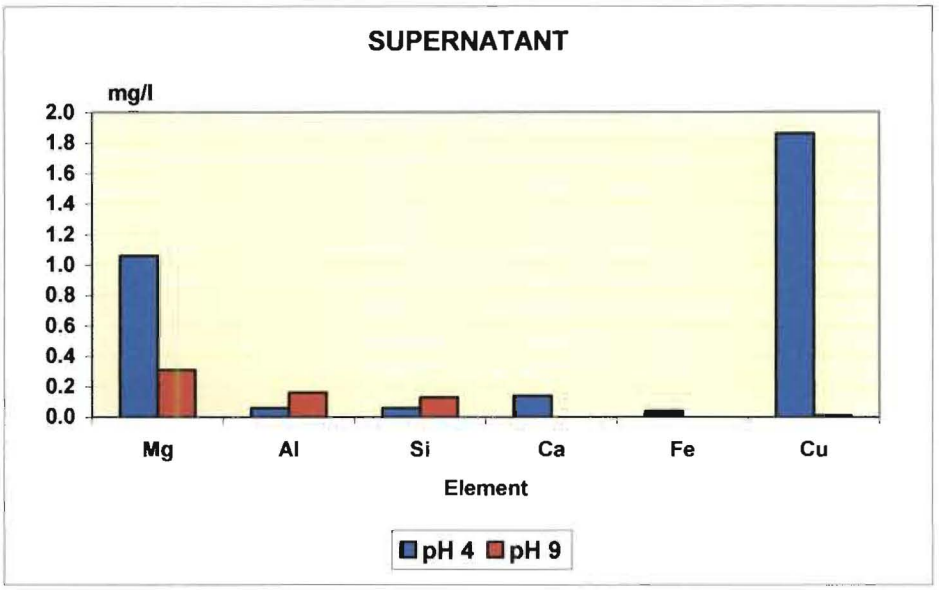

Figure 4.17: Supernatant Analysis for Pyroxene with Copper Sulphate Addition

4.1.3.3 Feldspar

As depicted in Figure 4.18, a higher concentration of aluminium ions was observed on feldspar surfaces at pH 4 compared to pH 9.

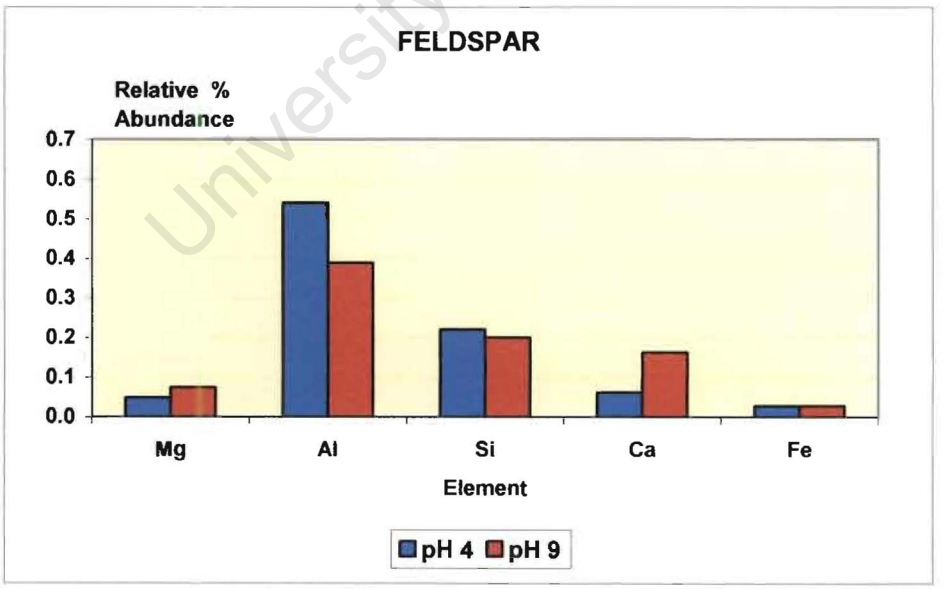

Figure 4.18: Relative % Abundance of Mg, Al, Si, Ca and Fe Ions on Feldspar Surfaces without Copper Sulphate Addition

The high surface concentration of aluminium ions at pH 4 could be attributed to the adsorption of Al^{3+} ions, which originated form the mineral itself, between pH 3.9 and 4.8 (Tranter and Raiswell, 1986).

The supernatant analyses (Figure 4.19) revealed high dissolution of aluminium ions at pH 9 and calcium ions at pH 4.

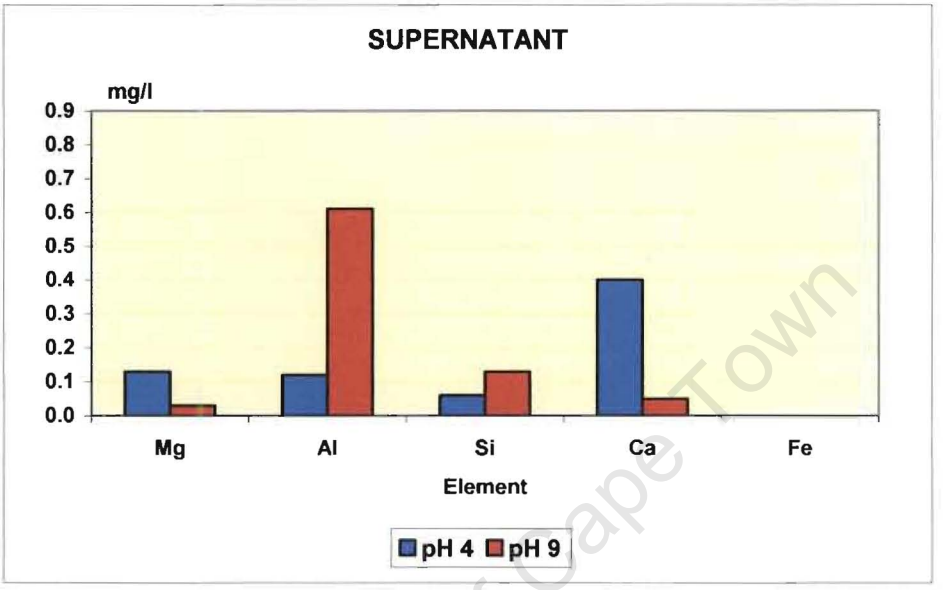

Figure 4.19: Supernatant Analysis for Feldspar without Copper Sulphate Addition

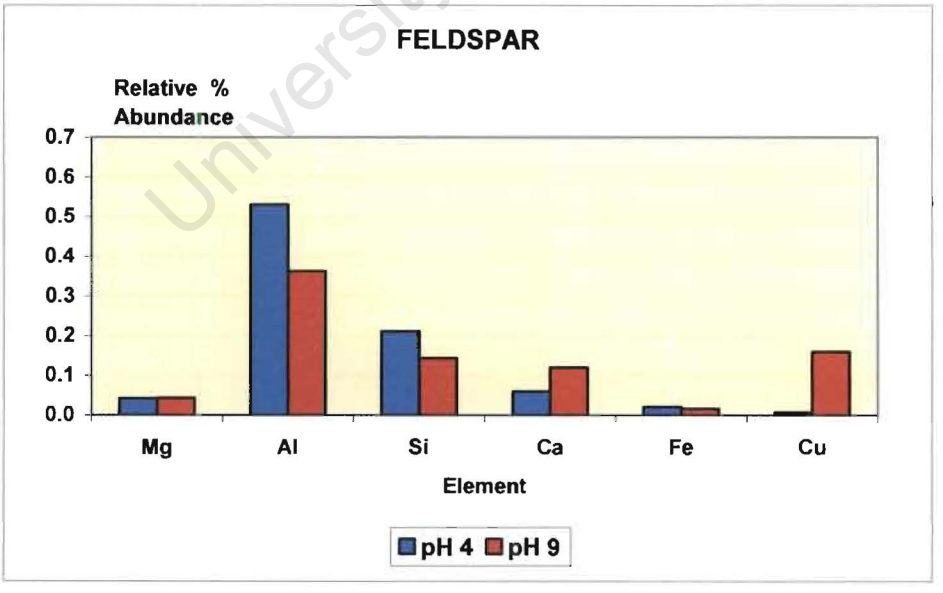

Figure 4.20: Relative % Abundance of Mg, Al, Si, Ca and Fe Ions on Feldspar Surfaces with Copper Sulphate Addition

As observed above for pentlandite and pyroxene, ToF-SIMS analyses also confirmed adsorption and/or precipitation of copper (II) ions onto the feldspar surfaces at pH 9 (Figure 4.20). Copper sulphate addition reduced the dissolution of aluminium ions at pH 9 and increased migration of calcium ions from feldspar surfaces into the solution at pH 4 (Figure 4.21).

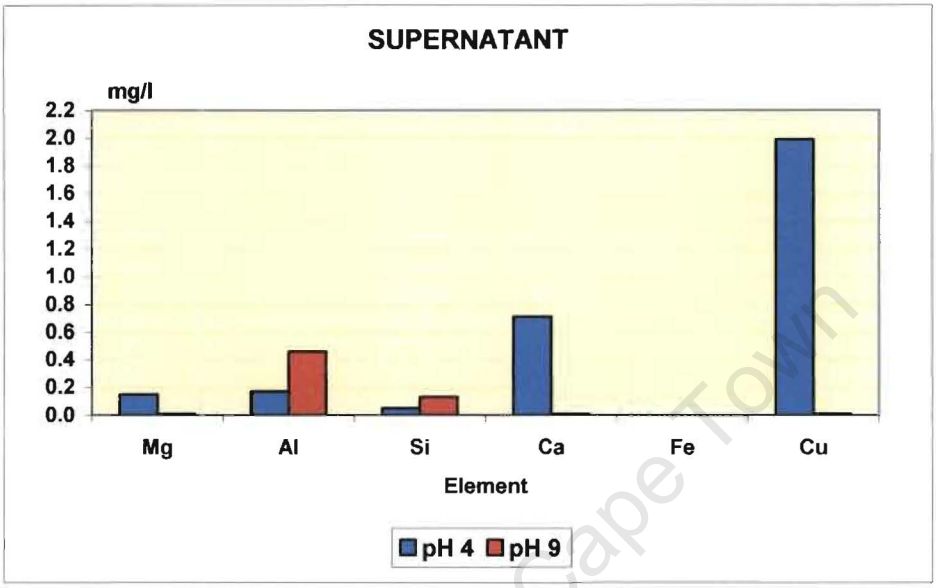

Figure 4.21: Supernatant Analysis for Feldspar with Copper Sulphate Addition

4.2 Mineral Mixture Study in Di-sodium Tetraborate Solution

Microflotation tests were carried out on mineral mixtures at pH 4 and pH 9 in order to determine possible interactions between the minerals and the reagent distribution on their surfaces.

4.2.1 Microflotation Tests

4.2.1.1 Reproducibility

The aim of the reproducibility tests was to determine the reliability of the procedure used during flotation of a 1:1 mineral mixture (pentlandite-pyroxene or pentlandite-feldspar) as well as the consistency of sulphur analysis carried out by a LECO analyser.

In order to determine the reproducibility, microflotation tests were carried out in triplicate on a 1:1 pentlandite-pyroxene mixture at pH 9 in the presence of xanthate (5 x 10^{-5}M). Concentrates were collected at time intervals of 3 and 20 minutes. The pentlandite and corresponding pyroxene recoveries and standard deviations for the total concentrate collected over a period of 20 minutes are given in Tables 4.3 and 4.4, respectively. The recovery-time curves for pentlandite and pyroxene are shown in Figure 4.22.

Table 4.3: Pentlandite Recovery and Standard Deviation for Pentlandite-Pyroxene Mixture

Time [min]	Pentlandite Recovery [%]				Std Dev	Rel Std Dev [%]
	Test 1	Test 2	Test 3	Mean		
20	51.1	56.8	54.2	54.0	2.9	5.3

Table 4.4: Pyroxene Recovery and Standard Deviation for Pentlandite-Pyroxene Mixture

Time [min]	Pyroxene Recovery [%]				Std Dev	Rel Std Dev [%]
	Test 1	Test 2	Test 3	Mean		
20	21.4	19.7	21.1	20.7	0.9	4.3

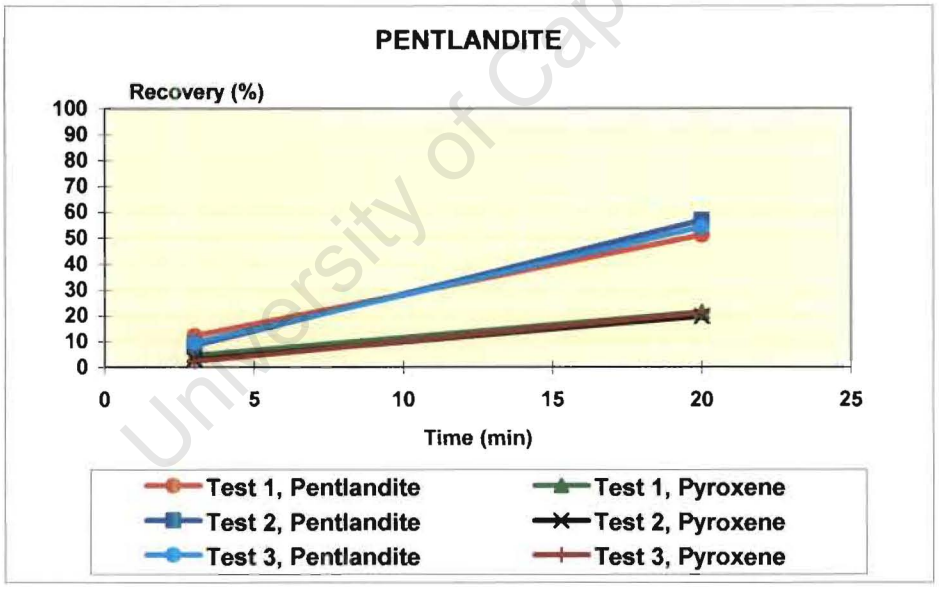

Figure 4.22: Microflotation Reproducibility (Minerals Mixture) in $Na_2B_4O_7$ at 10^{-3}M, I = 3 x 10^{-3}

The pentlandite and pyroxene recovery-time curves and the low standard deviations showed that reproducible results could be obtained using the flotation procedure and LECO sulphur analyses.

4.2.1.2 Pentlandite-Pyroxene Mixture

The microflotation data obtained on a 1:1 pentlandite-pyroxene mixture at pH 4 and pH 9 are shown in Figures 4.23 and 4.24 for pentlandite and pyroxene, respectively. During these tests, the SIBX and $CuSO_4$ concentrations were 5 x 10^{-5}M.

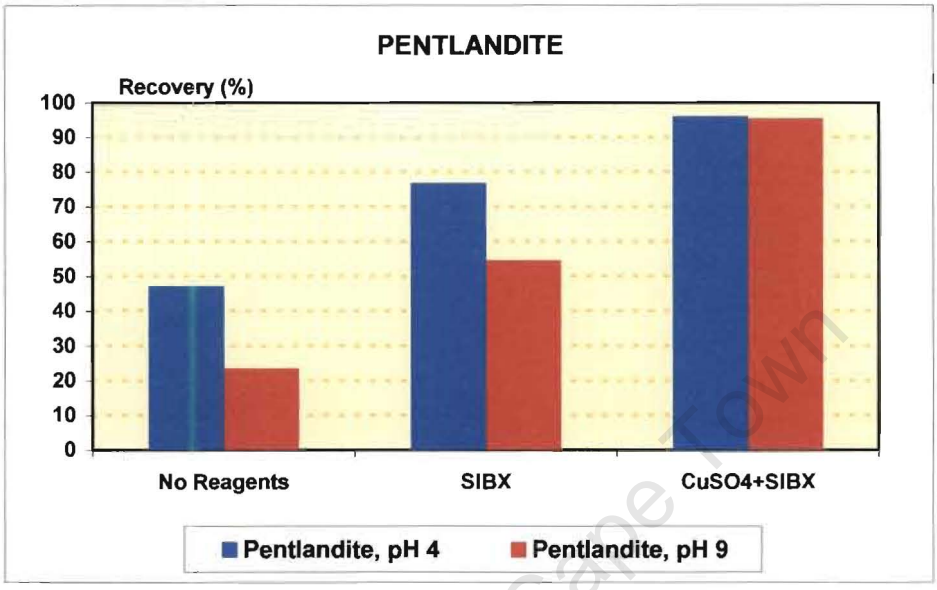

Figure 4.23: Pentlandite (in 1:1 Mixture with Pyroxene) Total Recovery in $Na_2B_4O_7$ at 10^{-3}M, I = 3 x 10^{-3}

Pentlandite collectorless floatability in mixture with pyroxene was low at pH 9 and could mostly be attributed to entrainment. This was also observed during the single minerals study. At pH 4, the mineral floated well without any reagent added, probably due to the removal by dissolution of oxide and hydroxide overlayers at acidic pH (Buckley and Woods, 1991). Pentlandite recovery was significantly enhanced in the presence of xanthate ions and even more in the presence of copper sulphate and xanthate. Zeta potential determinations suggested that copper (II) ions do not adsorb onto the mineral surfaces at pH 4 to the same extent as observed at pH 9. Nevertheless, the copper (II) ions surface coverage was sufficient to enhance pentlandite floatability at pH 4. It is, however, noteworthy that the pentlandite recoveries were slightly higher if the mineral was floated in mixture with pyroxene.

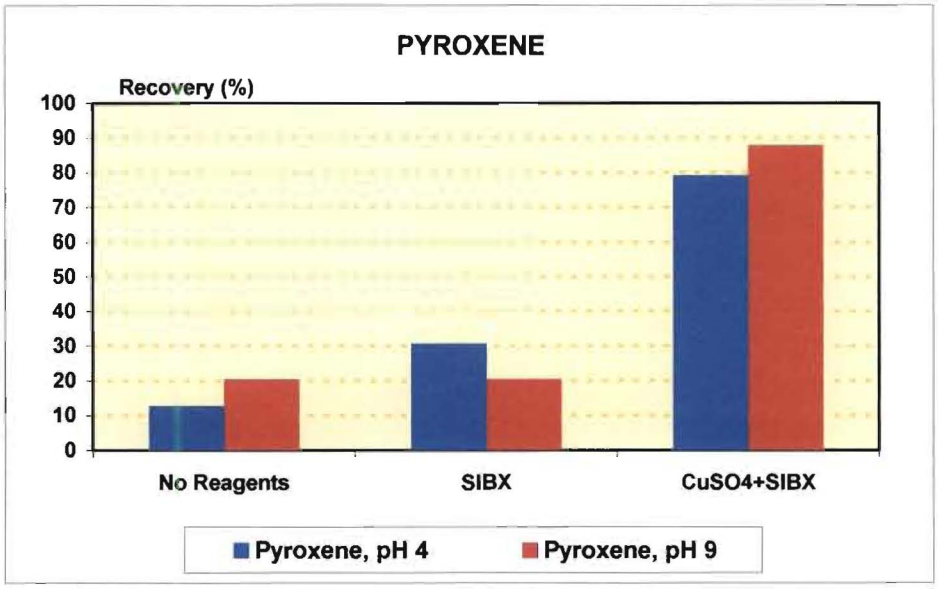

Figure 4.24: Pyroxene (in 1: 1 Mixture with Pentlandite) Total Recovery in $Na_2B_4O_7$ at 10^{-3}M, I = 3 x 10^{-3}

As seen in Figure 4.24, the pyroxene recovery was also significantly enhanced in the presence of copper sulphate followed by the addition of xanthate at the pHs tested. Xanthate on its own did not affect the pyroxene floatability at pH 9. To compare the single mineral pyroxene study, the recoveries without any reagent added and with xanthate were lower when pyroxene was floated in mixture with pentlandite. However, in the presence of copper and xanthate ions the opposite trend was observed for both pHs. This higher pyroxene recovery observed in the presence of copper sulphate could be a result of non-selective aggregation between pentlandite and pyroxene due to $Cu(OH)_2$ precipitate.

4.2.1.3 Pentlandite-Feldspar Mixture

The pentlandite-feldspar mixture results presented in Figures 4.25 and 4.26 showed a similar trend for pentlandite as observed for the pentlandite-pyroxene mixture (Figure 4.23). In the case of feldspar (Figure 4.26), the recoveries obtained were lower for all scenarios investigated compared to those of feldspar on its own (Figure 4.9). As will be shown later, this could be attributed to the preferential adsorption of copper and xanthate ions onto the pentlandite surfaces (Figures 4.27 and 4.28). For the mineral mixture, a higher feldspar recovery was only achieved at pH 9 in the presence of copper (II) and xanthate ions, which is consistent with the single mineral feldspar study. It is interesting to

note that feldspar flotation at pH 4 was reduced with the copper sulphate and xanthate addition.

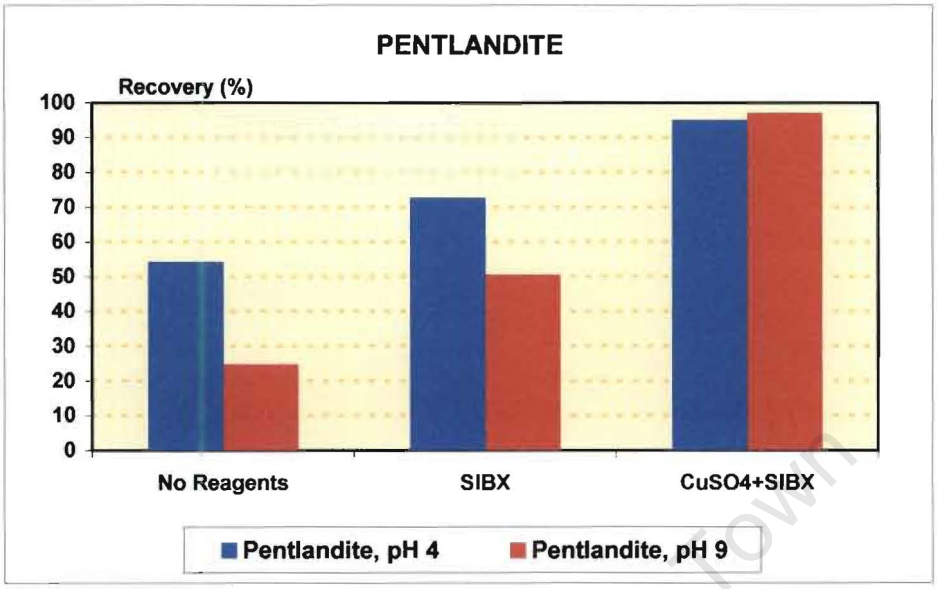

Figure 4.25: Pentlandite (in 1:1 Mixture with Feldspar) Total Recovery in $Na_2B_4O_7$ at 10^{-3}M, I = 3 x 10^{-3}

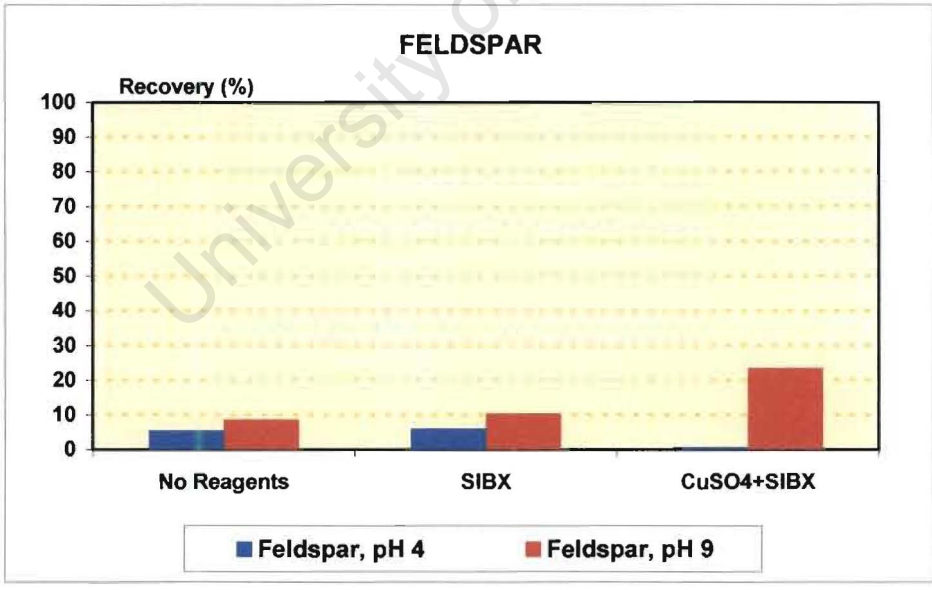

Figure 4.26: Feldspar (in 1:1 Mixture with Pentlandite) Total Recovery in $Na_2B_4O_7$ at 10^{-3}M, I = 3 x 10^{-3}

4.2.2 ToF-SIMS Analyses

ToF-SIMS analyses were carried out on the microflotation products of the tests conducted on the pentlandite-feldspar mixture at pH 9. The rationale for the selection was that a higher feldspar recovery was only obtained in the presence of copper sulphate and xanthate. The aim was to investigate and link the copper (II) and xanthate ion distribution on the mineral surfaces to floatability. Feldspar and pentlandite grains for ToF-SIMS analyses were separated by hand-picking from the first and second concentrate as well as tailings sample.

The comparison between Figures 4.27 and 4.28 reveals a significantly higher concentration of copper species on pentlandite compared to feldspar surfaces, indicating an increased affinity for the sulphide mineral studied. It would appear that the feldspar grains reporting to the concentrates had a higher copper concentration compared to those analysed in the tailings. In the case of pentlandite, copper coverage was the highest on the grains in the tailings. This could be attributed to the longer contact time of the grains with copper ions in solution and the redistribution of the copper ions on silicate and sulphide minerals with time.

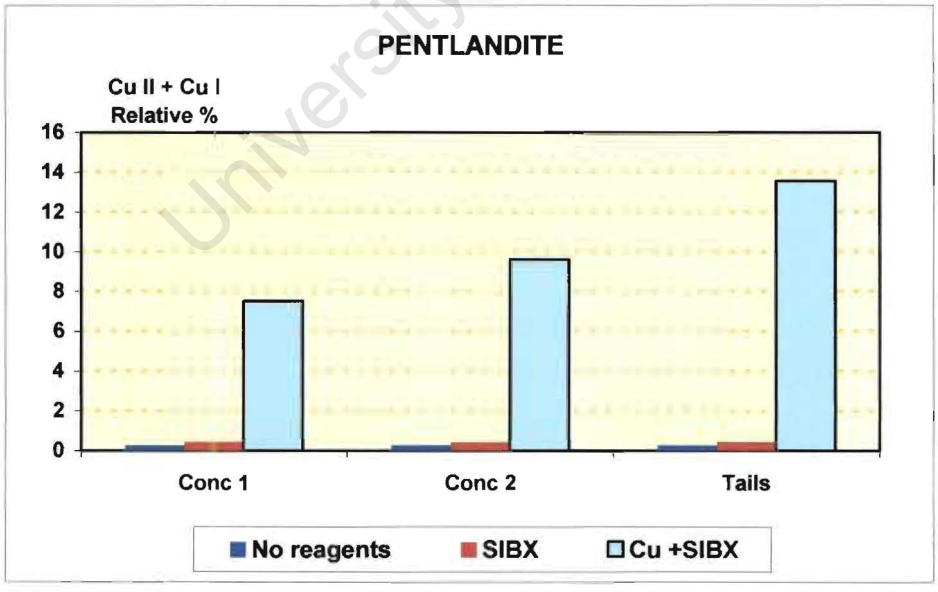

Figure 4.27: Relative Percent Abundance of Copper (II) Ions on Pentlandite Surfaces at pH 9

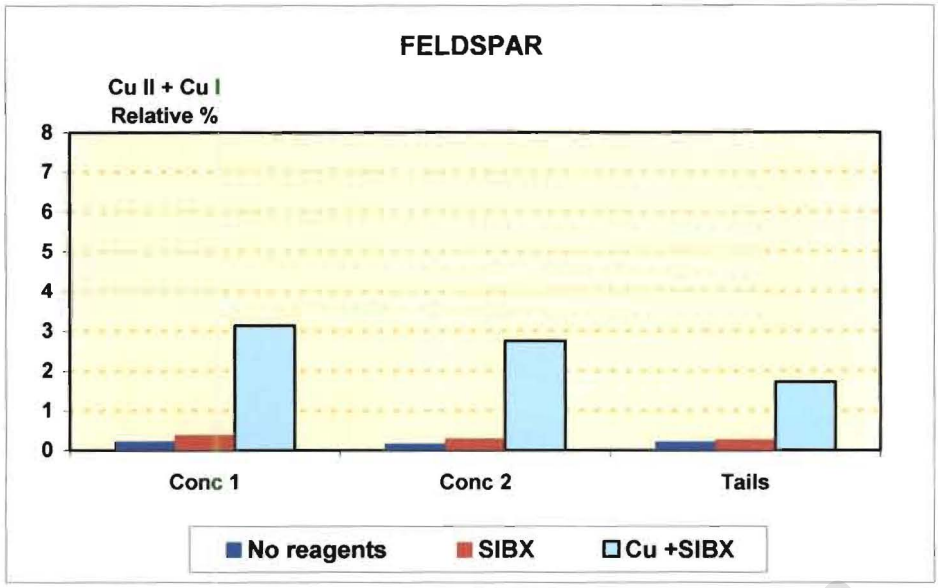

Figure 4.28: Relative Percent Abundance of Copper (II) Ions on Feldspar Surfaces at pH 9

The results presented in Figures 4.29 (pentlandite) and 4.30 (feldspar) clearly demonstrate that the presence of copper species increased the xanthate ion concentration on pentlandite as well as feldspar surfaces.

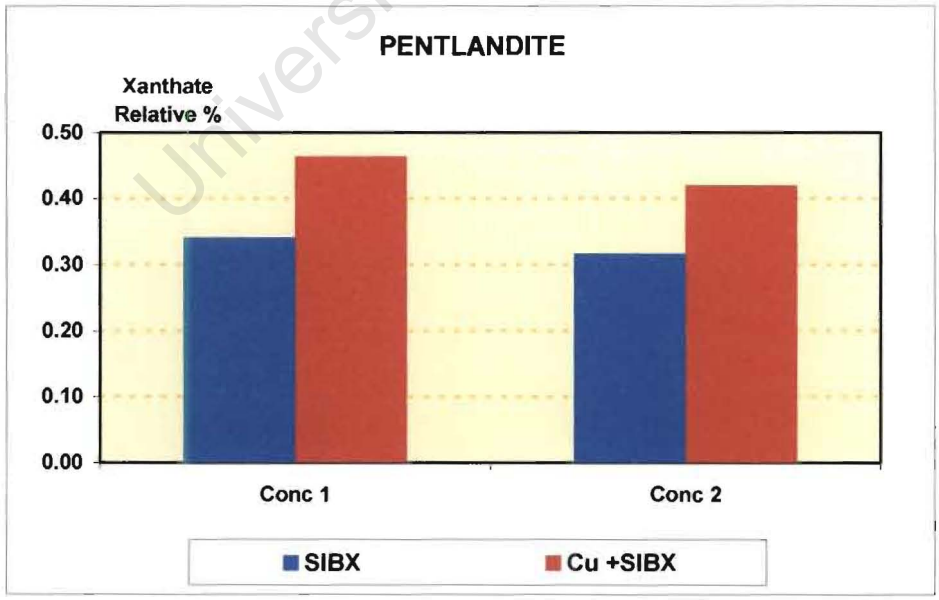

Figure 4.29: Relative Percent Abundance of Xanthate Ions on Pentlandite Surfaces at pH 9

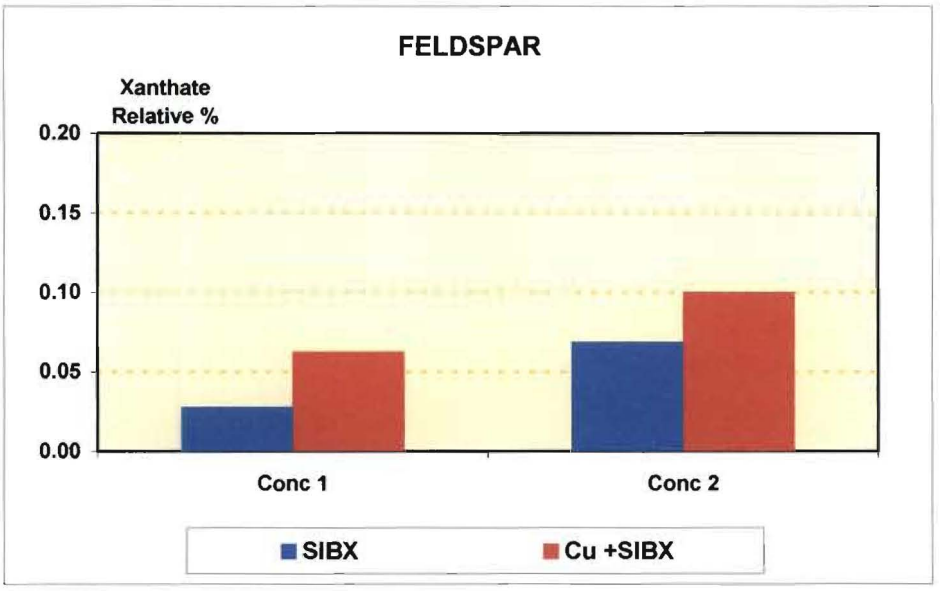

Figure 4.30: Relative Percent Abundance of Xanthate Ions on Feldspar Surfaces at pH 9

The ToF-SIMS analyses showed that the copper ion adsorption is non-selective. In the presence of copper ions the mineral surfaces become coated with copper species and subsequent addition and adsorption of xanthate ions was sufficient to cause true flotation of feldspar. Based on the pentlandite-feldspar ToF-SIMS results obtained, it can be proposed that subsequent adsorption of xanthate ions onto the copper (II) activated pyroxene surfaces enhanced pyroxene floatability in the presence of copper sulphate and xanthate (Figure 4.24). This is discussed further in Section 5.1.

4.3 Comparison of Flotation Response in Di-sodium Tetraborate Solution and Synthetic Water

In order to indirectly evaluate the effect that key ions, typically found in circuit water, have on surface alteration, microflotation tests were carried out using the pentlandite-pyroxene and pentlandite-feldspar mixtures. The aim was to determine if the ions present in process water would interfere with copper and xanthate ion adsorption and distribution on the mineral surfaces as well as establish if the trends observed in a simple electrolyte would be valid in a more complex pulp environment prevailing in an industrial flotation cell. The tests were carried out at pH 9, which is the process circuit pH.

4.3.1 Pentlandite-Pyroxene Mixture

The comparison of the microflotation data obtained in di-sodium tetraborate solution and synthetic water is displayed in Figures 4.31 and 4.32 for pentlandite and pyroxene, respectively.

As shown in the figures the pentlandite and pyroxene recoveries were depressed for all scenarios investigated when synthetic water was used during flotation. The most significant effect was observed in the presence of copper sulphate followed by xanthate addition.

During the experiments carried out in synthetic water, the mineral samples were suspended in synthetic water and then the required reagents were dosed. As will be shown later, the lower recovery in synthetic water could be attributed to the adsorption and/or precipitation of ions occurring in synthetic water onto the mineral surfaces. This topic is discussed further in Section 5.2.

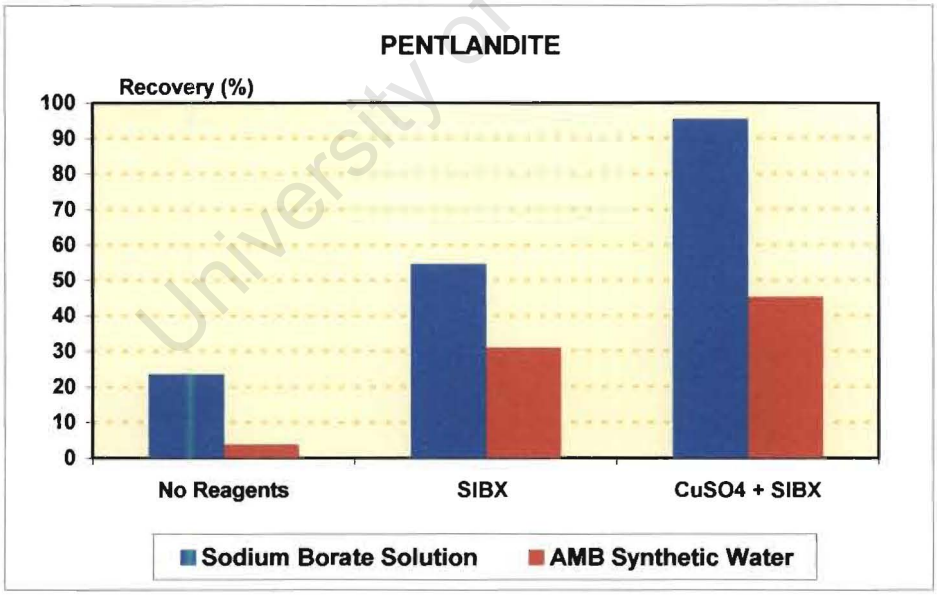

Figure 4.31: Pentlandite (in 1:1 Mixture with Pyroxene) Total Recovery in $Na_2B_4O_7$ at 10^{-3}M, I = 3 x 10^{-3} and Synthetic Water, I = 2 x 10^{-2}, at pH 9

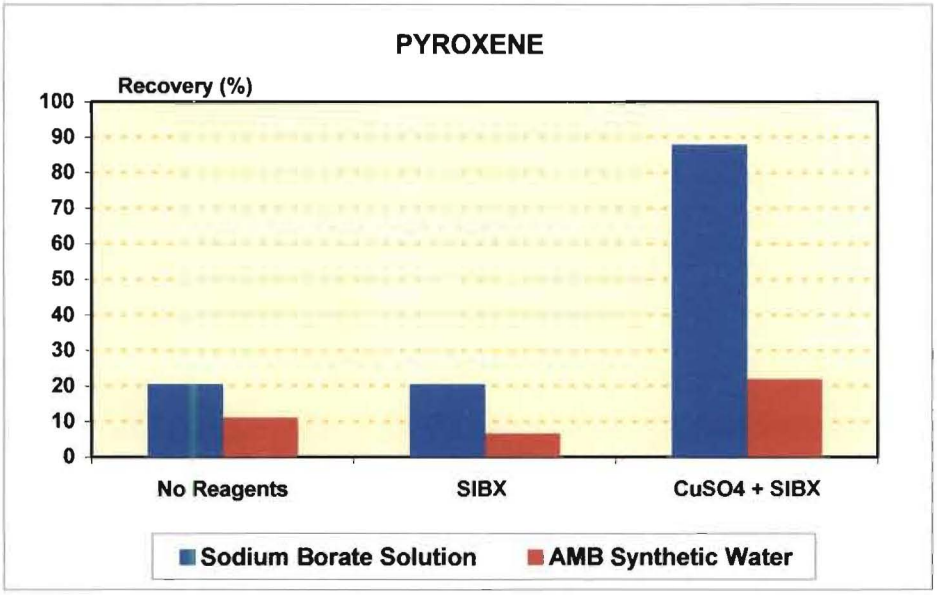

Figure 4.32: Pyroxene (in 1:1 Mixture with Pentlandite) Total Recovery in $Na_2B_4O_7$ at 10^{-3}M, I = 3 x 10^{-3} and Synthetic Water, I = 2 x 10^{-2} , at pH 9

Nevertheless, despite the significantly lower recoveries achieved, the trends obtained with xanthate as well as copper sulphate and xanthate addition, are in line with those observed in a simple electrolyte.

4.3.2 Pentlandite-Feldspar Mixture

The results achieved for the pentlandite-feldspar mixture (Figures 4.33 and 4.34) revealed very low feldspar recoveries (about 2%) in synthetic water for all conditions tested. The feldspar recovery remained low even in the presence of copper sulphate and xanthate in synthetic water. However, the pentlandite recovery for the pentlandite-feldspar mixture in synthetic water was higher in the presence of copper and xanthate ions compared to that in the mixture with pyroxene (Figure 4.31). This is attributed to the preferential adsorption of copper ions onto the pentlandite surfaces, when the pentlandite-feldspar mixture is floated. The different trend observed between pyroxene and feldspar in the presence of copper and xanthate ions also indicates that the copper (II) ions uptake by feldspar surfaces was more significantly reduced by the ions in synthetic water than for pyroxene. The different pyroxene and feldspar behaviour could probably be attributed to the different chemical composition of these siliceous minerals (Table 3.1). This is discussed further in Section 5.1.

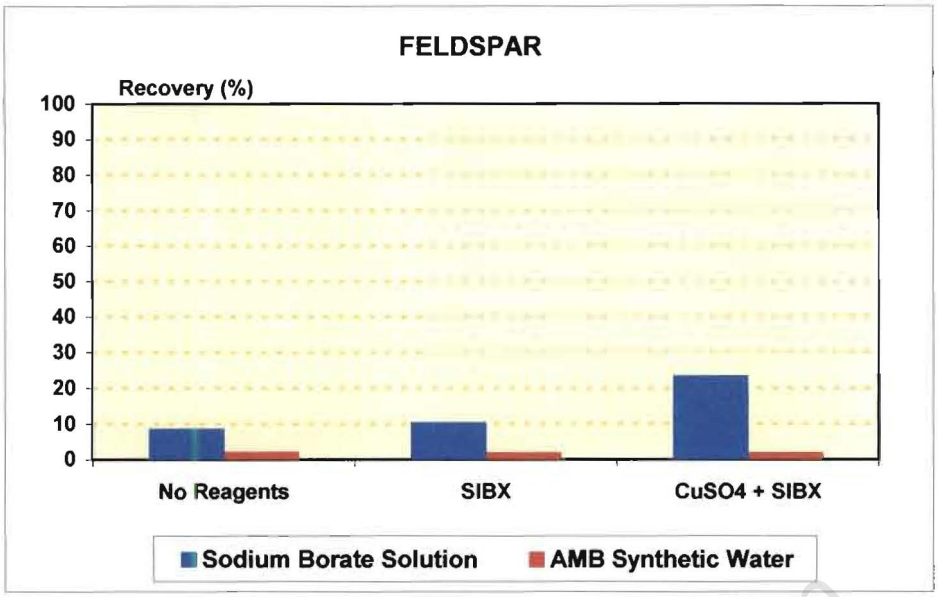

Figure 4.33: Feldspar (in 1:1 Mixture with Pentlandite) Total Recovery in $Na_2B_4O_7$ at 10^{-3}M, I = 3 x 10^{-3} and Synthetic Water, I = 2 x 10^{-2}, at pH 9

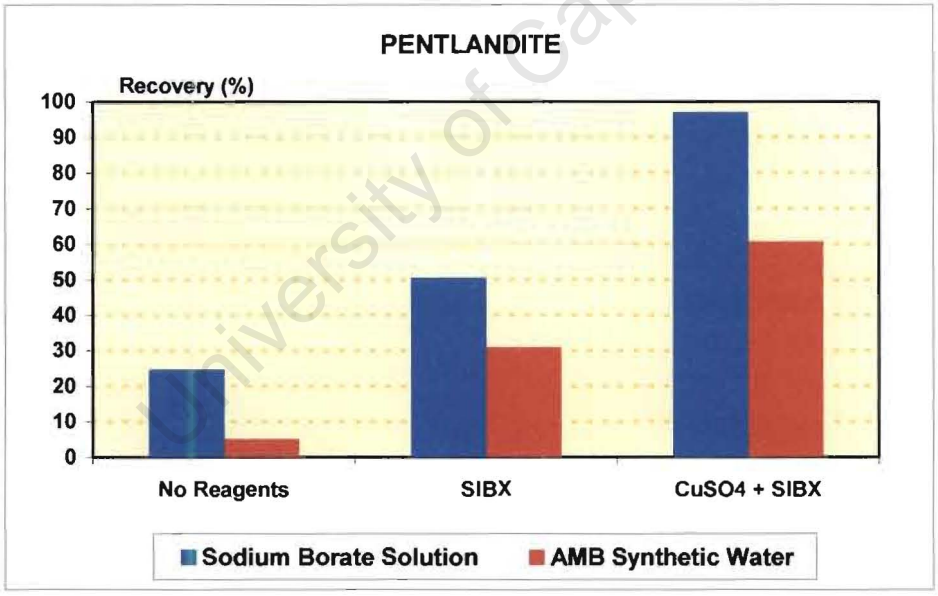

Figure 4.34: Pentlandite (in 1:1 Mixture with Feldspar) Total Recovery in $Na_2B_4O_7$ at 10^{-3}M, I = 3 x 10^{-3} and Synthetic Water, I = 2 x 10^{-2}, at pH 9

The results obtained indicate that the ions in synthetic water play a role not only in the degree of surface passivation and thus reduction in recoveries as observed for the pentlandite-pyroxene mixture but could also alter the trends in terms of floatability as

observed for the pentlandite-feldspar mixture, in di-sodium tetraborate solution (Figure 4.9) and synthetic water (Figure 4.33), in the presence of copper sulphate and xanthate. Therefore synthetic water rather then di-sodium tetraborate solution was selected for further tests in order to enable scaling up of the trends from a microflotation environment to a pulp condition in an industrial flotation cell at a concentrator.

4.4 Comparison of Pentlandite, Pyroxene and Feldspar Floatability in Synthetic Water

The results presented above for pH 9 showed that pentlandite, pyroxene and feldspar flotation recoveries were significantly depressed in synthetic water for all scenarios investigated. The highest pentlandite and pyroxene recoveries were obtained in the presence of copper (II) and xanthate ions. In terms of feldspar, the recovery seems to remain unchanged in synthetic water regardless of the reagent suite tested.

An attempt was made to increase the pentlandite recovery by adjusting the pH outside of the pH range where metal hydroxides are formed. It has been mentioned previously that Cu^{2+} ions as well as various positively charged copper hydroxide species ($CuOH^{+}$, $Cu_2(OH)_2^{2+}$) are predominant below pH 9.5. This can also be seen from the copper speciation diagram given in Section 5.1. As will be shown later, pH 6 also reduced the thickness of passivating metal oxide and hydroxide overlayers. The pH range outside of hydroxide precipitation would enhance the formation of copper-xanthate complexes (Wang et al, 1989c) and thereby increase hydrophobicity and ultimately the pentlandite recovery.

To confirm the above mentioned assumption, microflotation tests were performed at pH 6 in the presence of copper sulphate and xanthate. The preferred pH is pH 6 compared to pH 4 since in an operating circuit less acid would be consumed and corrosion of equipment would be reduced. For comparative purposes, the ultimate recoveries obtained and those previously given at pH 9 are plotted in Figure 4.35. The pentlandite recoveries displayed present the average recoveries for the pentlandite-pyroxene and pentlandite-feldspar mixtures.

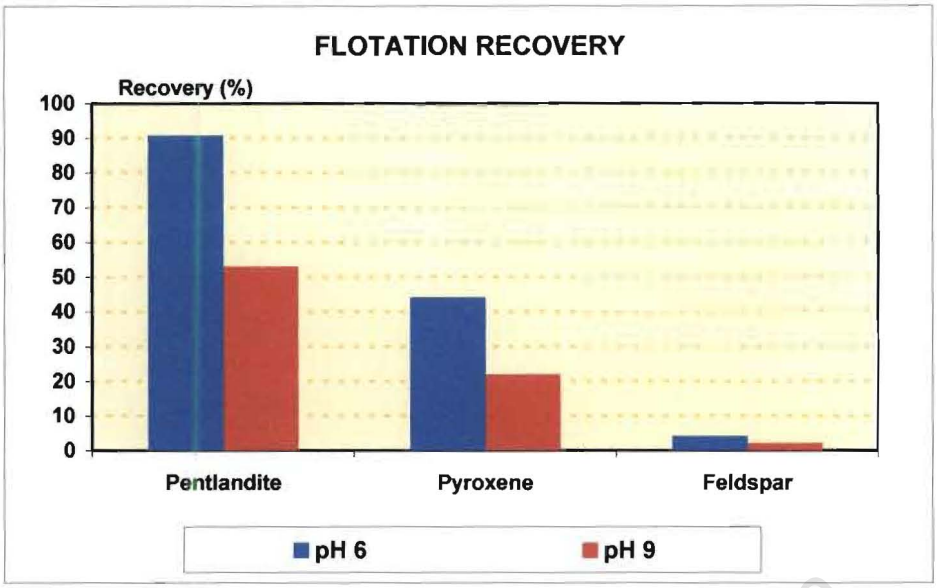

Figure 4.35: Total Pentlandite, Pyroxene and Feldspar Recoveries in Synthetic Water with Addition of Copper Sulphate and Xanthate, $I = 2 \times 10^{-2}$

The adjustment of pH 9 to pH 6 resulted in an increase of pentlandite recovery from 53% to 91%. The pentlandite recovery achieved at pH 6 was thus of a similar value as obtained with copper sulphate and xanthate in di-sodium tetraborate solution for both pHs tested (96%). Copper (II) ions also enhanced true flotation of pyroxene at pH 6 compared to pH 9. However, the recovery obtained (44%) is significantly lower compared to those in a simple electrolyte at the corresponding conditions (pH 4: 80%, pH 9: 88%). Feldspar recovery in synthetic water was low for both pHs tested and can mostly be attributed to entrainment.

As predicted, the lower pH significantly enhanced pentlandite recovery but did not improve selectivity between the sulphide and gangue minerals investigated. Due to the fact that feldspar recovery was not significantly affected in the presence of copper (II) ions in synthetic water, it was decided to carry out additional experiments only on the pentlandite-pyroxene mixture with the aim of further investigating the water quality effect on floatability as well as the possibility of improving selectivity while maintaining a high pentlandite recovery.

4.5 Effect of Water Quality on Floatability with an Emphasis on Calcium Ions

To further investigate the water quality effect on floatability, synthetic water with a calcium concentration of 80 ppm and 500 ppm was prepared and the flotation results obtained on 1:1 pentlandite-pyroxene mixture in the presence of xanthate ions compared to a simple electrolyte in order to determine the effect calcium ions have on pentlandite and pyroxene surface alteration and, ultimately, floatability for the system studied.

4.5.1 Microflotation Tests

The ultimate recoveries obtained at pH 6 and pH 9 are summarised in Figure 4.36 and 4.37, respectively. As shown in the figures, the pentlandite ultimate recovery was depressed in synthetic water and even more in the presence of a higher calcium concentration for both pHs studied. The same trend was observed for pyroxene. The pentlandite recovery was higher at pH 6 compared to pH 9 for all scenarios investigated. The higher pentlandite recovery has been attributed to a lower metal hydroxide and oxide mineral surface coverage at pH 6 compared to pH 9.

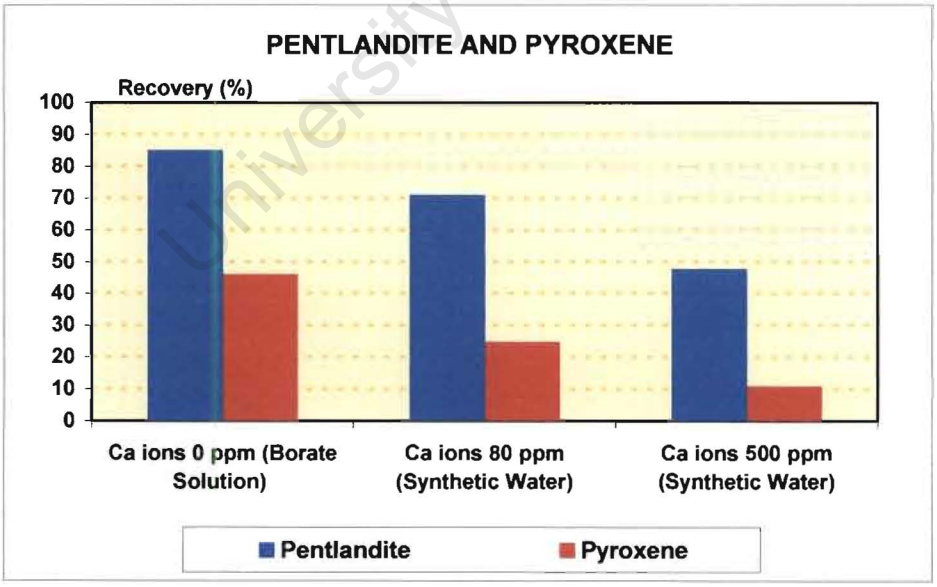

Figure 4.36: Pentlandite and Pyroxene Recovery in Synthetic Water at pH 6, $I = 2 \times 10^{-2}$

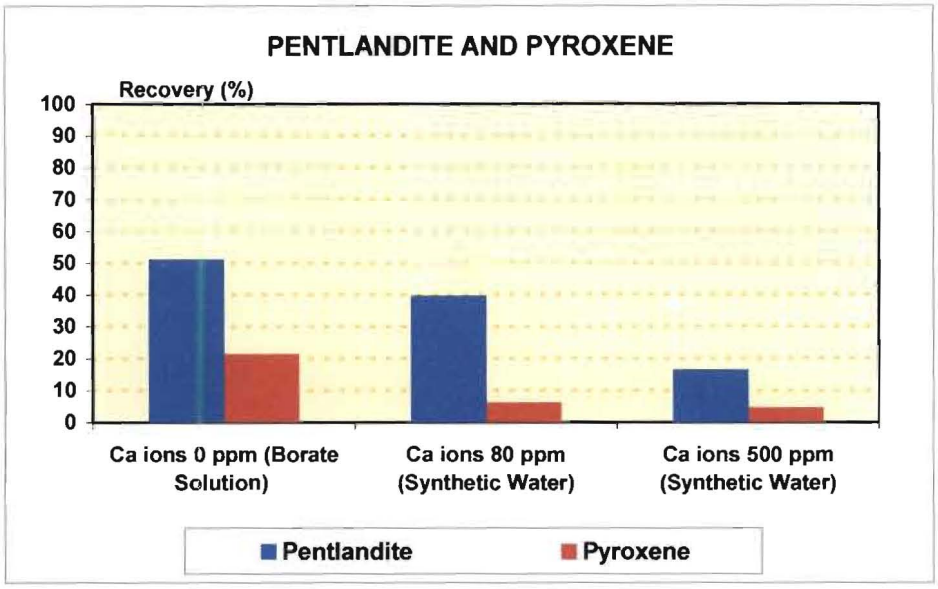

Figure 4.37: Pentlandite and Pyroxene Recovery in Synthetic Water at pH 9, I = 2 x 10^{-2}

4.5.2 Zeta Potential Determinations

In the presence of 500 ppm calcium ions, the zeta potential value of pentlandite in synthetic water increased significantly compared to 80 ppm of calcium ions (Figure 4.38). The calcium speciation diagram is shown and discussed in Section 5.2.

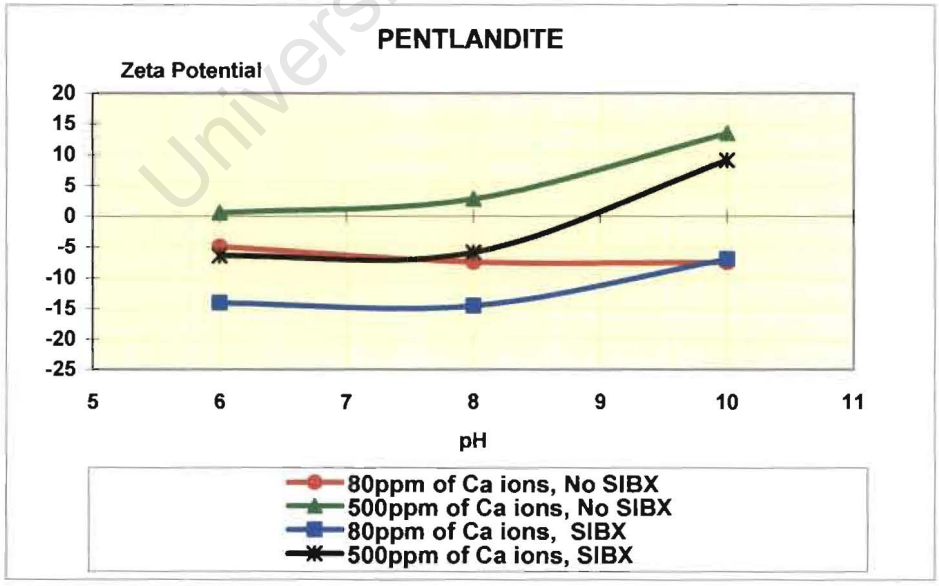

Figure 4.38: Zeta Potential of Pentlandite in Synthetic Water, I = 2 x 10^{-2}

The increase in zeta potential value is attributed to adsorption of positively charged calcium species, onto the pentlandite surfaces (Section 5.2). This change in the zeta potential value could also result from differences in ionic strength. The zeta potential increased with the alkalinity of the synthetic water. The addition of xanthate ions shifted the zeta potential versus pH curve to more negative values for both calcium concentrations, indicating that adsorption of xanthate ions onto the pentlandite surfaces occurred.

The zeta potential determinations for pyroxene (Figure 4.39) revealed that calcium ions also adsorbed onto the pyroxene surfaces. However, unlike on pentlandite, the similarity of the zeta potential versus pH curve in the presence or absence of xanthate ions (80 ppm of calcium) indicates no affinity of xanthate ions for pyroxene surfaces. In the case of pyroxene in the presence of 500 ppm of calcium ions, the mineral is more negative above pH 9 with the addition of xanthate ions. SIBX is present in solution in the anionic form ($SIBX^-$), which would adsorb electrostatically onto the positive pyroxene surfaces.

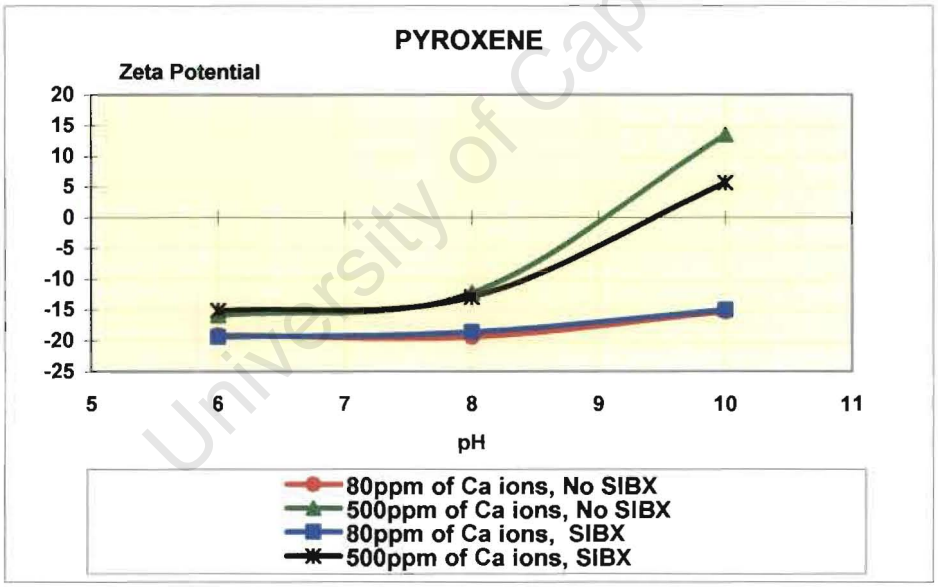

Figure 4.39: Zeta Potential of Pyroxene in Synthetic Water, $I = 2 \times 10^{-2}$

4.5.3 ToF-SIMS Analyses

To understand the mechanisms contributing to the lower pentlandite recovery in synthetic water, surface analyses of pentlandite grains, conditioned in the presence of pyroxene, at pH 6 and 9 without any reagents added in di-sodium tetraborate solution and synthetic

water (80 ppm of calcium) were performed. The results displayed in Figure 4.40 indicate a significantly higher relative percent abundance of [calcium, magnesium, aluminum and silicon] ions on the grains conditioned in synthetic water. It will be shown later that this resulted in a lower number of surface active sites available for xanthate ion adsorption and ultimately in the lower pentlandite recovery in synthetic water. The low concentration of the ions of interest observed on pentlandite in di-sodium tetraborate solution is attributed to the migration of these ions from pyroxene onto the pentlandite surfaces.

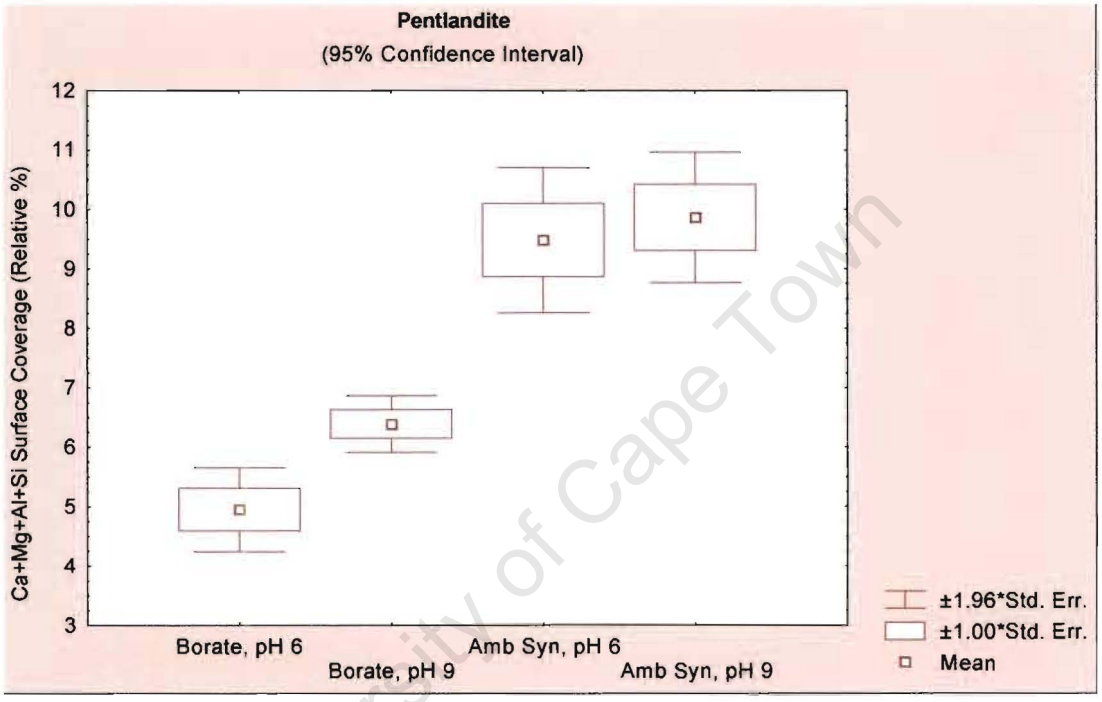

Figure 4.40: Relative % Abundance of Calcium, Magnesium, Aluminium and Silicon Ions on Pentlandite Surfaces in $Na_2B_4O_7$ at 10^{-3}M, I = 3 x 10^{-3} and Synthetic Water, I = 2 x 10^{-2}

The ToF-SIMS data for pentlandite given in Figure 4.41 showed a significantly higher surface coverage of calcium ions with the 500 ppm calcium concentration for both pHs investigated. The relative % abundance of these ions on pentlandite surfaces is higher at pH 6 compared to pH 9. As seen in Figure 4.41, magnesium ion surface coverage is higher at pH 9 compared to pH 6. There is no significant difference in magnesium ion relative % abundance observed for the calcium concentrations studied. The calcium and magnesium speciation diagrams are given and discussed later in Section 5.2.

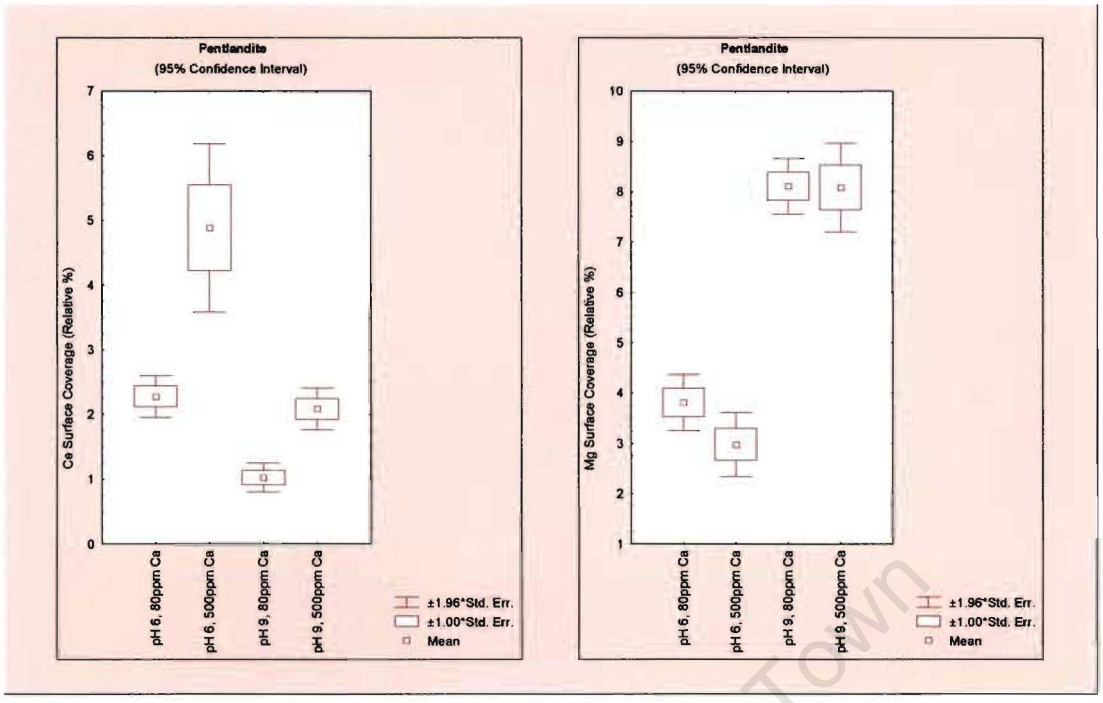

Figure 4.41: Relative % Abundance of Calcium and Magnesium Ions on Pentlandite Surfaces in Synthetic Water, I = 2 x 10^{-2}

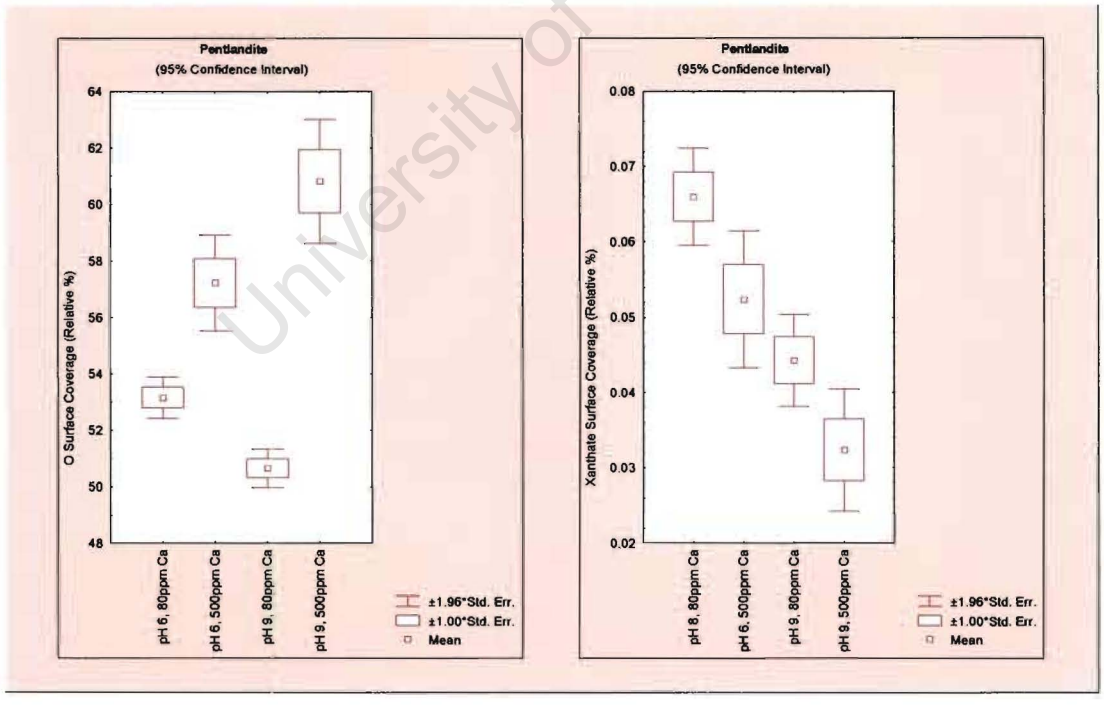

Figure 4.42: Relative % Abundance of Oxygen and Xanthate Ions on Pentlandite Surfaces in Synthetic Water, I = 2 x 10^{-2}

The data given in Figure 4.42 revealed a higher oxygen concentration on the pentlandite surfaces with the increased calcium concentration. The xanthate surface coverage (Figure 4.42) indicates a lower surface coverage of xanthate with the higher calcium ion concentration for pentlandite. The larger spread observed with the xanthate analyses could be attributed to the heterogeneous surfaces on and between the mineral grains, which affects the xanthate adsorption. Moreover, the ToF-SIMS data showed a significantly higher xanthate uptake by the pentlandite surfaces at pH 6 compared to pH 9 for both scenarios investigated.

The relative % abundance of iron and nickel ions (Figure 4.43) indicates that the higher calcium ion concentration increased the iron and reduced the nickel surface coverage at pH 6. At pH 9, there seems to be no significant difference in the iron or nickel ion concentration observed between the calcium concentrations tested. The surface analyses showed a higher surface concentration of iron ions at pH 6 compared to pH 9. The nickel ions surface coverage follows the opposite trend as observed for iron ions. At pH 9, there is a higher concentration of nickel hydroxide species (Figure 4.44).

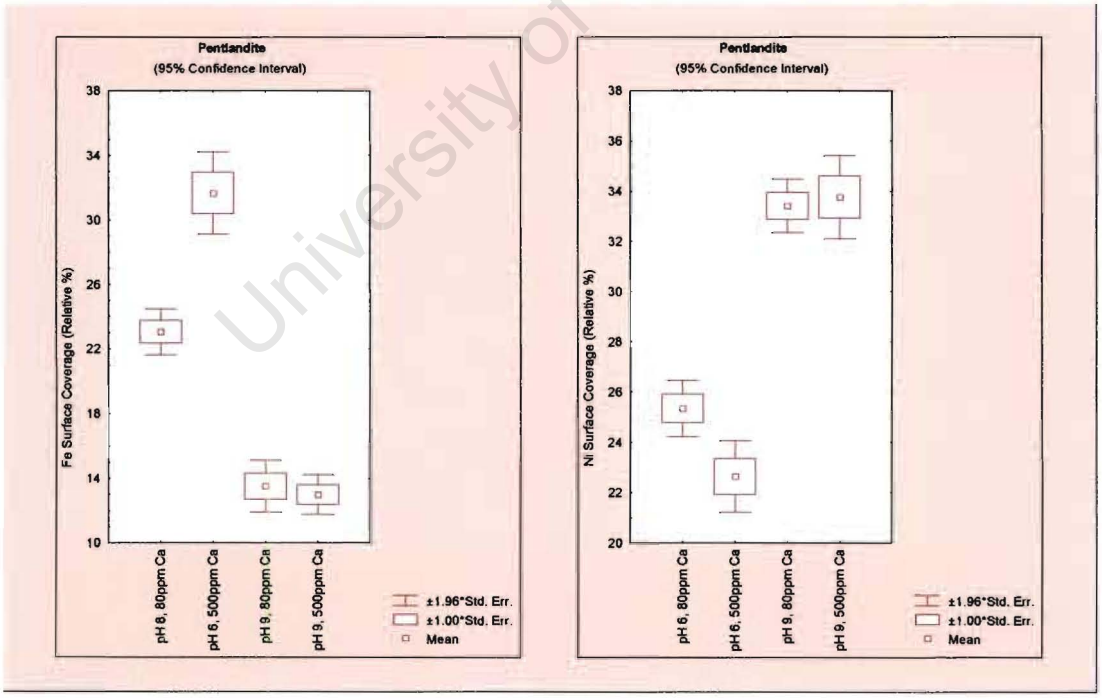

Figure 4.43: Relative % Abundance of Iron and Nickel Ions on Pentlandite Surfaces in Synthetic Water, I = 2 x 10^{-2}

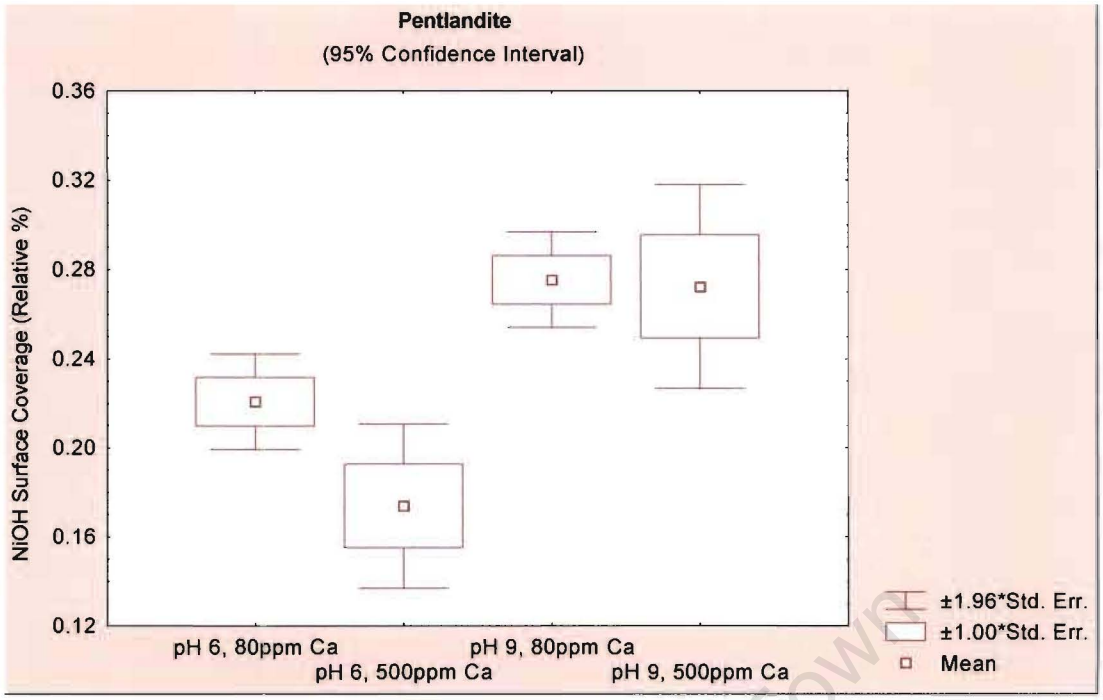

Figure 4.44: Relative % Abundance of $NiOH^+$ on Pentlandite Surfaces in Synthetic Water, $I = 2 \times 10^{-2}$

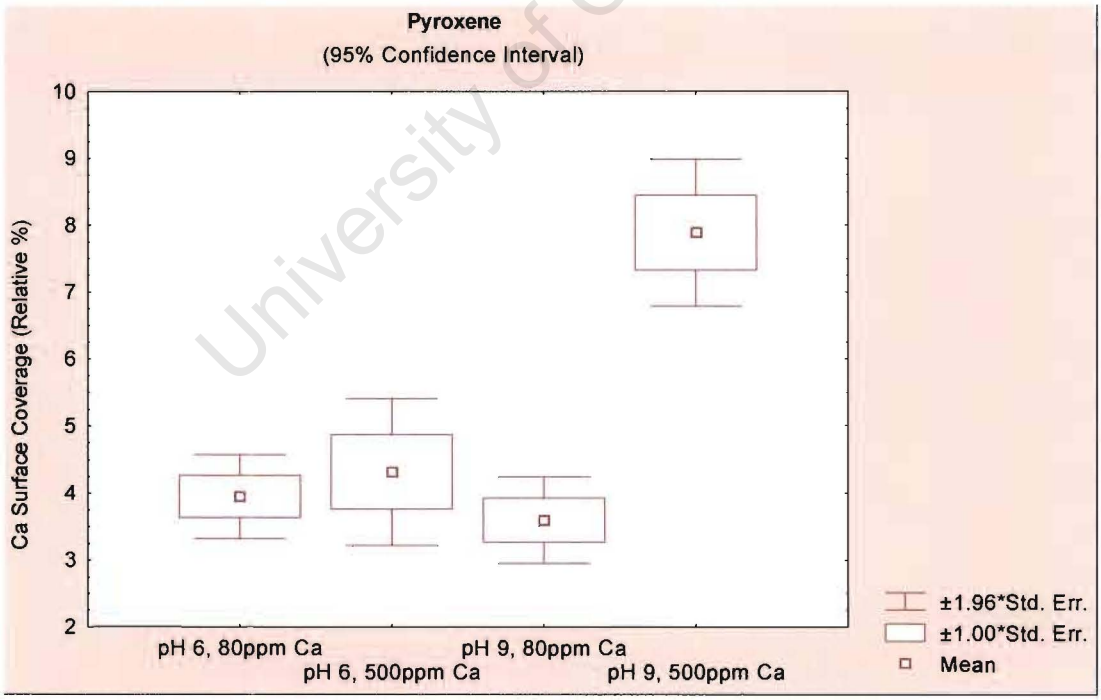

Figure 4.45: Relative % Abundance of Calcium Ions on Pyroxene Surfaces in Synthetic Water, $I = 2 \times 10^{-2}$

ToF-SIMS analysis carried out on pyroxene grains (Figure 4.45) showed that pyroxene surfaces also become enriched in calcium ions with the increasing calcium concentration at pH 9. However, there was no significant difference observed at pH 6.

4.6 Enhanced Selectivity of Pentlandite-Pyroxene System

The results presented above within the thesis showed that inadvertent activation by copper (II) ions contributed significantly to the true flotation of pyroxene. The aim of the tests below was to maximise pentlandite recovery and simultaneously minimise the percentage pyroxene reporting to the concentrate.

4.6.1 Microflotation Tests

Figures 4.46 and 4.47 show the results of the microflotation studies at pH 6 and pH 9 using a 1:1 pentlandite-pyroxene mixture. The ultimate recovery of pentlandite obtained in the absence of any reagent and in the presence of SIBX and [$CuSO_4$ + SIBX] is shown. At pH 6, the addition of SIBX and of $CuSO_4$ both increased recovery significantly. In terms of the recovery of pyroxene in the same set of tests, the addition of SIBX significantly increased recovery and the addition of $CuSO_4$ caused an even further increase in recovery at pH 6.

Since the microflotation results showed that both pentlandite and pyroxene recoveries were enhanced by the addition of copper (II) ions followed by xanthate addition, the effect being more significant at pH 6 than pH 9, it was important to determine conditions at which the separation between pentlandite and pyroxene was maximised in the presence of copper (II) ions. To this end it was noted that DETA has been reported to depress pyrrhotite flotation in the processing of copper-nickel ores (Yoon et al. 1995, Kelebek et al. 1996) by removing activating ions such as nickel and copper from the pyrrhotite surface due to a chelating mechanism, which is related to the formation of metal-DETA complexes. In the case of pyroxene, the copper and nickel ions present in an operating circuit would activate the mineral surface as copper and nickel hydroxides and oxides. The speciation diagram for copper and nickel are shown in Chapter 5. Therefore it was decided to test the effect of DETA in the pentlandite-pyroxene system to determine whether it would influence the separation of pentlandite from pyroxene. The mechanism proposed would involve complexing of the activating copper (II) ion species preferentially from the pyroxene

compared to the pentlandite. The results obtained in the study of the flotation of pentlandite-pyroxene mixtures using DETA are shown in Figures 4.46 (pH 6) and 4.47 (pH 9). Combinations of [$CuSO_4$ + SIBX], [DETA + SIBX] and [$CuSO_4$ + DETA + SIBX] were used. At pH 6 the recovery of pentlandite was hardly affected by DETA in the presence of copper sulphate but it caused a slight reduction in pyroxene recovery. At pH 9 DETA actually increased the recovery of pentlandite without affecting pyroxene recovery. In summary, there were indications that DETA preferentially deactivated pyroxene at pH 6 by removing adsorbed ions. The different pentlandite response to DETA addition at pH 6 compared to pH 9, in the presence of copper ions, could be attributed to a different bond of copper species onto pentlandite. This is discussed further in Section 5.3.

It is well known that the presence of very fine particles in flotation plants often detrimentally affects the recovery and selectivity of valuable minerals due to the effect of slime coatings. The effect of such coatings and also agglomeration of coarser particles on the floatability of pentlandite and pyroxene was thus investigated using synthetic process water only at pH 9, this being the typical pH of an operating circuit. The results shown (Figure 4.48) revealed that in the presence of xanthate ions pentlandite recovery decreased from 30.9% to 23.4% when the pentlandite was first conditioned and then floated in the presence of –38µm pyroxene particles. To eliminate or minimize the agglomeration phenomenon between pentlandite and pyroxene particles, the use of sodium polyphosphate as a dispersing agent was investigated. The results of these tests, using a combination of [polyphosphate + $CuSO_4$ + DETA + SIBX] where the sodium polyphosphate has an approximate chain length of 50 and is added at a concentration of 3.1×10^{-6} M, are shown in Figures 4.46 and 4.47. At pH 6 the polyphosphate had a significant effect on the selectivity to pentlandite, the separation factor of pentlandite recovery:pyroxene recovery changing from about 2.4 in the absence of polyphosphate to 4.3 in its presence (an increase of 79%). At pH 9 this ratio in fact decreased from 2.56 to 2.0.

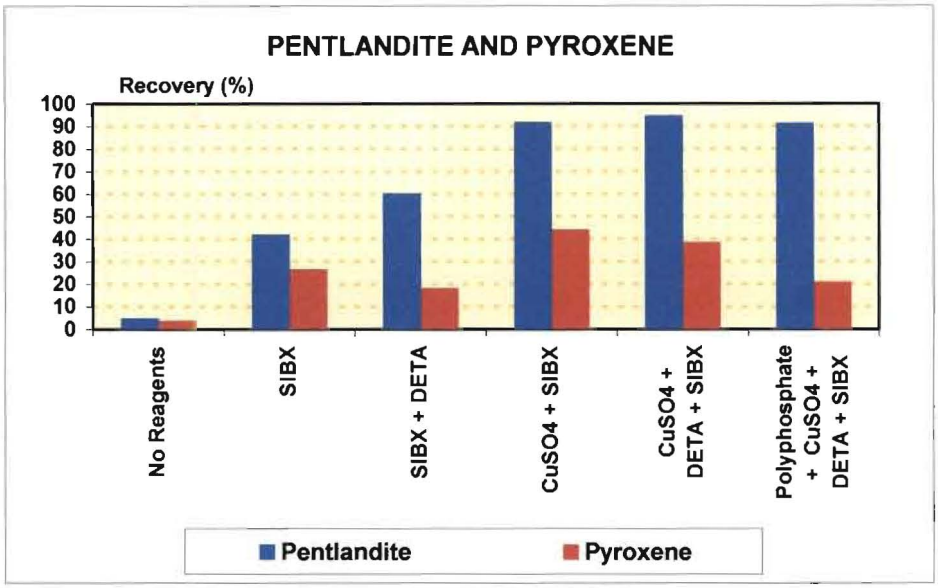

Figure 4.46: Pentlandite and Pyroxene Ultimate Recovery in Synthetic Water at pH 6, $I = 2 \times 10^{-2}$

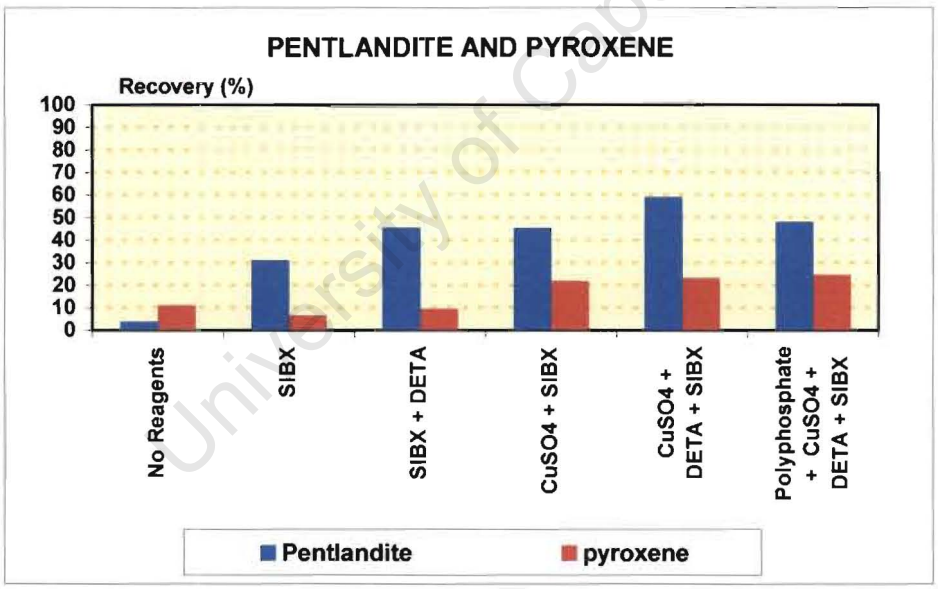

Figure 4.47: Pentlandite and Pyroxene Ultimate Recovery in Synthetic Water at pH 9, $I = 2 \times 10^{-2}$

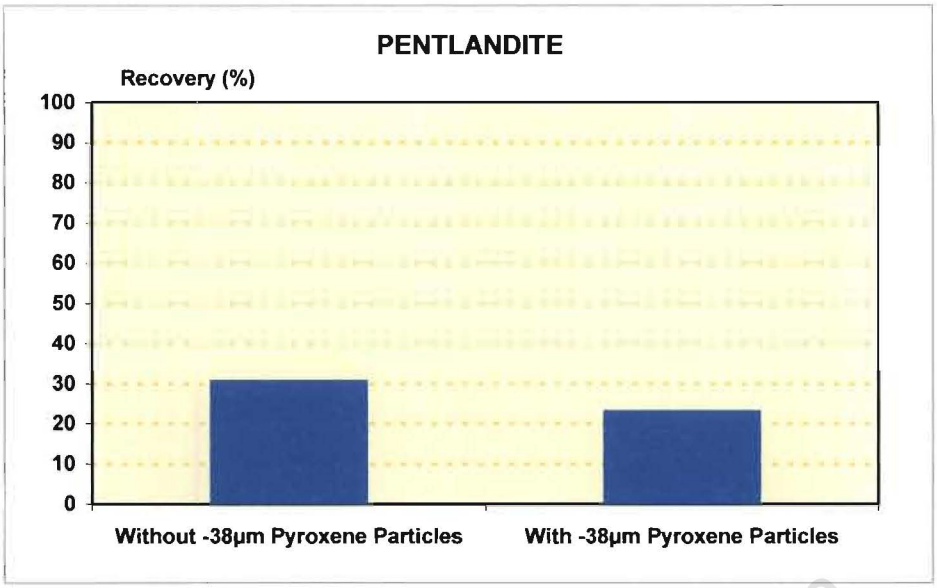

Figure 4.48: Pentlandite Ultimate Recovery in Synthetic Water at pH 9, I = 2 x 10^{-2}

4.6.2 Zeta Potential Determinations

Zeta potential studies were carried out on pentlandite and pyroxene in the presence of SIBX (5 x 10^{-5}M), $CuSO_4$ (5 x 10^{-5}M), polyphosphate (3.1 x 10^{-6}M) [$CuSO_4$ + SIBX], [$CuSO_4$ + DETA (5 x 10^{-5}M)] and [$CuSO_4$ + DETA + SIBX], [polyphosphate + $CuSO_4$ + DETA + SIBX], respectively at pH values of 6, 8 and 10. These results are plotted in Figures 4.49 and 4.50, and showed that both minerals have zeta potential values in the range between 0 and ±20mV, which promotes slimes coating and also aggregation of coarser particles. This would not only contribute to a lower pentlandite recovery but also a reduction in the concentrate grade. The addition of polyphosphate shifted the zeta potential versus pH curve compared to the no reagent curve to more negative values for both minerals studied indicating either adsorption of the polyphosphate anion onto the pentlandite mineral surfaces or complexing of the positive metal ions in solution. Thus the repulsive forces prevent attachment and increase detachment of pyroxene from pentlandite surface.

In the case of pentlandite the most significant observations were that at pH 10, where DETA caused a significant decrease in zeta potential whereas SIBX a significant increase in the zeta potential value. In the case of pyroxene, DETA caused a decrease in zeta potential of copper (II) activated surfaces at the pH range investigated.

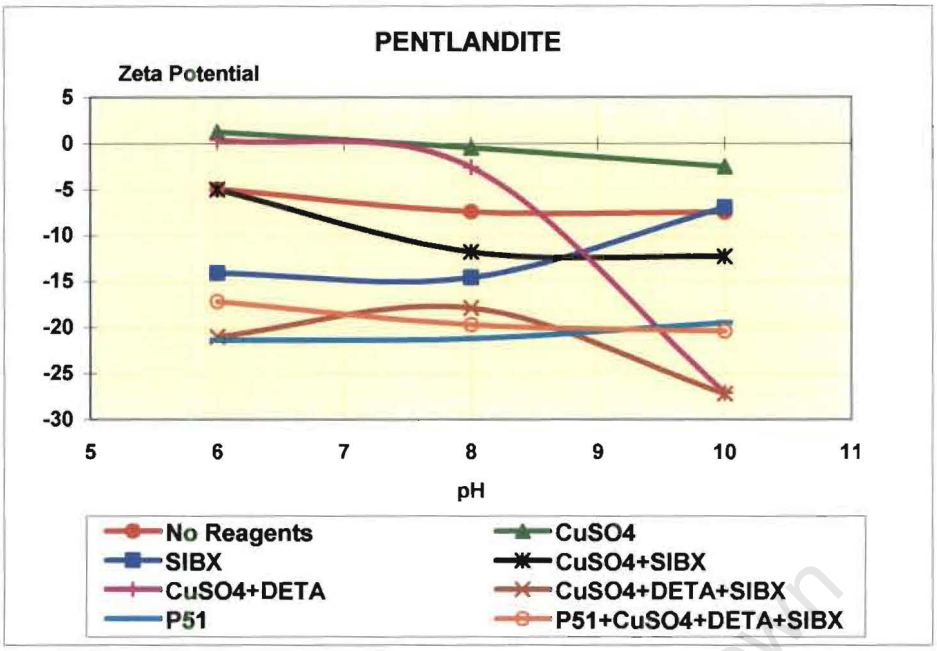

Figure 4.49: Zeta Potential of Pentlandite in Synthetic Water, I = 2 x 10^{-2}

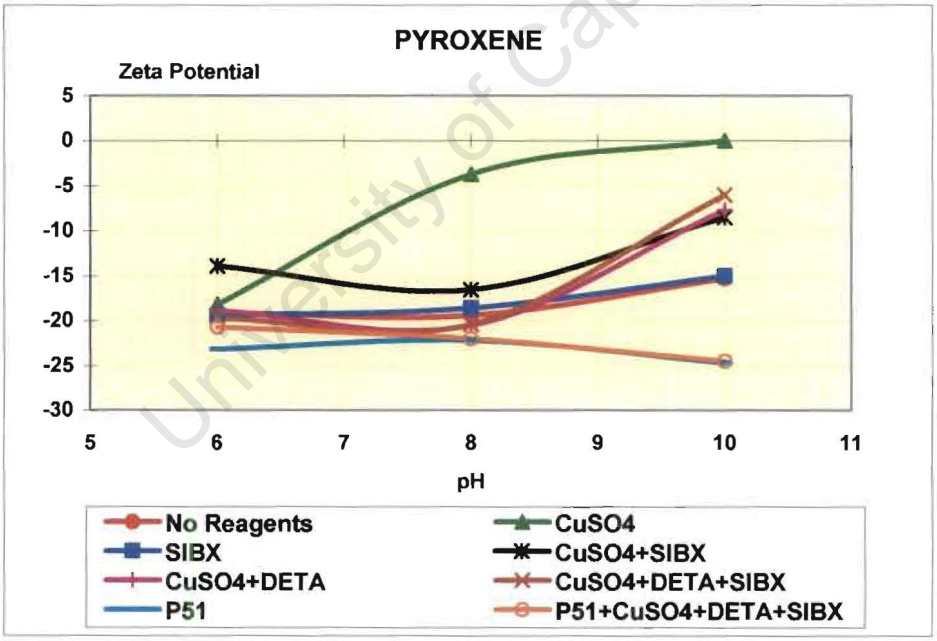

Figure 4.50: Zeta Potential of Pyroxene in Synthetic Water, I = 2 x 10^{-2}

4.6.3 ToF-SIMS Analyses

ToF-SIMS analyses were carried out on a pentlandite sample conditioned with pyroxene for 20 minutes in the presence of xanthate ions and indicated the presence of a lower hydroxyl group surface coverage and a higher sulphur concentration at pH 6 compared to pH 9. These tests also showed a higher relative percent coverage of xanthate ions on the penlandite surface at pH 6 compared to pH 9. The ToF-SIMS data obtained on the pentlandite grains conditioned in the absence and presence of DETA in combination with xanthate indicated that DETA contributed to the removal of surface oxidation products thus exposing a more hydrophobic "virgin" pentlandite surface.

Because of the specific interest in the activating role of nickel (II) ions on pyroxene surfaces, ToF-SIMS analyses were carried out on pyroxene grains conditioned on their own and in the presence of pentlandite (Figure 4.51).

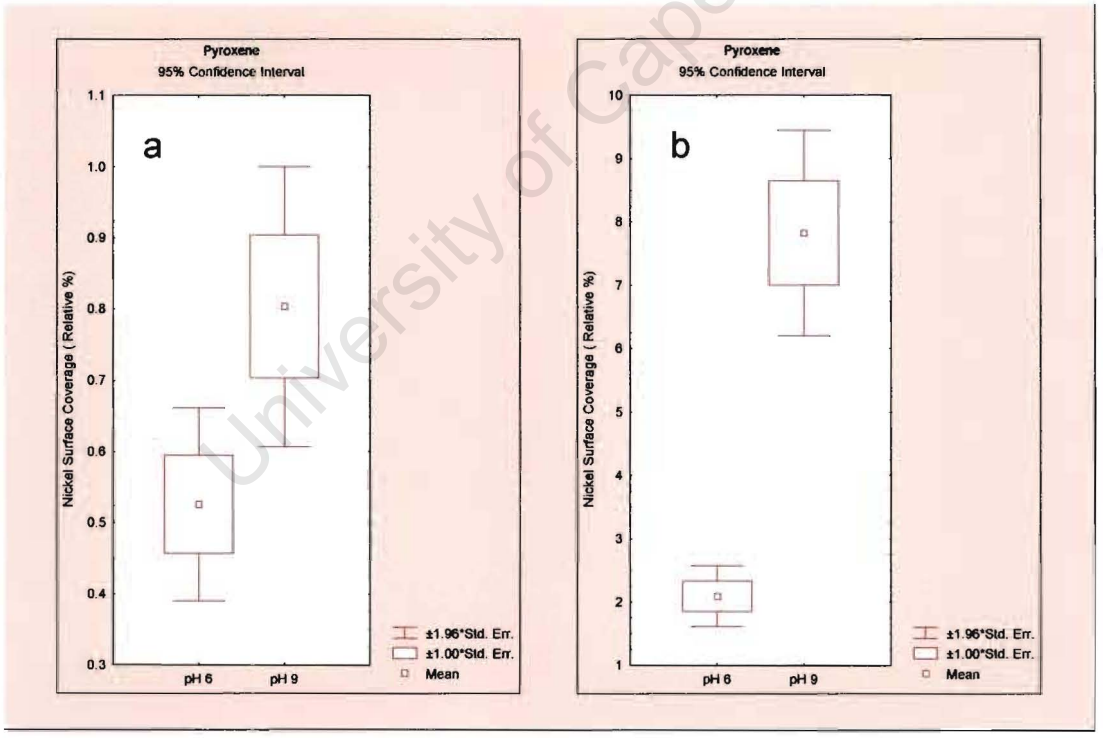

Figure 4.51: Relative % Abundance of Ni Ions on Pyroxene Only (a) and Pyroxene Exposed to Pentlandite (b) in Synthetic Water (no reagents present)

The ToF-SIMS data revealed a higher surface concentration of nickel (II) ions on pyroxene in the presence of pentlandite compared to pyroxene on its own for both pHs studied. This can be attributed to a transfer mechanism of Ni (II) ions from pentlandite to pyroxene mineral surfaces. Note that the scales for Figure 4.51 are not the same for pyroxene on its own and pyroxene in mixture with pentlandite.

Figure 4.52 shows the results of the ToF-SIMS analysis of pyroxene in the presence of pentlandite with respect to Ni and Cu as a function of various reagent regimes. In the presence of $CuSO_4$ at pH 9 the concentrations of both metals on the surface is greater than those at pH 6. When the mineral was conditioned in the presence of DETA, the concentration of copper (II) and nickel (II) ions found on the surface was significantly reduced for both pHs relative to the case of [$CuSO_4$ + SIBX] alone. These results are consistent with the zeta potential measurements. The addition of polyphosphate continued to reduce the concentration of copper (II) and nickel (II) ions on the surface, this effect being particularly significant at pH 9.

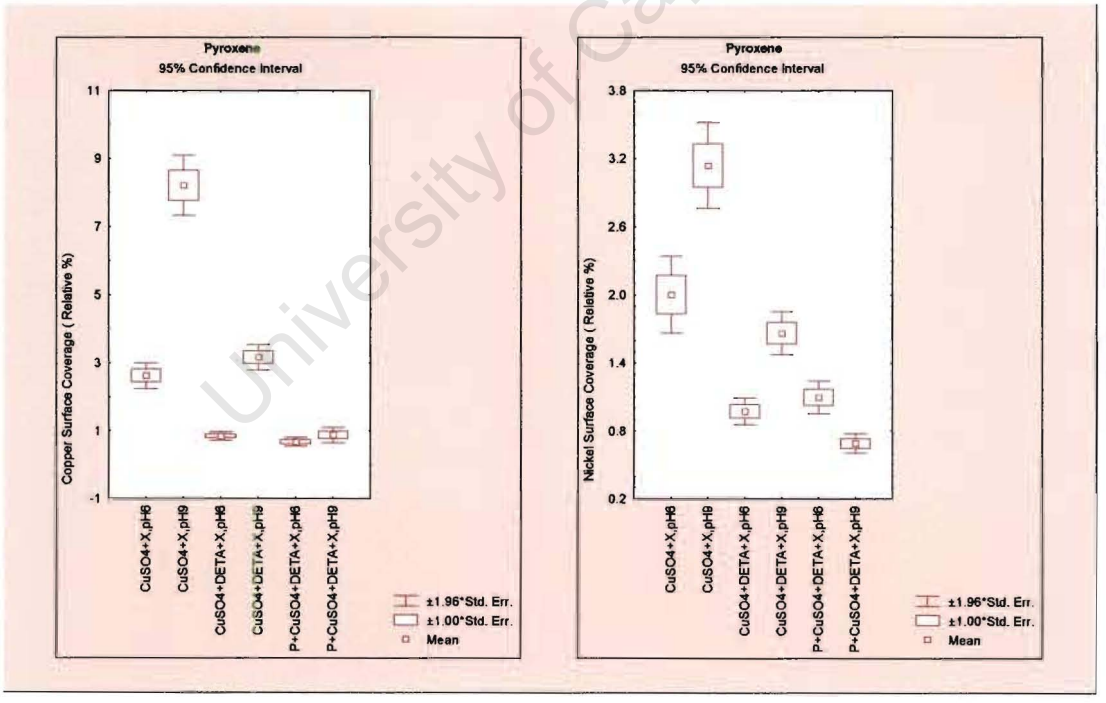

Figure 4.52: Relative % Abundance of Cu and Ni Ions on Pyroxene Surfaces in Synthetic Water, I = 2 x 10^{-2}

ToF-SIMS analysis of pentlandite grains (Figure 4.53) also indicated lower copper (II) ion concentration on pentlandite surfaces in the presence of DETA for both pHs tested. At pH 9, the combination of polyphosphate and DETA reduced the copper species concentration even further. However, the surface coverage of copper on pentlandite surfaces was significantly higher compared to the residual concentration observed on pyroxene mineral surfaces. The nickel species concentration on pentlandite surfaces seems to be reduced in the presence of [polyphosphate + $CuSO_4$ + DETA + SIBX] compared to [$CuSO_4$ + DETA + SIBX].

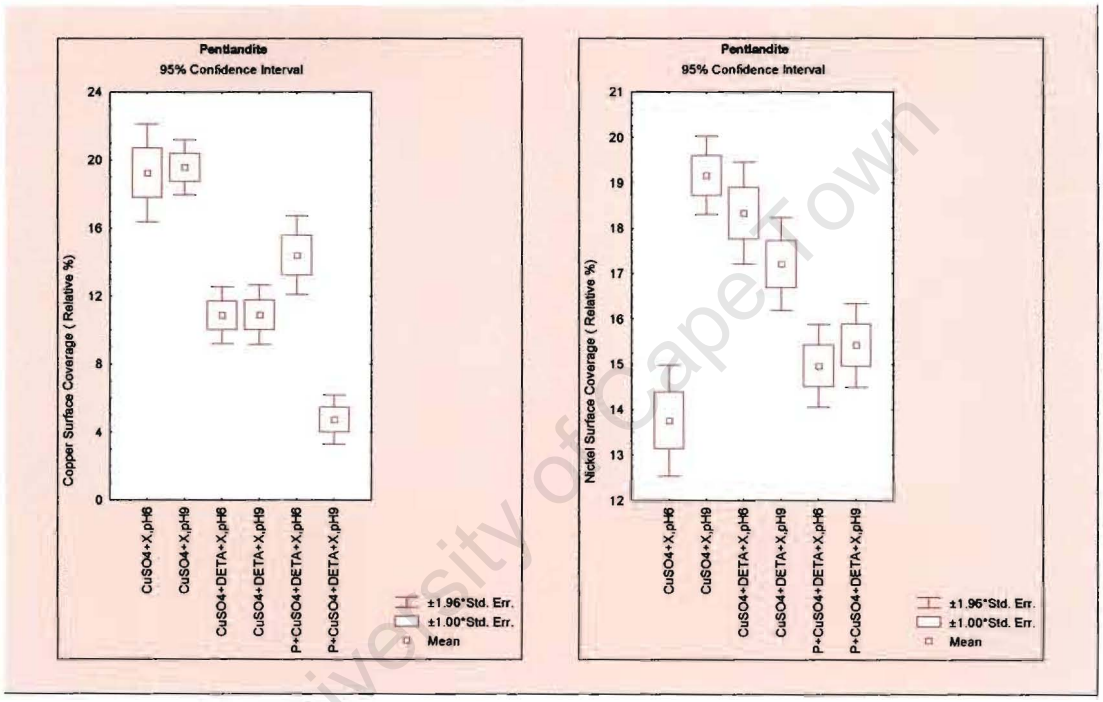

Figure 4.53: Relative % Abundance of Cu and Ni Ions on Pentlandite Surfaces in Synthetic Water, I = 2 x 10^{-2}

Figures 4.54a and 4.54b show the ToF-SIMS images of pyroxene at pH 6 comparing nickel, copper and xanthate ion images for the [$CuSO_4$ + SIBX] trial with and without DETA addition. The images clearly demonstrate that the pyroxene surfaces have significantly lower concentrations of nickel, copper and xanthate ions with the addition of DETA.

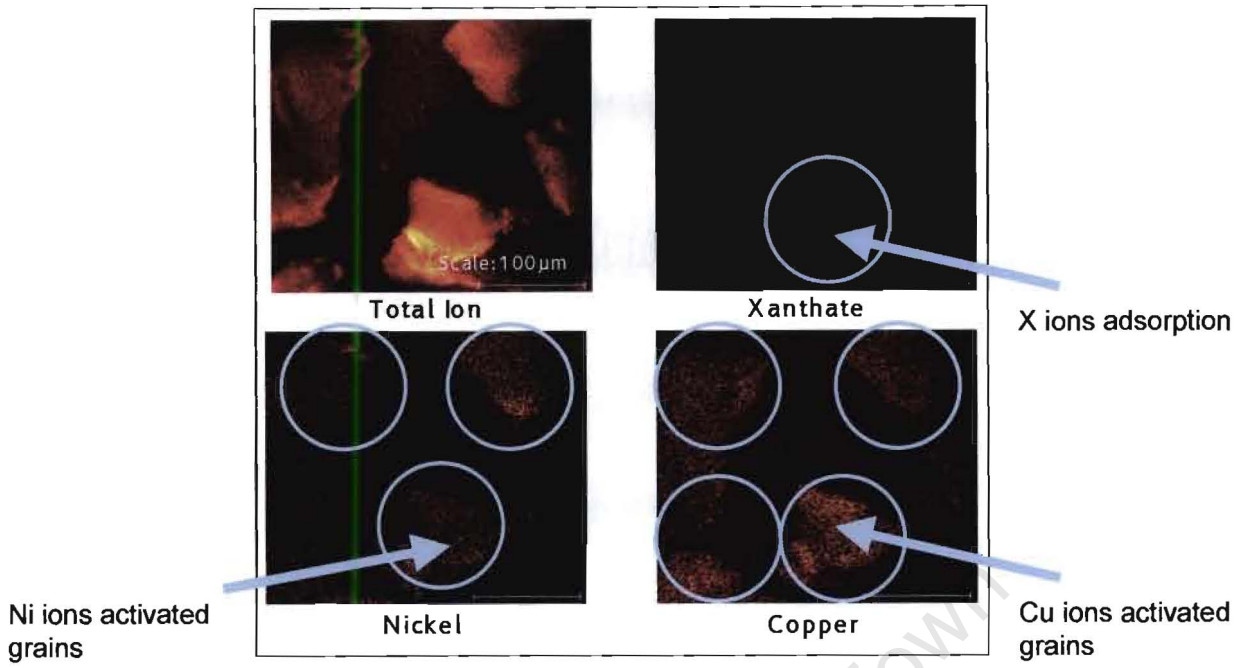

Figure 4.54a: ToF-SIMS Images of Pyroxene Conditioned with Copper and Xanthate Ions at pH 6 in Synthetic Water, I = 2 x 10^{-2}

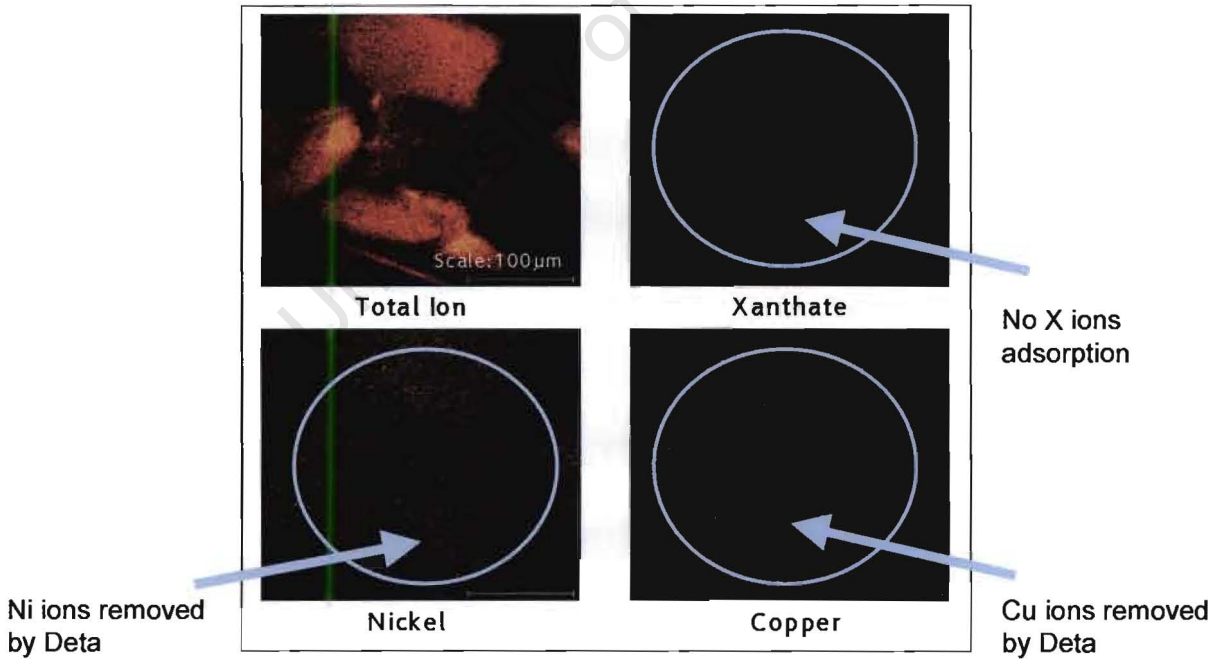

Figure 4.54b: ToF-SIMS Images of Pyroxene Conditioned with Copper, DETA and Xanthate Ions at pH 6 in Synthetic Water, I = 2 x 10^{-2}

To demonstrate the cleaning effect polyphosphate has on mineral surfaces, the Merensky ore sample was conditioned in the presence of polyphosphate using a batch flotation cell. An ore sample was selected instead of the pentlandite-pyroxene mixture with the aim of enhancing the polyphosphate slime cleaning effect since microflotation tests were performed at a coarser size distribution and thus only agglomeration of valuable and gangue minerals was reduced.

Surface analysis of pentlandite grains indicated that polyphosphate had a significant cleaning effect by reducing the surface concentrations of calcium, magnesium, aluminium and silicon ions (Figure 4.55). This reflects a possible chelating effect of polyphosphate with calcium and magnesium ions (Section 2.5) as well as dispersion of siliceous gangue particles from pentlandite surfaces.

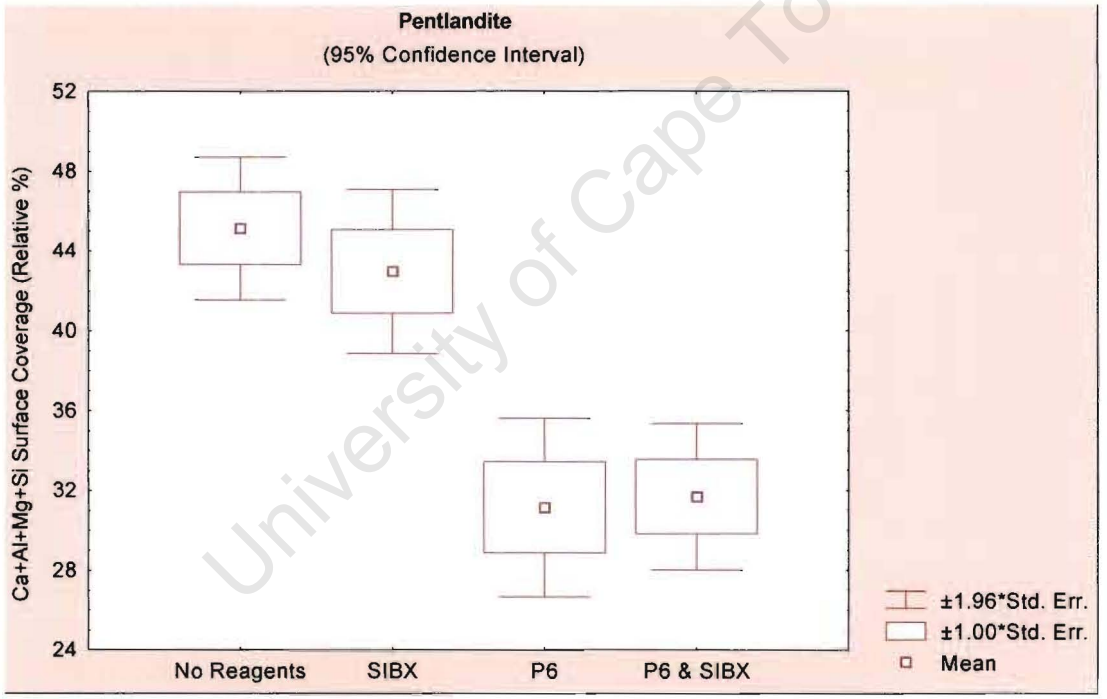

Figure 4.55: Relative % Abundance of Calcium, Magnesium, Aluminium and Silicon Ions on Pentlandite Surfaces at pH 9

4.7 Flotation Study on Ore Sample

Batch flotation tests (Figure 4.56) and small scale continuous flotation trials (Figure 4.57) were conducted on a Merensky Reef ore sample with the objective of investigating whether the trends obtained using a microflotation cell and a "simple pulp environment" would be observed in a "more complex pulp environment" prevailing in an industrial flotation cell. Both figures show the sulphide nickel recovery versus silica recovery. The cumulative recovery for each cell is plotted in Figure 4.57. The sulphide nickel data corresponds to pentlandite recovery and the silica values relate to pyroxene and feldspar recovery.

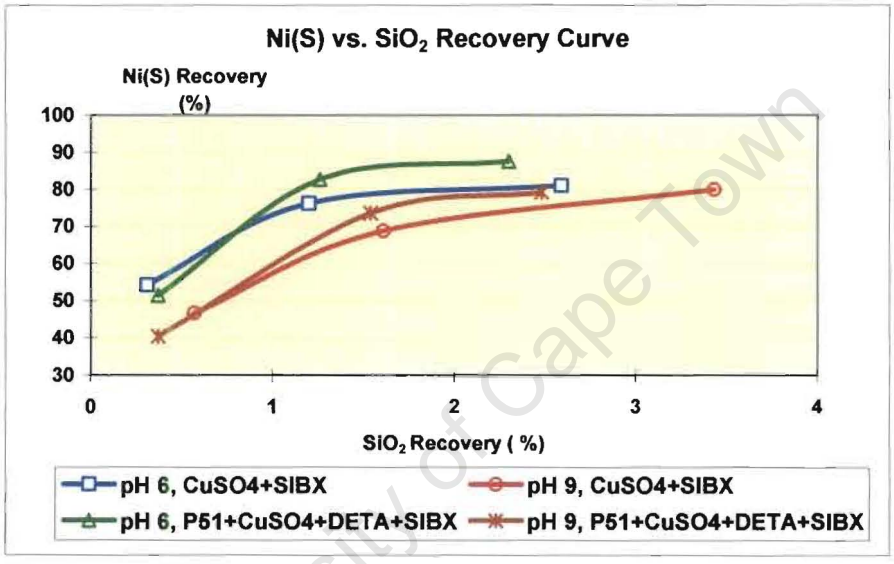

Figure 4.56: Batch Flotation Tests Using Merensky Ore Sample

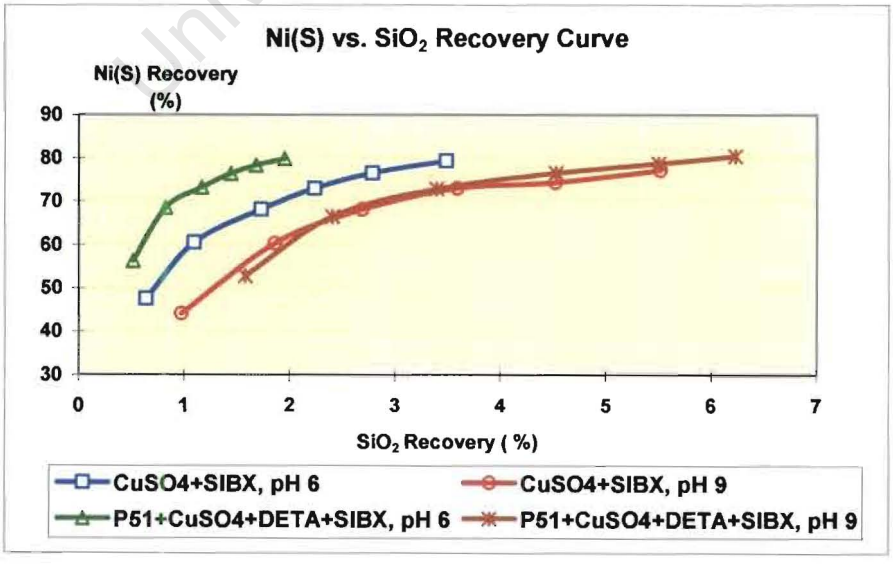

Figure 4.57: Continuous Flotation Trials Using Merensky Ore Sample

The results obtained clearly demonstrate that the optimum selectivity to pentlandite occurred when a reagent combination of [polyphosphate +$CuSO_4$ + DETA + SIBX] at pH 6 was used. Thus the metallurgical data obtained confirmed the microflotation results.

The batch flotation data obtained for the above given conditions has shown a significant improvement in the ultimate recovery and the concentrate grade compared to the standard reagent regime, while the continuous trials significantly improved the selectivity, however, at a similar ultimate recovery. The difference observed between the batch flotation tests and the continuous trials can probably be attributed to the froth phase rather than pulp phase. During the continuous runs, the froth was less mobile at pH 6 compared to pH 9. This resulted in a significantly lower mass pull and thus a significantly higher concentrate grade at pH 6. The most important observation, however, is that the ultimate valuable mineral recovery has not been reduced by the lower mass pull in the presence of polyphosphate and DETA.

CHAPTER 5

DISCUSSION

5.1 A Simple Electrolyte Study

It was postulated that activation of gangue minerals occurred as a result of the presence of copper (II) ions followed by xanthate adsorption, which would result in true flotation of the siliceous gangue minerals. To test the hypothesis, pyroxene and feldspar were conditioned and floated on their own and in a 1:1 mixture with pentlandite in the presence of xanthate as well as in the presence of copper ions followed by the addition of xanthate. An electrolyte solution was used in order to simplify the system studied. Di-sodium tetraborate solution was selected as a background electrolyte for its buffer capacity, which simulates the buffering effect of pulp solution at operating circuits.

Zeta potential determinations and ToF-SIMS analysis obtained during the study clearly demonstrated that copper ions adsorbed onto pentlandite as well as pyroxene and feldspar surfaces (Figures 4.3, 4.4, 4.5, 4.12, 4.16, 4.20). Microflotation data showed that subsequent adsorption of xanthate ions onto the copper (II) activated mineral surfaces caused true flotation of pyroxene and feldspar. A higher copper concentration was found on all mineral surfaces at pH 9 compared to pH 4 (Figures 4.16 and 4.20). The reasons for the different behaviour at these pHs are discussed further later in this Section. This resulted in a significantly higher flotation of pyroxene and feldspar on their own at pH 9 compared to pH 4 (Figures 4.8 and 4.9) as well as when these minerals were in a 1:1 mixture with pentlandite (Figures 4.24 and 4.26). The ToF-SIMS analysis carried out on the microflotation products of the tests conducted on the pentlandite-feldspar mixture at pH 9 (Figure 4.30) showed that the presence of copper species increased the xanthate ion concentration on feldspar surfaces to the level, which was sufficient to cause true flotation of feldspar. Based on the pentlandite-feldspar ToF-SIMS results obtained, it can be proposed that subsequent adsorption of xanthate ions onto the copper (II) activated pyroxene surfaces enhanced pyroxene floatability in the presence of copper sulphate and xanthate. Nagaraj and Brinen (1995 and 1996) studied copper ion adsorption, and its effect on subsequent sulphide collector adsorption, on pyrite and pyroxene minerals under flotation related conditions at pH 9. They found that xanthate ions adsorbed onto copper

ion activated mineral surfaces. Unfortunately, they did not carry out flotation tests and thus link the copper and collector surface coverage to floatability.

This thesis explores the relative roles, which the chemical conditions such as pH and E_h and the chemical environment such as solution species present as well as the roles ions in the water play in influencing the flotation of the pentlandite on the one hand and the siliceous gangue minerals (pyroxene and feldspar) on the other hand. The interactions between copper and xanthate species in solution and on the surface are investigated.

The floatability of all minerals studied is explained below in terms of the interactions between the minerals and various copper as well as xanthate species present.

Due to the lack of reliable equilibrium constant values available in the literature for sodium isobutyl xanthate species, ethyl xanthate was used to demonstrate a possible xanthate speciation. A calculation of the speciation of ethyl xanthate at pH 9 was performed for a range of E_h conditions (Figure 5.1).

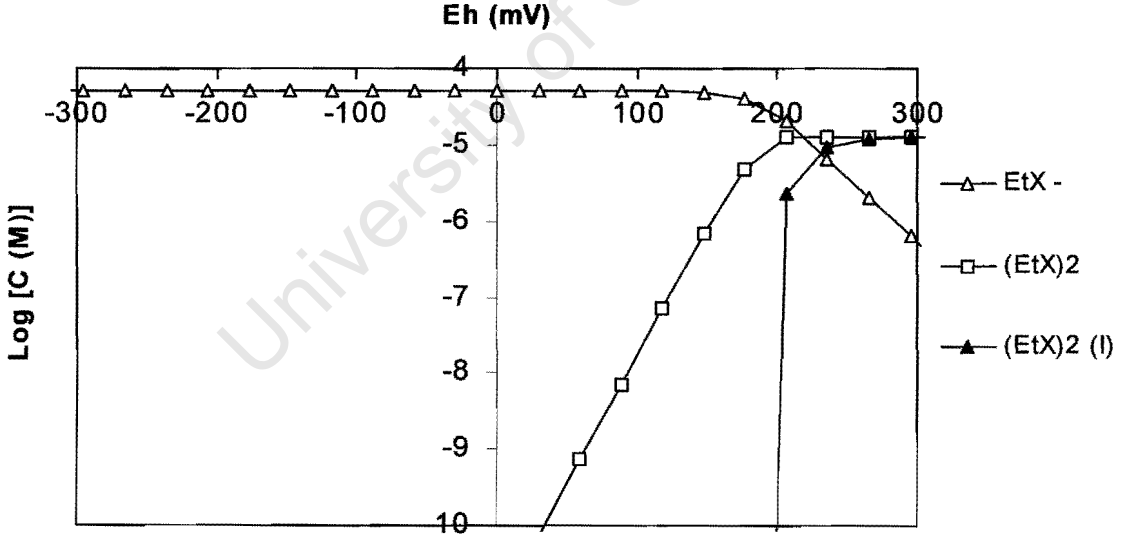

Figure 5.1: Speciation Diagram for Ethyl Xanthate (EtX) at pH 9

The equilibrium constants used for this SOLGAS Water calculation are given in Table 5.1 as well as the equilibrium constants for the other solution speciation calculations described in this section.

Table 5.1: Species and Equilibrium Constants Used for Solution Speciation Calculations

Species	Equilibrium Constant	Stoichiometric contributions				
		Cu^{2+}	e^-	H^+	EtX^-	Ca^{2+}
Solution species						
Cu^{2+}	0	1	0	0	0	0
e^-	0	0	1	0	0	0
H^+	0	0	0	1	0	0
EtX^-	0	0	0	0	1	0
Ca^{2+}	0	0	0	0	0	1
Cu^{1+}	2.59	1	1	0	0	0
$Cu(OH)^{1+}$	-7.70	1	0	-1	0	0
$Cu(OH)_2$	-13.80	1	0	-2	0	0
$Cu(OH)_3^-$	-26.80	1	0	-3	0	0
$Cu(OH)_4^{2-}$	-39.60	1	0	-4	0	0
$Cu_2(OH)^{2+}$	-10.70	2	0	-2	0	0
$(EtX)_2$	-2.54	0	-2	0	2	0
HetX	1.52	0	0	1	1	0
$CaOH^+$	-12.70	0	0	-1	0	1
Solids						
$(EtX)_2$ (liquid)	2.37	0	-2	0	2	0
CuEtX	23.01	1	1	0	1	0
$Cu(EtX)_2$	26.75	1	0	0	2	0
$Cu(OH)_2$	-7.70	1	0	-2	0	0
$Ca(OH)_2$	-22.81	0	0	-2	0	1

Xanthates are the most commonly used sulphydryl collectors in beneficiation of sulphide minerals. It is accepted that thiol collectors on their own do not exhibit any affinity for silicate minerals. For the minerals used during the study, xanthate adsorbs selectively onto pentlandite surfaces, not onto pyroxene and feldspar surfaces (Figures 4.3, 4.4, 4.5). In general, the selectivity is attributed to the reagent structure, which incorporates functional group with specific affinity for one cation and/or more cations that are present on the mineral surfaces. In the case of the minerals studied, the selectivity is attributed to the affinity between nickel sites on pentlandite surfaces and sulphur ions in the xanthate structure. A schematic representation of xanthate adsorption onto pentlandite surfaces is given in Figure 5.2.

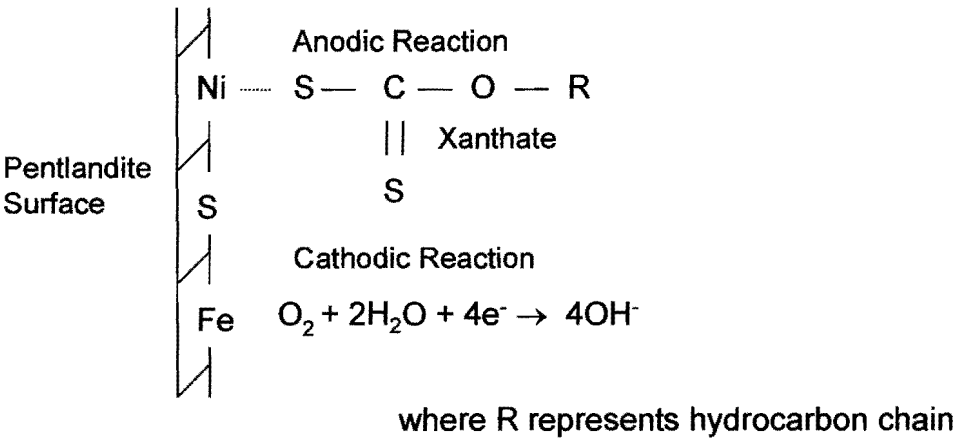

Figure 5.2: Schematic Representation of Xanthate Adsorption onto Pentlandite

The zeta potential determinations obtained during the study on pyroxene and feldspar (Figures 4.4 and 4.5) in the presence or absence of xanthate ions are consistent with respect to the xanthate adsorption mechanism described above and showed no affinity of xanthate for the siliceous minerals. The microflotation data showed that the addition of xanthate had no influence on the flotation response of pyroxene and feldspar in the single mineral system at pH 4 or 9 (Figures 4.8 and 4.9). For these minerals the only possibility of xanthate playing a role would be via its dimer. These results thus suggest that the xanthate dimer in the liquid form is not present, as this would adsorb onto the mineral surfaces where it may alter the zeta potential determinations and increase the flotation response. As seen from Figure 5.1, the formation of dixanthogen is favored at E_h values above 200 mV, whereas in this study, the E_h values were always in the region of 100 mV.

SIBX is therefore present in solution in the anionic form ($SIBX^-$). This is consistent with the speciation data presented in Figure 5.1, which shows that the anionic xanthate form is dominant over a wide range of xanthate concentrations and E_h values. The anionic xanthate is not expected to adsorb electrostatically onto the negative pyroxene and feldspar surfaces (Figures 4.4 and 4.5). Upon the fracturing of a silicate mineral crystal, the mineral negative surface charge arises from the breakage of oxygen-metal (e.g. Ca^{2+}, Fe^{3+}, Mg^{2+}) bond, which is almost entirely ionic in character and should break more easily than the stronger oxygen-silicon bond (Deju and Bhappu, 1965). Deju and Bhappu (1965) reported that the ratio of the ionic character of the oxygen-silicon bond is 2.3 times that of the oxygen-carbon bond. The ratio of electronegativity of the two bonds has substantiated

this finding, since it amounts to 51% for the oxygen-silicon bond and only 22% for the oxygen-carbon bond. This means a ratio of 51 to 22, or 2.3 to 1. On this basis, they assumed that the oxygen-silicon bond is the strongest one occurring in silicate minerals.

The lack of change in either the zeta potential curve or the flotation response indicates that the xanthate ions do not adsorb chemically either onto pyroxene and/or feldspar. For the mineral mixtures, however, it does appear that the pyroxene recovery at pH 4 is enhanced in the presence of xanthate (Figure 4.24). This could be attributed to inadvertent activation of pyroxene surfaces by pentlandite dissolution products, such as nickel ions (Figure 4.11), rather than the direct xanthate effect. ToF-SIMS data (Figure 4.51) has shown the presence of Ni ions on pyroxene surfaces. It would appear that pyroxene surfaces have a higher affinity for the metal cations compared to feldspar. The possible cause for the difference in flotation response observed for pyroxene and feldspar could be attributed to the different chemical composition of these siliceous minerals. Pyroxene is predominantly magnesium-iron silicate while feldspar is aluminium-calcium silicate. It is proposed that the higher floatability of pyroxene compared to that of feldspar arises from the magnesium silicate surface patches on pyroxene, which behave in a similar way as naturally hydrophobic talc [$Mg_3(Si_4O_{10})\ (OH)_2$]. It is also possible that iron ions might be exchanged by nickel ions when pyroxene is in a mixture with pentlandite. This results in inadvertent activation of pyroxene. Moreover, a feldspar dissolution study carried out by Tranter and Raiswell (1986) showed that aluminium ions could leach out and precipitate back onto the feldspar surfaces as aluminium hydroxy species. Thus the feldspar surfaces might preferably adsorb aluminium hydroxy species, which originated from the feldspar dissolution, compared to nickel and copper ions and thus a lower degree of inadvertent activation is observed.

Unlike pyroxene and feldspar, pentlandite shows a positive response with the addition of SIBX. In this case, the zeta potentials are more negative across the entire pH range, compared to pentlandite in the absence of SIBX (Figure 4.3). This indicates that chemisorption of xanthate ions onto the pentlandite surfaces is occurring. The reaction between xanthate and a nickel surface site arises from an anodic process involving oxidation of the collector (equations 23, 24), which is coupled to a cathodic process, the reduction of dissolved oxygen (equation 25) at other surface sites to remove the electrons donated by the oxidation process (Hodgson and Agar, 1989).

$$Ni + X^- \rightarrow NiX + e^- \quad (23)$$

$$NiX + X^- \rightarrow NiX_2 + e^- \quad (24)$$

$$O_2 + 2H_2O + 4e^- \rightarrow 4OH^- \quad (25)$$

Hodgson and Agar (1989) also reported, based on their voltametric studies, that the formation of nickel dixanthogen (24) originated from chemisorbed xanthate on the pentlandite surfaces and was occurring concurrently with the adsorption of xanthate on the pentlandite surfaces during the progressive oxidation process. As seen from the zeta potential data, the degree of adsorption decreases with increasing pH until pH 10, i.e. a smaller shift in zeta potential vs. pH curve is observed, where the zeta potentials for pentlandite with and without the addition of SIBX are approximately equal. This trend is attributed to a higher degree of pentlandite surface passivation by nickel and iron hydroxide species with increasing pH, which would hinder xanthate ion adsorption. An increase in the flotation response of pentlandite in the presence of xanthate ions is observed in the single mineral system (Figures 4.7) as well as in the mixed mineral system (Figures 4.31 and 4.34). The higher floatability of pentlandite at pH 4 compared to pH 9 is attributed to the lower iron and nickel hydroxy species surface coverage and a higher xanthate ion concentration on pentlandite surfaces at pH 4.

The data obtained during the study revealed that unlike xanthate adsorption, copper ion adsorption is non-selective, i.e. adsorption onto pentlandite (sulphide mineral) as well as pyroxene and feldspar (siliceous minerals) has been observed. Both silicate and sulphide minerals became more positively charged above pH 4 in the presence of copper (II) ions. The possible mechanisms for copper ion adsorption and inadvertent activation are proposed below. The copper speciation diagram at pH 9 for a solution containing 5×10^{-5} M copper (II) ions is shown in Figure 5.3.

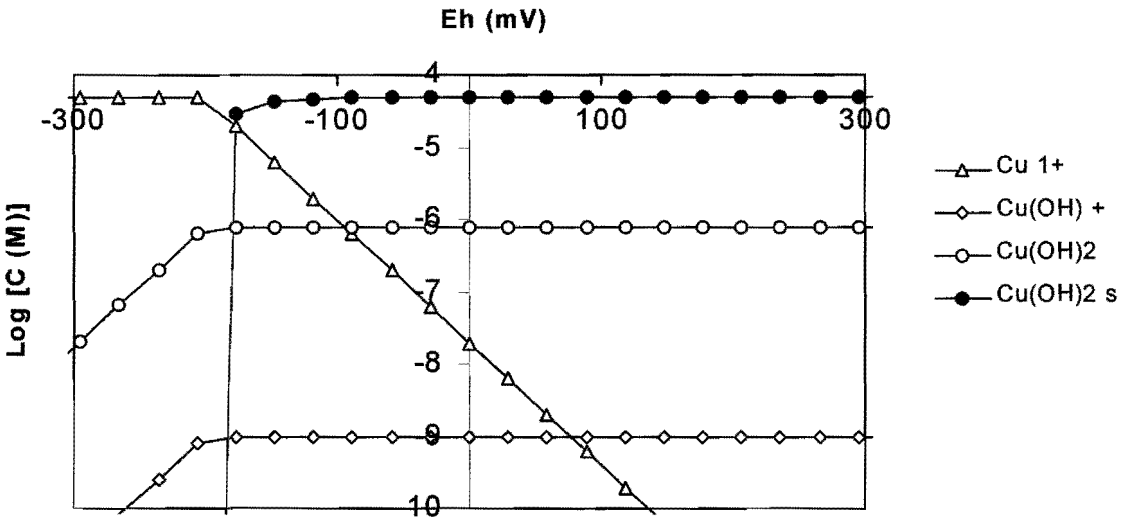

Figure 5.3: Copper Speciation Diagram for pH 9 over a Range of E_h Conditions

At oxidising E_h values (*i.e.* above 0 mV) at pH 9 the solubility of copper (II) ions is approximately equal to the concentration of $Cu(OH)_2$ species in solution which is 7.9×10^{-7} M. The remainder of the copper (II) ions added, i.e. 4.92×10^{-5} M from an initial solution concentration of 5×10^{-5} M, would then be present as $Cu(OH)_2$ precipitate, assuming no adsorption onto the mineral surfaces. $Cu(OH)_2$ precipitate would first appear at about pH 7 (Figure 5.4). Although the data in Figure 5.4 were determined at an E_h of 300 mV, the onset of $Cu(OH)_2$ is not strongly dependent on E_h (Gerson, personal communication). At low pH the positive copper (II) ion species predominate. The adsorption of the positive copper ions at acidic pH onto the negatively charged surface of pyroxene and feldspar would cause the zeta potential to increase relative to untreated pyroxene and feldspar. This is indeed what is observed (Figures 4.4 and 4.5). At high pH, the precipitation of $Cu(OH)_2$ would lead to a marked decrease in zeta potential observed above pH 8, due to the fact that $Cu(OH)_2$ does not carry charge.

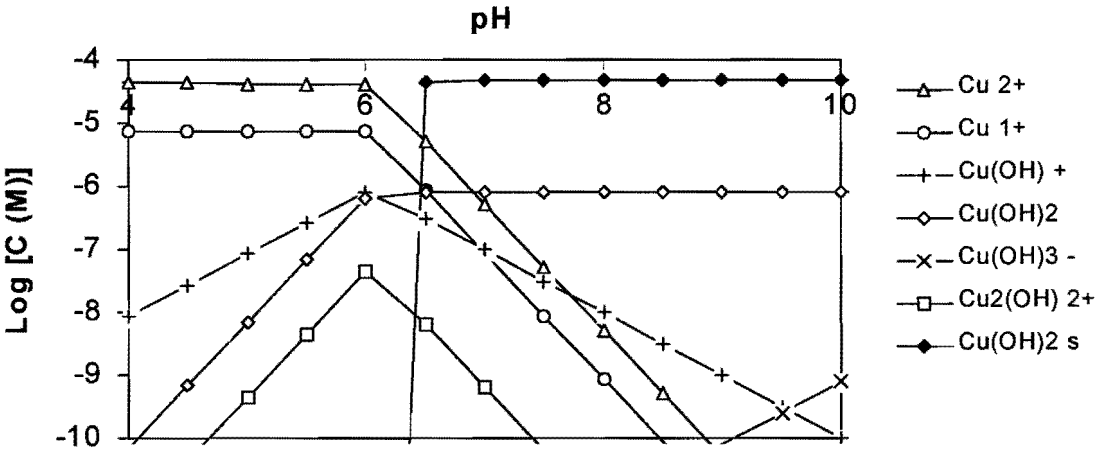

Figure 5.4: Copper Speciation for Copper Concentration of 5 x 10^{-5}M as a Function of pH at Constant E_h of 300 mV

Fuerstenau (1976) reported that adsorption of copper ions onto the quartz surfaces may be a result of hydrogen bonding between adsorbed hydrogen ion and the hydroxy complex (Figure 5.5).

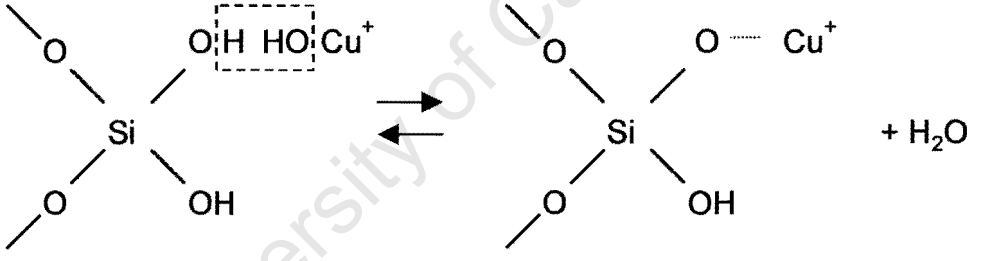

Figure 5.5: Hydrogen Bonding (Copper Ions)

He also proposed that an alternative mechanism could be the adsorption of the hydroxy complex by the formation and splitting out of water (Figure 5.6).

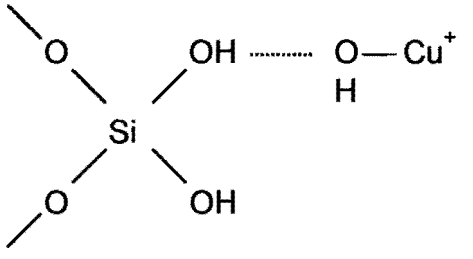

Figure 5.6: Hydroxy Complex Formation (Copper Ions)

The third possible mechanism involves nucleation and growth of a hydroxide precipitate at the surface. These adsorption mechanisms would result in a more positive mineral surface charge. It is assumed, despite the difference in chemical composition between quartz, pyroxene and feldspar, that these mechanisms play a role in copper ion adsorption onto both pyroxene and feldspar surfaces as well. An ion exchange mechanism is ruled out since exchange of e.g. Mg^{2+} for Cu^{2+} would not lead to higher pyroxene and feldspar surface charge observed in the presence of copper (II) ions.

The effect of the presence or absence of copper ions on the zeta potential of pentlandite (Figure 4.3) is not the same as for the silicate minerals. In the case of pentlandite, as for pyroxene and feldspar, the zeta potential curve for the copper (II) ion treated mineral sample is more positive above pH 4 than for the untreated sample. However, the increase in relative zeta potential occurs between pH 4 and pH 6, above which the difference between the two curves remains approximately constant. The positive zeta potential of the untreated pentlandite between pH 4 and 8.5 rules out the possibility of an electrostatic attraction with the positive copper (II) ions, which dominate the copper (II) solution species up to pH 7 (Figure 5.4). At high pH, in the case of the copper (II) ion treated pentlandite, the shape of the zeta potential curve mirrors that of the untreated pentlandite sample. This suggests that the deposition of $Cu(OH)_2$ does not play a significant role in the pentlandite surface alteration. It can therefore be concluded that the copper (II) adsorption processes occurring on the pentlandite surfaces are not the same as those observed for pyroxene and feldspar surfaces. Moreover, the nature of the interaction between the copper (II) ions in solution and the pentlandite surfaces is most likely to be chemical (charge transfer mechanism) rather than electrostatic (attraction between opposite charges). In the case of pentlandite, the adsorption of Cu (II) ions involves an oxidation-reduction reaction during which Cu(II) ion oxidises the sulphur of the mineral ($S^{2-} \rightarrow S_{ox}$) and is itself reduced to Cu(I). The copper ions adsorption inhibits mineral oxidation by stabilisation of chemically reactive sites. The kinetics of the Cu(II) ion adsorption occurs faster than $Cu(OH)_2$ precipitation and thus it is sufficient at high pH to remove enough copper (II) ions from solution to reduce $Cu(OH)_2$ precipitation, which starts at about pH 7 as shown in Figure 5.4. A schematic representation of copper ion adsorption onto the pentlandite surfaces is shown in Figure 5.7.

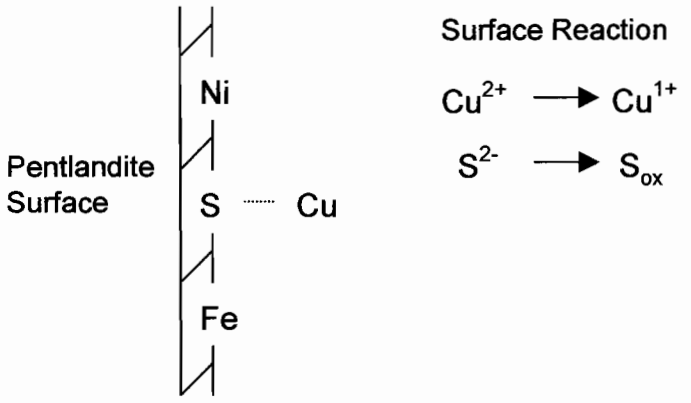

Figure 5.7: Schematic Representation of Copper Ion Adsorption onto Pentlandite

The ToF-SIMS analyses of single minerals indicate that the copper ion surface concentration on the pentlandite surfaces (Figure 4.12) is higher compared to that on the pyroxene (Figure 4.16) and feldspar (Figure 4.20) surfaces. The same trend is observed when the minerals are present in a 1:1 mixture (Figures 4.27 and 4.28). The surface analyses thus demonstrate a higher affinity of copper ions for pentlandite compared to pyroxene and feldspar. This is attributed to the fast kinetics of the Cu(II) ion adsorption onto the pentlandite sulphur sites as well as to a stronger chemical bond in the case of pentlandite.

The zeta potential curves for pyroxene and feldspar treated with copper (II) ion and SIBX are significantly more negative compared to pyroxene and feldspar treated with copper ions only (Figures 4.4 and 4.5). As SIBX on its own did not alter the zeta potential for pyroxene or feldspar, it follows that xanthate ions must be adsorbing onto the copper ion activated mineral surfaces. Nagaraj and Brinen (1996), using XPS, found that copper was present as Cu^{1+} rather than Cu^{2+} after collector treatment of copper activated pyroxene. This suggests that a chemical reaction is occurring during the adsorption of xanthate onto the copper activated pyroxene and feldspar surfaces, which involves the formation of Cu(I)-X complexes. The second possible mechanism could be electrostatic attraction between positively charged copper species and negatively charged xanthate ions. A schematic representation of the xanthate interaction with the copper ion activated silicate mineral surfaces is given in Figure 5.8.

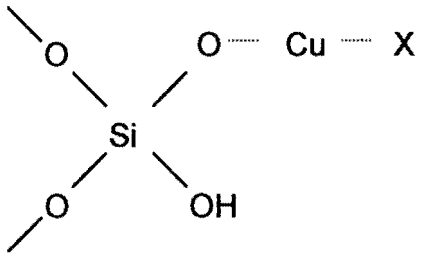

Figure 5.8: Schematic Representation of Xanthate Adsorption onto Copper Activated Silicate Mineral

In the pentlandite system treated with both copper and SIBX ions (Figure 4.3), the shape of the zeta potential curve is almost identical to that of the copper (II) ion treated pentlandite sample but at a zeta potential approximately 20 mV lower. This may indicate that the surface concentration of SIBX remains fairly constant across the pH range studied. In the case of pentlandite a chemical reaction rather than electrostatic attraction between copper and xanthate ions occurs due to a high affinity of xanthate ions for copper (I) ions. As proposed by Hodgson and Agar (1989) it can also be deduced that in the present case copper (II) ions are reduced to Cu(I) ions during the adsorption onto the pentlandite sulphur sites and that subsequently, in the presence of xanthate ions, Cu(I)-X complexes are formed. A shematic representation of xanthate adsorption onto the copper activated pentlandite surfaces is shown in Figure 5.9.

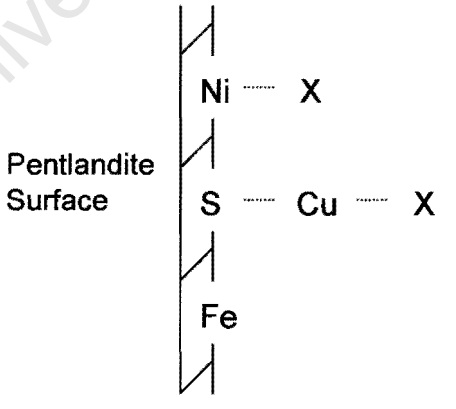

Figure 5.9: Schematic Representation of Xanthate Adsorption onto Copper Activated Pentlandite

To highlight the possible interactions between copper and xanthate ions and the subsequent effect on copper and xanthate speciation, the speciation diagrams for a solution containing 5×10^{-5} M SIBX and copper ions at pH 4 and 9 as a function of E_h are shown in Figures 5.10a and 5.10b, respectively.

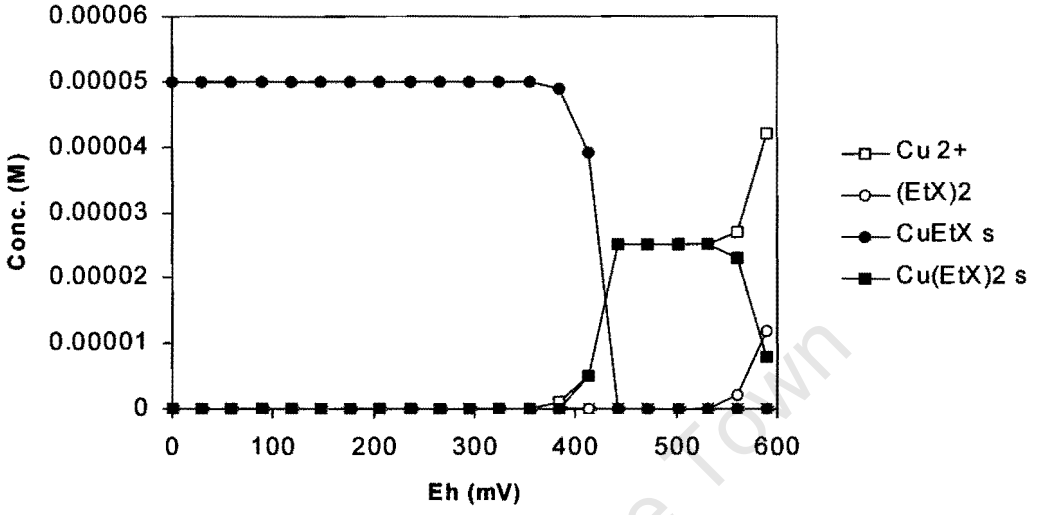

5.10 (a)

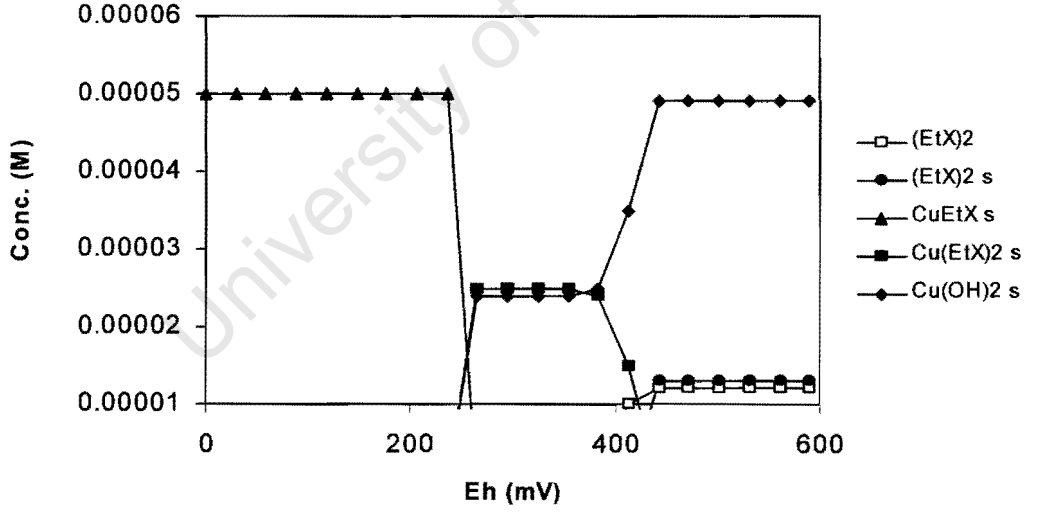

5.10 (b)

Figure 5.10: Speciation Diagrams at (a) pH 4 and (b) pH 9 for 5×10^{-5} M Ethyl Xanthate and Copper

At pH 9, three competing processes are likely to be occurring in terms of copper (II) ions adsorption from solution. It could be a chemical adsorption process in the case of

pentlandite (oxidation-reduction reaction during which Cu^{2+} ion oxidises the sulphur of pentlandite and is itself reduced to Cu^{1+}), or in the case of both pentlandite and silicate minerals electrostatic attraction (attraction between opposite charges) and $Cu(OH)_2$ precipitation (non-selective process at alkaline pH). At pH 4, $Cu(OH)_2$ precipitation does not occur (Figure 5.10 a) and thus only a chemical reaction and electrostatic attraction could play a role in copper (II) ion adsorption onto the mineral surfaces. The predominant copper-xanthate species present at pH 9 is likely to be a mixture of $Cu(OH)_2$ and either Cu(I) and/or Cu(II) xanthate species. Because of the fact that the system is kinetically controlled, copper ions in solution will adsorb readily to the sulphur ions on pentlandite surfaces before any equilibrium concentration of the copper hydroxy species is reached. Residual xanthate ions in solution will then react with the precipitated $Cu(OH)_2$ colloids, which are likely to be converted to hydrophobic Cu(I)-X colloids according to the following mechanism (Gerson, personal communication):

$$[2Cu(OH)_2 \rightarrow 2Cu(II)X_2 \rightarrow 2Cu(I)X + X_2],$$

This is reflected in the single mineral pyroxene and feldspar flotation study carried out at pH 9 where the addition of xanthate ions to the copper (II) ion treated sample resulted in a marked increase in flotation response (Figures 4.8 and 4.9) due presumably to the formation of hyrophobic Cu(I)-X. For pentlandite, although the speciation diagram (Figure 5.4) shows precipitation of $Cu(OH)_2$ at pH 9, kinetically the Cu-S species forms rapidly at the surface before the thermodynamically favoured hydroxy species can form. Thus, contrary to expectations led by the speciation diagrams, the increase in flotation response upon the addition of xanthate ions to the copper (II) ion treated sample is even more profound (Figure 4.7), resulting in a recovery of almost 100%. This is because the adsorbed copper (II) ions (as in the Cu-S species and not the expected precipitated $Cu(OH)_2$ species) complexed with xanthate ions and a higher pentlandite hydrophobicity was achieved.

Comparing the single mineral system (pentlandite, pyroxene, feldspar) to the mineral mixures study (pentlandite-pyroxene, pentlandite-feldspar) in the absence or in the presence of xanthate and copper (II) ions, it was observed that pentlandite recoveries were slightly higher if the mineral was floated in the mixture with pyroxene and/or feldspar

compared to being on its own. The siliceous mineral recoveries were however lower, except in the case of the pyroxene recovery in the presence of copper (II) and xanthate ions. The possible reason for the higher pyroxene recovery is agglomeration between pyroxene and pentlandite particles. This is discussed in Section 5.3. Similar to these observations Chander (1990) found, in the absence of conventional collectors, that the flotation of chalcopyrite and pyrite improved with an increased proportion of quartz in the chalcopyrite or pyrite quartz mixture. He suggested that this behaviour could be attributed to preferential precipitation or adsorption of the metal hydroxides onto the quartz surface. This finding, in the absence of xanthate, can explain the higher pentlandite and lower feldspar and pyroxene recoveries obtained in mineral mixtures compared to those in the single mineral studies. In the presence of copper (II) and xanthate ions, Tof-SIMS analyses obtained on a 1:1 pentlandite-feldspar mixture show preferential adsorption of copper (II) ions (Figures 4.27, 4.28) and xanthate ions (Figures 4.29 and 4.30) onto the pentlandite rather than feldspar surfaces. Thus the preferential adsorption of copper (II) and xanthate ions onto the pentlandite surfaces, in addition to the preferential precipitation or adsorption of the metal hydroxides onto the feldspar surface, resulted in the higher pentlandite and lower feldspar and pyroxene recoveries compared to those obtained in the single pentlandite, pyroxene and feldspar system.

In summary, the results obtained showed that xanthate ions on their own do not adsorb onto the pyroxene and feldspar surfaces. In addition, the data revealed that inadvertent activation by copper ions occurs and if it is followed by xanthate adsorption, true flotation of pyroxene and feldspar is observed. The testwork also showed that the pentlandite recovery is significantly enhanced in the presence of xanthate ions and even more so in the presence of copper (II) and xanthate ions. The pentlandite recovery was higher at the acidic pH compared to the alkaline pH for all scenarios investigated.

5.2 Effect of Water Quality on Floatability with an Emphasis on Calcium Ions

In order to indirectly evaluate the effect that key ions, typically found in circuit water, have on surface alteration, microflotation tests were carried out using the pentlandite-pyroxene and pentlandite-feldspar mixtures. The aim was to determine whether the ions present in process water would interfere with copper and xanthate ion adsorption and distribution on the mineral surfaces as well as establish whether the trends observed in a simple

electrolyte would be valid in a more complex pulp environment prevailing in an industrial flotation cell. During the experiments, the mineral samples were suspended in synthetic water and then the required reagents were dosed.

A comparison between recoveries obtained in di-sodium tetraborate solution as opposed to synthetic water at pH 9 revealed that pentlandite (Figures 4.31 and 4.34) as well as pyroxene (Figure 4.32) and feldspar (Figure 4.33) are all depressed in synthetic water for all scenarios investigated. The most significant effect was observed in the case of presence of copper (II) ions followed by xanthate addition. It is noteworthy that for pentlandite, pyroxene and feldspar the recoveries were reduced from 96% to 53%, 88% to 22% and 22% to 2%, respectively, when compared to those in di-sodium tetraborate solution. The lower recoveries are associated with the formation of a passivating layer on the mineral surfaces (Figure 4.40) due to sorption of the ions present in the synthetic water. The sorption mechanisms, which play a role in surface passivation of the sulphide and siliceous gangue minerals are described below.

It is accepted that sulphide mineral surfaces in a pulp, in the absence or presence of collector, are energetically and chemically heterogeneous and contain a variety of active sites (Ralston, 1991). Ralston also pointed out that the most energetic sites are likely to be hydrophilic. Clusters of water molecules will adhere to the hydrophilic sites. Sulphide mineral surfaces typically consist of hydrophilic and hydrophobic patches and the relative population of each of these mineral sites would influence the sulphide mineral floatability. In the case of this study, all mineral surfaces came into contact with the ions in synthetic water prior to the addition of copper (II) and xanthate ions. Thus e.g. Ca^{2+} and Mg^{2+} ions, which are predominant at the pH range of interest (Figures 5.11 and 5.12) adsorb onto the active sites of all minerals. The possible mechanisms involved in calcium ion adsorption onto all minerals studied are discussed later in this section. When copper (II) ions are subsequently added, most of the active surface sites, especially the high energy sites, are already occupied by the ions which were present in the water and thus a lower degree of copper ion concentration on the mineral surface due to fewer sites being available is observed. This lower degree of chemically adsorbed copper (II) ions onto the pentlandite surfaces will result in a higher concentration in solution of copper ions and hence will result in a higher concentration of the thermodynamically favoured $Cu(OH)_2$ precipitate at alkaline pH (Figure 5.3). As has been discussed in Section 5.1, the hydrophilic precipitate

[$Cu(OH)_2$] would not increase the mineral hydrophobicity as significantly, when compared to the formation of Cu-S bond. The lower hydrophobicity will result in the reduction of the pentlandite floatability.

The main aim of this research was to increase the pentlandite recovery while keeping the flotation of pyroxene and feldspar as low as possible so as to improve the overall selectivity. In order to evaluate this, microflotation tests were carried out on the mineral mixtures in synthetic water in the presence of copper (II) and xanthate ions. In the first instance, flotation at pH 6 resulted in a significant increase in the pentlandite as well as pyroxene recovery compared to pH 9 (Figure 4.35). The higher recovery observed at pH 6 is attributed to a higher degree of copper (II) ion adsorption compared to pH 9 where $Cu(OH)_2$ species is dominant and precipitates on the mineral surface (cf. copper speciation diagram, Figure 5.3). At pHs which do not favour hydroxide formation, and hence precipitation, the formation of Cu(I)-X complexes is enhanced (Wang et al, 1989) and thus hydrophobicity and ultimately floatability increases. At pH 6, feldspar recovery remained virtually unchanged compared to pH 9 and can mostly be attributed to entrainment. These results indicate that feldspar has a lower affinity for copper (II) and nickel (II) ions compared to pyroxene and is therefore less susceptible to inadvertent activation by these ions and thus to recovery due to true flotation. The possible reasons for this phenomenon were discussed in Section 5.1.

The effect, which the concentration of the ions in the water has on floatability was also investigated using the pentlandite-pyroxene mixture, in the presence of xanthate ions at pH 6 and pH 9. Specifically the concentration of calcium ions was increased from 80ppm to 500ppm in synthetic water.

As depicted in the calcium speciation diagram in Figure 5.11, the predominant calcium species over the pH range of interest (up to pH 11) is Ca^{2+}.

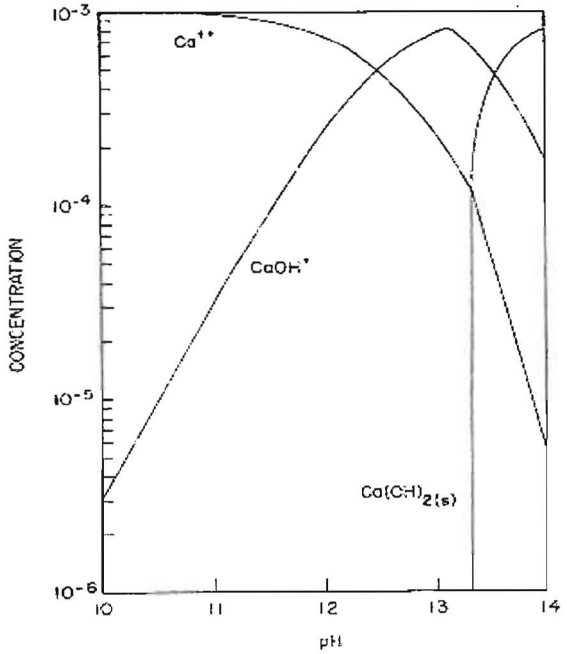

Figure 5.11: Speciation Diagram for 1 x 10^{-3} M Ca^{2+} (Fuerstenau, 1976)

Tof-SIMS data shown in Figure 4.41 clearly demonstrates that adsorption of calcium ions onto the pentlandite surface occurs at both pHs investigated and increases with the increasing calcium concentration. These observations are also supported by the zeta potential data shown in Figure 4.38, where the zeta potential becomes more positive as concentration increases. These observations are consistent with the proposal of Hodgson and Agar (1989) that calcium ions chemisorb onto the pentlandite surface by replacing metal ions (26) and thus changing the stoichiometry of the surface as follows:

$$Fe_{4.5}Ni_{4.5}S_8 + Ca^{2+} \rightarrow (Fe_{4.5-x}Ni_{4.5-x}Ca_{ads}S_8) + xFe^{2+} + xNi^{2+} + (4x - 2)e \qquad (26)$$

The zeta potential determinations of pentlandite in the presence of synthetic water indicate a more positive surface charge at pH 9 compared to pH 6. This would indicate that more calcium ions are exchanging/adsorbing onto the pentlandite surface at pH 9.

Given their chemical similarity between calcium and magnesium ions (See speciation diagrams, Figures 5.11 and 5.12) it is probable that magnesium ions would behave in a similar way to calcium ions. The magnesium speciation diagram is shown in Figure 5.12.

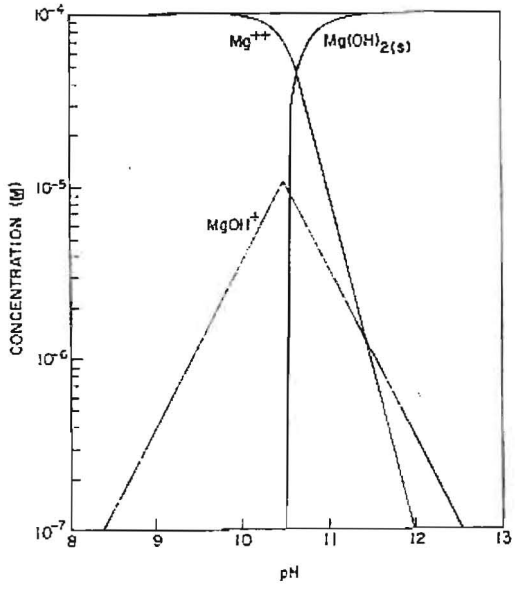

Figure 5.12: Speciation Diagram for 1 x 10^{-4} M Mg^{2+} (Fuerstenau, 1976)

In this study, it was also interesting to observe the changes in the surface concentration of nickel and iron ions on pentlandite (Figure 4.43). At pH 6, the higher calcium concentration increased the iron and decreased the nickel ion surface coverage while at pH 9, there was no significant difference observed either in the iron or the nickel relative % surface abundance with the varying calcium ion concentration. The nickel and iron speciation diagrams are given in Figure 5.13 and Figure 5.14, respectively. The diagrams show that the Ni^{2+}, $NiOH^+$, Fe^{2+} and $FeOH^+$ species are dominant at pH 6, while $Ni(OH)_2$, $NiOH^+$, $Fe(OH)_2$ and $FeOH^+$ species are dominant at pH 9.

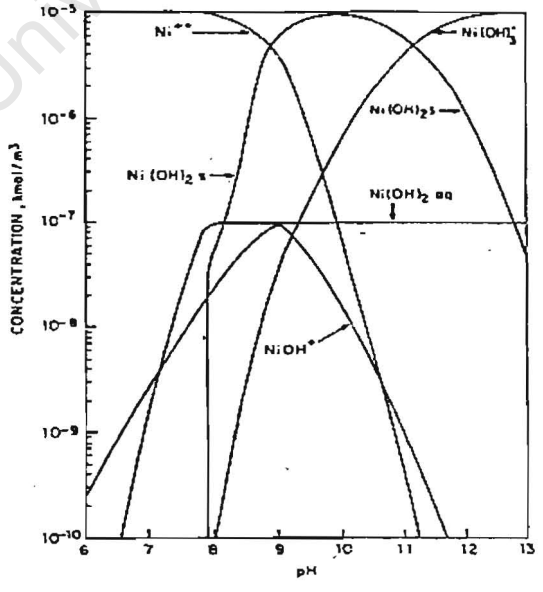

Figure 5.13: Speciation Diagram for 1 x 10^{-5} M Ni^{2+} (Acar and Somasundaran, 1992)

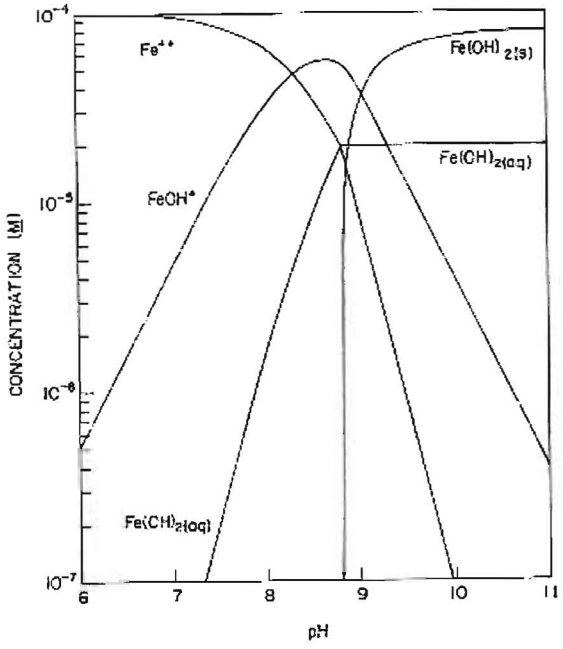

Figure 5.14: Speciation Diagram for 1 x 10^{-4} M Fe^{2+} (Fuerstenau, 1976)

Based on the nickel and iron speciation diagrams, it is proposed that at pH 6 the pentlandite iron ions, which were replaced by the calcium ions, form iron hydroxy overlayers on the pentlandite surfaces. At pH 9, both iron and nickel hydroxy species are re-adsorbing onto the pentlandite surfaces as iron and nickel hydroxy species, thus forming overlayers masking the calcium concentration on the pentlandite surfaces. The relative % abundance of nickel ions on pentlandite surfaces at pH 9 was higher compared to iron ions. This is an opposite trend compared to pH 6. The difference observed could probably be attributed to the lower isoelectric point (iep) of iron oxides and hydroxides [FeO (iep: 6.7-8.2), Fe_3O_4 (iep: 6.5), Fe_2O_3 (eip: 6.7-8.2), FeOOH (iep: 7)] compared to nickel oxides (iep: 10.3) and nickel hydroxides (iep: 11.1) (Acar and Somasundaran, 1992). Thus an iron hydroxy species overlayer is formed at pH 6 while nickel hydroxy overlayer at pH 9.

The microflotation results obtained (Figures 4.36 and 4.37) showed that the lowest pentlandite and pyroxene recovery was obtained at the high calcium concentration of 500 ppm. The lower pentlandite recovery observed with the increased calcium concentration is supported by previous work carried out by Hodgson and Agar (1989). Their voltametric studies showed that Ca^{2+} ions interfere with X^- ions adsorption onto the pentlandite surfaces. This is also consistent with the earlier proposal that Ca^{2+} ions inhibit Cu^{2+} ion

adsorption. As discussed in section 5.1, xanthate ions chemisorb onto the nickel sites. Thus the replacement of nickel ions by calcium ions would reduce the number of nickel surface sites available for xanthate adsorption. This is consistent with the ToF-SIMS data (Figure 4.42), which also showed a lower xanthate surface coverage at the higher calcium ion concentration. Moreover, the xanthate surface coverage was lower at pH 9 compared to pH 6 for both calcium concentrations tested. This phenomenon was discussed in Section 5.1. The other factor contributing to the lower pentlandite recovery could be a higher oxygen mineral surface coverage (Figure 4.42) observed with the increased calcium concentration for both pHs investigated. This would suggest that the mineral surfaces were more oxidised and passivated by metal hydroxy species. Therefore a lower recovery was observed.

In terms of pyroxene, the lower recovery obtained in the synthetic process water indicates that the presence of e.g. Ca^{2+} and Mg^{2+} ions in some way inhibits the possibility of inadvertent activation of pyroxene by the pentlandite dissolution products (Ni^{2+}). This may be associated with the fact that Ca-O (ΔHo = -151850 gram calories per mol) and Mg-O (ΔHo = -144090 gram calories per mol) bonds are thermodynamically stronger than the Ni-O (ΔHo = -57640 gram calories per mol) bond and that thus bonding of Ca and Mg to the oxidic surface of the pyroxene is more favoured than in the case of Ni. [(ΔHo) values from CRC Handbook of Chemistry and Physics (1985-1986)].

In summary, the data obtained during the present study showed that major ions typically found in process water play a significant role in floatability of minerals in a pentlandite-pyroxene and pentlandite-feldspar mixture. Furthermore, the study revealed a higher pentlandite recovery at pH 6 compared to pH 9. This has been explained in terms of the various dominant species in the system at these pHs. For ease of reference the predominant species of elements of interest at pH 6 and pH 9 are summarized in Table 5.2.

Table 5.2: Predominant Species of Elements of Interest at pH 6 and pH 9

Element of Interest	pH 6	pH 9
Fe	Fe^{2+}, $FeOH^{+}$	$Fe(OH)_2$, $FeOH^{+}$
Ni	Ni^{2+}, $NiOH^{+}$	$Ni(OH)_2$, $NiOH^{+}$
Cu	Cu^{2+}	$Cu(OH)_2$
Ca	Ca^{2+}	Ca^{2+}
Mg	Mg^{2+}	Mg^{2+}

The lower mineral floatability observed in the synthetic process water compared to the electrolyte solution is attributed to the formation of passivating layers of the ions present in the water. The lower recovery at pH 9 compared to pH 6 is associated with the formation of nickel, iron and copper hydroxy species. The ions present in the water and the hydroxy species would interfere with xanthate adsorption and thus reduce mineral surface hydrophobicity.

It follows therefore that it is of great importance to carry out tests in water with a composition similar to that existing on a typical concentrator.

5.3 Enhanced Pentlandite-Pyroxene Selectivity

The aim of this study was to maximise pentlandite recovery and simultaneously minimise the percentage pyroxene reporting to the concentrate. The flotation data (Figure 4.35) showed that the pentlandite recovery in synthetic water at pH 6, in the presence of copper and xanthate ions, was similar to that observed in a simple electrolyte at pH 4 and pH 9 (Figure 4.23). However, the pyroxene recovery was also increased at pH 6 compared to pH 9 (Figure 4.35) and thus selectivity between the sulphide and gangue minerals did not improve. The higher pyroxene recovery is probably due to inadvertent copper (II) and nickel (II) ion activation as observed from the ToF-SIMS analysis (Figures 4.52 and 4.51) and zeta potential determinations (Figure 4.50). Both surface analysis techniques provide strong evidence of xanthate ion adsorption onto the copper activated pyroxene surfaces. As discussed above Fe ions also emanate from the pentlandite. In that context, Fuerstenau and Fuerstenau (1982) reported that the first hydroxy complex of iron ions

could also activate pyroxene minerals. Subsequently, the formation of insoluble iron-hydroxy-xanthate compounds could occur (Wang et al, 1989).

The microflotation data (Figures 4.46 and 4.47) obtained in the presence of Cu(II) ions followed by xanthate addition for the pentlandite-pyroxene mixture showed that copper (II) and xanthate ions surface coverage observed is sufficient to induce true flotation of pyroxene for both pHs studied. Up to pH 7, the positive copper (II) ions dominate the copper solution species (Figure 5.4). As shown in Section 5.1, it is proposed that the adsorption of xanthate ions onto copper activated pyroxene at pH 6 is due to hydrogen bonding and the adsorption of the hydroxy complexes by the formation and splitting out of the water. The floatability observed at pH 9 would suggest that copper on pyroxene is reduced from cupric to cuprous upon collector adsorption resulting in the formation of Cu(I)-X complexes, thus rendering these previously hydrophilic colloids hydrophobic as indicated in Section 5.1.

The comparative single pyroxene and mixed pentlandite-pyroxene study carried out in the presence of xanthate ions showed that pyroxene surfaces could also be inadvertently activated by Ni (II) ions as a result of pentlandite dissolution due to superficial oxidation. Buckley and Woods (1991) found that during oxidation of pentlandite, iron was removed from the pentlandite lattice to form a hydrated iron oxide overlayer, which left metal deficient pentlandite in addition to a restructured nickel-iron sulphide. Further oxidation resulted in some nickel being included in the oxide overlayer. Hodgson and Agar (1989) proposed a similar oxidation reaction for pentlandite (27).

$$Fe_{4.5}Ni_{4.5}S_8 \rightarrow (Fe_{4.5-x}Ni_{4.5-x}S_8) + xFe^{2+} + xNi^{2+} + 4xe \qquad (27)$$

ToF-SIMS analyses (Figure 4.51) indicated a higher surface concentration of nickel ions on pyroxene in the presence of pentlandite compared to pyroxene on its own for both pHs studied. The possible mechanisms involved in Ni (II) ion adsorption onto the pyroxene surfaces were described in Section 2.2 (Mackenzie and O'Brien, 1969) and the proposed adsorption mechanisms are shown in Figure 5.15 and 5.16.

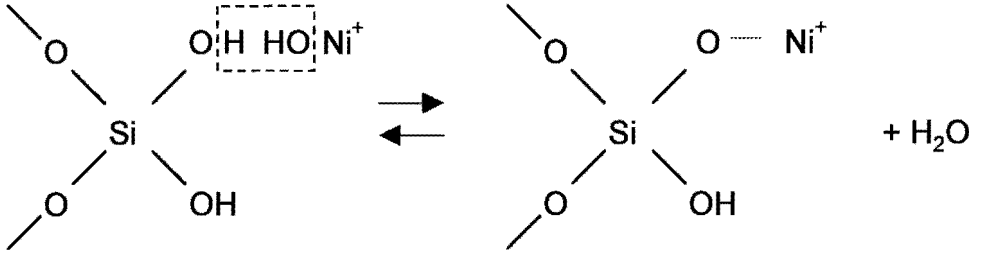

Figure 5.15: Hydrogen Bonding (Nickel Ions)

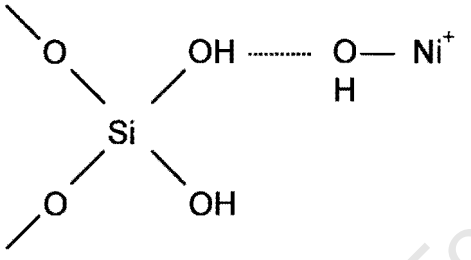

Figure 5.16: Hydroxy Complex Formation (Nickel Ions)

The higher pyroxene recovery observed at pH 6 compared to pH 9 in the mixture with pentlandite is attributed to the higher concentration of positively charged Ni (II) species at the lower pH as seen in the speciation diagram for nickel (Figure 5.13). Xanthate anions could then adsorb onto the $Ni(OH)^+$ sites due to electrostatic attraction.

The zeta potential determinations (Figures 4.49 and 4.50) indicated that not only inadvertent activation but also agglomeration contribute to the recovery of pyroxene. This is due to pentlandite and pyroxene having a surface charge of a similar value in the pH range studied, which promotes slime coating of pyroxene onto pentlandite and also agglomeration of coarser particles. This would contribute not only to a reduction in the concentrate grade but also to a lower pentlandite recovery.

In terms of pentlandite floatability, a higher recovery at pH 6 compared to pH 9 (Figures 4.46 and 4.47) could be attributed to the dissolution of hydroxide overlayers at the lower pH, which resulted in a sulphide-sulphur enriched surface at pH 6. The adjustment of the conditioning pH outside the pH range where metal hydroxides are formed thus leads to an increase in pentlandite hydrophobicity and an improved recovery. In addition, it has been

shown previously in Figure 4.42 that there is a higher xanthate ion surface coverage on pentlandite at pH 6 compared to pH 9. The significant increase in the recovery in the presence of Cu (II) ions followed by the addition of xanthate is attributed to the formation of Cu(I)-X complexes, which would enhance hydrophobicity.

The microflotation results obtained during this study (Figures 4.46 and 4.47) clearly showed that the selectivity between pentlandite and pyroxene was significantly enhanced in the presence of DETA and polyphosphate. Kelebek et al. (1996) has demonstrated that although DETA complexes readily with nickel and copper hydroxide species, it does not compete with the surface lattice Cu-S and Ni-S. In the case of pyroxene, the copper and nickel ions would be present on the mineral surfaces as copper and nickel hydroxides and oxides. Thus it would appear that the mechanism involved is related to the removal of hydroxy species of Ni and Cu from the pyroxene surface due to the formation of metal DETA complexes as described in Section 2.4.

Given that ToF-SIMS is not a quantitative technique, ToF-SIMS analyses of pyroxene grains (Figure 4.52) indicate that the complexing agent reduces the copper and nickel ions on the pyroxene surfaces more significantly at pH 9 compared to pH 6. This could be attributed to the higher concentration of these ions on the pyroxene surfaces at pH 9 prior to the addition of DETA as has been shown from ToF-SIMS data (Figure 4.52). As shown previously (Section 5.2), at pH 9 $Cu(OH)_2$ and $Ni(OH)_2$ precipitation occurs and thus the relative percent abundance of copper (II) and Ni(II) ions on the pyroxene surfaces would be higher compared to pH 6, where the metal cations would bond due to hydrogen bonding or hydroxy complex formation as discussed in Section 5.1.

The zeta potential determinations (Figure 4.50) show a similar trend compared to the ToF-SIMS data. A significant decrease in the pyroxene zeta potential versus pH curve in the presence of copper (II) ions followed by DETA addition also indicated that DETA removes copper (II) species from the mineral surface. The lack of change in the zeta potential versus pH curve with the subsequent addition of xanthate ions indicates no xanthate ion adsorption on pyroxene surface in the presence of copper sulphate and DETA.

A similar pattern, in terms of reduced copper (II) ion concentration in the presence of DETA, was observed for pentlandite above pH 8 (Figure 4.49). The shift to a more

negative surface charge suggests that DETA complexes with Cu (II), Ni (II) and Fe (II) hydroxide and oxide species. The surface charge on pentlandite in the presence of copper sulphate, DETA and xanthate is significantly more negative compared to that obtained with copper sulphate and DETA only. This clearly showed, unlike on pyroxene, that xanthate ions adsorb onto the pentlandite surface.

The difference in the [$CuSO_4$ + DETA] zeta potential versus pH curve at acidic pH for pentlandite and pyroxene can probably be attributed to the nature of the bond of copper onto the sulphide and siliceous mineral. Most of the copper (II) ions would bond to sulphur for pentlandite, while on pyroxene, copper ions would be present as copper hydroxide species. At pH 9, even in the case of pentlandite, some of the copper ions would be present on the mineral surfaces as hydroxides and thus DETA would have the same effect on both minerals investigated as seen from the zeta potential pH curves in Figures 4.50 and 4.51. This is consistent with the observations by Kelebek (1996).

The polyphosphate was added with the aim of reducing slime coating and agglomeration. In the presence of polyphosphate, zeta potential determinations (Figures 4.49 and 4.50) showed a shift in the surface charge to more negative values for both minerals studied. The mineral surfaces thus moved from a region of electrostatic forces of attraction to a region of repulsion. This reduced slime coating and agglomeration between pentlandite and pyroxene particles. Feiler et al. (1999) also found that adsorption of polyphosphate onto the valuable mineral surfaces could significantly hinder the adsorption of slimes. Furthermore, his results showed that in a system where adsorption of the slimes to the valuable minerals has already occurred, addition of polyphosphate caused desorption of the slimes. The critical concentrations of polyphosphate for desorption to occur correlated with the concentration of polyphosphate at which the short-range interparticle forces changed from attractive to repulsive.

In the system studied, polyphosphate also reduced the Cu (II) ion adsorption onto pyroxene and pentlandite at pH 9 (Figures 4.52 and 4.53). As demonstrated in Figure 4.55, polyphosphate significantly reduced the relative % surface abundance of calcium, magnesium, aluminium and silicon ions. The sequestering effect of polyphosphates has been discussed in Section 2.5.

In summary, at pH 6 the introduction of polyphosphate and DETA to the copper (II) and nickel (II) ion activated mineral system resulted in a lower pyroxene floatability, while maintaining a high pentlandite recovery. At pH 9 the combination of polyphosphate and DETA reduced the pentlandite recovery while the pyroxene recovery remained fairly constant, despite having a significantly lower Cu (II) and Ni (II) ions surface coverage on pyroxene. The lower pentlandite recovery at pH 9 could be attributed to a lower copper (II) ion surface coverage with the addition of polyphosphate compared to the copper sulphate and DETA scenario. In terms of pyroxene recovery, it is interesting to note that the lowest pyroxene recovery obtained was 21% in the presence of copper sulphate for both pHs investigated. This might suggest that the recovery of 21% reflects the lowest possible pyroxene recovery, while maintaining a high pentlandite recovery, in the presence of copper sulphate for the system studied.

From an economic point of view, large scale testwork needs to be carried out to evaluate the proposed process with respect to cost versus recovery of the valuable minerals (platinum bearing and sulphide minerals). The potential benefits of this process would also reduce transport and smelting costs.

CHAPTER 6

CONCLUSIONS

The aim of the study was to investigate the extent to which metal ion activation occurs and influences flotation and how this can be managed so as to increase the separation of pentlandite from pyroxene and feldspar. The aim was to minimise the gangue mineral floatability and simultaneously maximise the pentlandite recovery.

At the commencement of this investigation it was hypothesised, on the basis of published findings on similar but different systems, that activation of gangue minerals would occur as a result of the presence of copper (II) and nickel (II) ions followed by xanthate adsorption, which would result in true flotation of the siliceous gangue minerals. The results obtained during the study have clearly demonstrated and confirmed that in the mineral system being investigated here inadvertent activation of the siliceous gangue by heavy metal ions, Cu (II) and Ni (II), contributes significantly to the true flotation of these minerals. The chemical form of the copper and nickel depends on the pH of the solution. ToF-SIMS analyses and zeta potential determinations indicate the presence of xanthate on copper (II) ion activated pyroxene and feldspar surfaces confirming that the inadvertent metal ion adsorption causes the pyroxene and feldspar to be susceptible to xanthate adsorption. In the absence of copper ions, no xanthate ion adsorption was observed. The adsorption of xanthate ions onto copper activated silicate minerals studied at acidic pHs was probably due to electrostatic attraction. In that pH the copper forms the Cu(II) species. In the case of pH 9, the colloidal $Cu(OH)_2$ form on the surface of the siliceous minerals and these are converted to hydrophobic Cu(I)-X in the presence of xanthate as observed by Nagaraj and Brinen (1996), thus increasing hydrophobicity of the gangue minerals. Pyroxene was activated by the metal cations more significantly compared to feldspar in di-sodium tetraborate solution as well as in the synthetic water. There was no true flotation of feldspar observed in the synthetic water for any scenario investigated. It is suggested that the higher floatability of pyroxene compared to that of feldspar arises from the magnesium silicate surface patches on pyroxene, which behave in a similar way as naturally hydrophobic talc. It is also possible that iron ions might be exchanged by nickel ions when pyroxene is in a mixture with pentlandite. This results in inadvertent activation of pyroxene by Ni (II) ions. Moreover, the feldspar surfaces might preferably adsorb aluminium hydroxy

species, which originated from the feldspar dissolution, compared to nickel and copper ions and thus a lower degree of inadvertent activation is observed.

In the case of pentlandite, it was postulated that surface oxidation, valuable-gangue mineral aggregation and formation of passivating layers can all detrimentally affect pentlandite hydrophobicity and, ultimately, recovery. The recovery was significantly enhanced in the presence of xanthate ions and even more so in the presence of copper (II) and xanthate ions. The microflotation results showed that the pentlandite recovery was higher at pH 6 compared to pH 9 for all scenarios investigated. The higher recovery observed at pH 6 compared to that at pH 9 is attributed to a lower metal hydroxide pentlandite surface coverage at the former pH. Thus the pentlandite surface was left with a sulphide sulphur-rich residual surface layer. Therefore, in the presence of copper (II) ions, a higher degree of copper (II) ion adsorption onto the pentlandite sulphide sulphur sites in the form of Cu(I)-S occurred at pH 6 compared to pH 9. At pH 9, although the copper ion speciation diagram shows precipitation of $Cu(OH)_2$, Cu-S species forms more rapidly on the pentlandite surface and thus the system is kinetically and not thermodynamically controlled. Moreover, the results showed a higher xanthate ion surface coverage on penlandite surfaces at pH 6 compared to pH 9. At the pH range in which hydroxide species and thus precipitation is not favoured, the formation of Cu(I)-X complexes is enhanced and thus floatability increased.

It was further hypothesised, on the basis of the findings by Yoon et al. (1995) and Kelebek et al. (1996) in a study investigating pyrrhotite depression in the processing of copper-nickel ores and Edwards et al. (1980) in a study evaluating the effect of slime coating of chrysotile and lizardite on pentlandite flotation, that it would be possible to alleviate the inadvertent activation of gangue minerals by using a complexing agent such as diethylenetriamine and reduce the sulphide-gangue aggregation with the addition of a dispersant (sodium polyphosphate). The microflotation results obtained in the presence of DETA and polyphosphate confirmed the above hypotheses. DETA in combination with polyphosphate greatly reduced pyroxene inadvertent activation, however, the effectiveness was most noticeable at pH 6. The mechanism responsible for the observed selectivity could be explained by the ability of DETA to deactivate Ni (II), Cu (II) and possibly other ions through the formation of stable chelates. Furthermore, DETA reduced the level of surface oxidation products on pentlandite surfaces and also prevented xanthate ion

adsorption onto the copper activated pyroxene surfaces. In the presence of polyphosphate, zeta potential determinations showed a shift in the surface charge to more negative values for both minerals studied. The mineral surfaces thus moved from a region of electrostatic forces of attraction to a region of repulsion. This reduced slime coating and aggregation between pentlandite and pyroxene particles. Polyphosphate also reduced the thickness of the calcium and magnesium passivating layers on pentlandite surfaces. The study has shown that the optimum conditions, in terms of pentlandite recovery and selectivity, comprise the combination of polyphosphate, copper sulphate, DETA and SIBX at pH 6.

It is well known that the nature of process water can influence the flotation of minerals. It was hypothesised that the presence of ions typically found in process water, viz. Ca^{2+} and Mg^{2+} would thus play an important role in flotation. The flotation recoveries for all minerals studied were lower in synthetic process water, which contained these ions compared to those in a simple electrolyte solution. The recoveries were reduced even further with the increased calcium ion concentration in the synthetic process water. The lower floatability of all minerals studied is attributed to the passivation of all mineral surfaces by the ions present in synthetic water, which would adsorb onto the active sites of the minerals and thus interfere with the subsequent adsorption of copper (II), nickel (II) and xanthate ions. This process is non-selective and desirable only in terms of the gangue minerals. In the case of pentlandite, Hodgson and Agar (1989) showed that calcium ions chemisorb onto the pentlandite surface by replacing metal ions and thus changing the stoichiometry of the surface. The zeta potential determinations of pentlandite in the presence of synthetic water indicate that more calcium ions are exchanging/adsorbing on the pentlandite surface at pH 9 compared to pH 6. Due to the chemical similarity between calcium and magnesium ions, it is probable that magnesium ions would behave in a similar way to calcium ions. The higher calcium ion concentration resulted in a lower pentlandite recovery.

In terms of pyroxene, the lower recovery obtained in the synthetic process water may be associated with a lower degree of inadvertent activation of pyroxene by pentlandite dissolution products due to the fact that Ca-O and Mg-O bonds are thermodynamically stronger than the Ni-O bond and thus bonding of Ca and Mg to the oxidic surface of the pyroxene is more favoured than in the case of Ni.

Finally, it is well known that microflotation cell is a useful diagnostic tool for the determination of the relative flotation response of pure minerals and mineral mixtures in frothless, non-turbulent systems. Despite these drawbacks, the study has shown that the microflotation results have significance for flotation due to the fact that the same trends were obtained in a batch cell, which represents a more complex pulp environment prevailing in an industrial flotation cell.

Additional work in this area could focus on the optimisation of DETA and polyphosphate dosages in combination with copper sulphate and xanthate addition. Furthermore, an evaluation of other complexing agents such as triethylenetetramine (TETA), ethylenediaminetetraacetic acid (EDTA) and ethylenediamine (EDA) as well as an investigation of the effect of polyphosphate chain length on a mineral grade-recovery relationship should be carried out. It is also suggested to study further the role that various ions present in process water (e.g. Mg^{2+}, SO_4^{2-}) play in mineral surface alteration and subsequently in flotation.

LIST OF REFERENCES

Acar, S. and Somasundaran, P., 1992. Effect of dissolved mineral species on the electrokinetic behaviour of sulphides. Minerals Engineering, Vol. 5, No.1, pp. 27-40.

Agar, G.E., Kipkie, W.B. and Wells, P.F., 1982. The separation of chalcopyrite and pentlandite from INCO Metals' Sudbury area ores. XIV International Mineral Processing Congress, Toronto, Canada, pp. IV-1.1- 1.12.

Bandini, P., Prestidge, C.A. and Ralston, J., 2000. Colloidal iron oxide slime coatings and galena particle flotation. Flotation 2000, Adelaide, Australia, Conference Abstracts, pp. 36-38.

Barskii, L.A., Rybas, V.V., Fat'yanova, M.A. and Ponomarev, G.P., 1986. Influence of sulphur-containing ions on selective flotation of copper-nickel ores. Fiziko-Tekhnicheskie Problemy Razrabotki Poleznykh Iskopaemykh, No.4, pp. 99-106.

Bolin, N.J., 1983. A study of feldspar flotation. Erzmetall, 36(9):427-432.

Boyd, D.A., 1979. An investigation into electron spectroscopy as a means of studying the chemistry of froth flotation. Johnson Matthey Report No. 78J1.

Bozkurt, V., Xu, Z. and Finch, J.A., 1997. Pentlandite/pyrrhotite interaction: xanthate adsorption in presence of Ni ions. In Processing of complex ores. Ed. J.A. Finch, S.R. Rao and I. Holubec, CIM, Montreal, pp. 101-114.

Bozkurt, V., Xu, Z. and Finch, J.A., 1998. Xanthate adsorption on pentlandite and pyrrhotite: Effect of mineral interactions. In Innovations in mineral and coal processing, Ed. Atak, Onal and Celik, Rotterdam, pp. 93-98.

Bozkurt, V., Xu, Z. and Finch, J.A., 1999. Effect of depressants on xanthate adsorption on pentlandite and pyrrhotite: single vs. mixed minerals. Canadian Metallurgical Quarterly, Vol. 38, No. 2, pp. 105-112.

Bradshaw, D.J., 1997. Synergistic effects between thiol collectors used in the flotation of pyrite. PhD Thesis, University of Cape Town.

Bradshaw, D.J. and O'Connor, C.T., 1996. Measurement of the sub-process of bubble loading in flotation. Minerals Engineering, Vol. 9, No. 4, pp. 443-448.

Broomhead, J.A. and Layers, G., 1976. Leaching studies with pentlandite and pyrrhotite. Proc. Australas. Inst. Min. Metall., No. 259, pp. 19-22.

Buckenham, M. H. and Rogers, J., 1954. Flotation of quartz and feldspar by dodecylamine. Trans. Instn. Min. Metall, 64, pp. 11-30.

Buckley, A.N. and Woods, R., 1991. Surface composition of pentlandite under flotation-related conditions. Surface and Interface Analysis, Vol. 17, pp. 675-680.

Chaberek, S. and Martell, A.E., 1959. Organic sequestering agents. John Wiley & Sons, Inc., New York.

Chander, S., 1990. Floatability of pyrite in the absence of conventional collectors. Paper presented at the Spring Information Transfer Session, May 17-18, Pennsylvania State University, University Park, PA.

Changgen, Li and Yongxin, Lu, 1983. Selective flotation of scheelite from calcium minerals with sodium oleate as a collector and phosphates as modifiers. II. The mechanism of the interaction between phosphate modifiers and minerals. International Journal of Mineral Processing, 10, pp. 219-235.

Clarke, P., Fornasiero, D., Ralston, J. and Smart, R.St.C., 1995. A study of the removal of oxidation products from sulphide mineral surfaces. Minerals Engineering, Vol. 8, No.11, pp. 1347-1357.

Corbridge, D.E.C., 1990. Phosphorus: An outline of its chemistry, biochemistry and technology. 4th Eddition, Elsevier, Amsterdam.

CRC Handbook of Chemistry and Physics, 66th edition 1985-1986, Editor-in-Chief R.C. Weast, CRC Press, Inc. Boca Raton, Florida

Deju, R.A. and Bhappu, R.B., 1965. Surface properties of silicate minerals. State Bureau of Mines and Mineral Resources, New Mexico Institute of Mining and Technology, Circular 82, pp. 1-6.

Deju, R.A. and Bhappu, R.B., 1966. A chemical interpretation of surface phenomena in silicate minerals. Society of Mining Engineers, December, pp. 329-332.

de Vaux. D., 1997. An introduction to Time of Flight Secondary Ion Mass Spectrometry. Anglo bi-annual operations director's technical seminar.

Edwards, C.R., Kipkie, W.B. and Agar, G.E., 1980. The effect of slime coatings of the serpentinite minerals, chrysotile and lizardite, on pentlandite flotation. International Journal of Mineral Processing, 7, pp. 33-42.

El-Salmawy, M.S., Nakahiro, Y. and Wakamatsu, T., 1993. The role of alkaline earth cations in flotation separation of quartz from feldspar. Minerals Engineering, Vol. 6, No.12, pp.1231-1243.

Eriksson, G., 1979. An algorithm for the computation of aqueous multi-component multiphase equilibria. Anal. Chem. Acta 112, pp. 375-383.

Feiler, A., Jenkins, P. and Ralston, J., 1999. Modification of particle adsorption and desorption processes using polyphosphates with reference to the management of "slimes" in mineral processing operations. Polymers in Mineral Processing, Edited by J.S. Laskowski, Quebec City, pp. 123-137.

Finkelstein, N.P. and Allison, S.A., 1976. The chemistry of activation, deactivation and depression in the flotation of zinc sulphide: a review. In Fuerstenau, M.C. (Ed.), A.M. Gaudin Memorial Volume, Flotation. 1: American Institute of Mining, Metallurgical and Petroleum Engineers, New York, pp. 414-451.

Finkelstein, N.P., 1997. The activation of sulphide minerals for flotation: a review. International Journal of Mineral Processing, 52, pp. 81-120.

Forssberg, K.S.E. and Jonsson, H., 1981. Absorption of heavy metal ions on pyrrhotite. Scandinavian Journal of Metallurgy, Vol. 10, pp. 225-230.

Forssberg, K.S.E., Antti, B.M. and Palsson, B.I., 1984. Computer-assisted calculations of thermodynamic equilibria in the chalcopyrite-ethyl xanthate system, Reagents in the minerals industry, edited by Jones, M.J. and Oblatt, R., The Institution of Mining and Metallurgy, pp. 251-264.

Forward, F.A., Veltman, H. and Vizsolyi, A., 1960. Production of high purity lead by amine leaching. Proc. International Mineral Processing Congress, London: IMM, pp. 823-837.

Fuerstenau, M.C., 1975. Role of metal ion hydrolysis in oxide and silicate flotation systems. Advances in Interfacial Phenomena, AICHE Symposium Series, No. 150, Vol.71, pp.16-23.

Fuerstenau, M.C., 1976. Flotation. A.M. Gaudin Memorial Volume, Volume 1, Published by American Institute of Mining, Metallurgical, and Petroleum Engineers, Inc., New York, pp. 148-196.

Fuerstenau, M.C., Palmer, B.R. and Gutierrez, B., 1977. Mechanisms of flotation of selected iron-bearing silicates. Society of Mining Engineers, Vol. 262, pp. 234-236.

Fuerstenau, D.W., 1982. Activation and flotation of sulphide minerals. Principles of Flotation, ed. R.P. King, South African Institute of Mining and Metallurgy, Johannesburg, pp. 188-198.

Fuerstenau, D.W. and Fuerstenau, M.C., 1982. The flotation of oxide and sulphide minerals. Principles of Flotation, ed. R.P. King, South African Institute of Mining and Metallurgy, Johannesburg, pp. 109-158.

Fuliang, W. and Fenglou, Li, 1997. Study of influence of calcium and magnesium ions on floatability of galena. Mining and Metallurgy, Vol. 6. No. 4, pp. 30-37.

Fullston, D., Fornasiero, D. and Ralston, J., 1998. Zeta potential study of the oxidation of copper sulphide minerals. Colloids and Surfaces, A: Physicochemical and Engineering Aspects, pp. 1-9.

Gaudin, A.M., Fuerstenau, D.W. and Mao, G.W., 1959. Activation and deactivation studies with copper on sphalerite. Mining Engineering, SME, 11, pp. 430-436.

Gerson, A., 2002. Personal Communication

Hayes, R.A., 1987. The effect of E_h on the collectorless flotation of sulphide minerals. M. Appl. Sci. Thesis, South Australian Institute of Technology, Adelaide, Australia.

Healy and Trahar, 1989. Challenges in Mineral Processing, ed. by K.V.S. Sastry and M.C. Fuerstenau, pp. 3-14, AIME, Littleton, CO.

Heiskanen, K., Kirjavainen, V. and Laapas, H., 1991. Possibilities of collectorless flotation in the treatment of pentlandite ores. International Journal of Mineral Processing, 33, pp. 263-274.

Heyes, G.W. and Trahar, W.J., 1984. The flotation of pyrite and pyrrhotite in the absence of conventional collectors. Electrochemistry in Mineral and Metal Processing, P.E. Richardson, et al., Ed., Vol. 84-10, The Electrochem. Soc., Inc. Pennington, NJ, pp. 219-232.

Hodgson, M. and Agar, G.E., 1989. Electrochemical investigations into the flotation chemistry of pentlandite and pyrrhotite: Process water and xanthate interactions. Canadian Metallurgical Quarterly, Vol. 28, No.3, pp. 189-198.

Hudiburgh, G.W. and Clifford, K.R., 1976. Amine flotation of feldspar from a magnetite concentrate. Society of Mining Engineers, AIME, Vol. 260, pp. 161-165.

Hunter, R.J., 1993. Introduction to modern colloid science. Oxford University Press.

Huynh, L., Feiler, A., Michelmore, A., Jenkins, P. and Ralston, J., 2000. Control of slime coatings by the use of anionic phosphates: A fundamental study. Flotation 2000, Adelaide, Australia, Conference Abstracts, pp. 41-43.

Ishihara, T. and Kagami, Y., 1964. Nippon Kogyo Kaishi, 80:881.

Jonassen, H.B. and Dexter, T.H., 1949. Inorganic complex compounds containing polydentate groups. I. The complex ions formed between copper (II) ions and ethylenediamine. Journal of the American Chemical Society, Issue 71, pp. 1553-1556.

Joy, A.S., Manser, R.M., Lloyed, K. and Watson, D., 1966. Flotation of silicates - 2. Adsorption of ions on feldspar in relation to its flotation response. Trans. Instn. Min. Metall., 75, C81-86.

Kakovskii, I.A., 1957. Physical properties of some flotation reagents and their salts with ions of heavy non-ferrous metals. Proc. 2nd Int. Conf. Surface Activity, London, pp. 225-237.

Kakovskii, I.A. and Arashkevich, V.M., 1968. The study of properties of organic disulphides. Preprint, VIIIth I.M.P.C., Leningrad.

Kartio, I.J., Basilio, C.I. and Yoon, R.H., 1996. An XPS study of sphalerite activation by copper. In Woods, R., Doyle, F., Richardson, P.E. (Eds.), Electrochemistry in Mineral and Metal Processing IV, The Electrochemical Society, pp. 25-34.

Kelebek, S., 1993. The effect of oxidation on the flotation behaviour of nickel-copper ores. XVIII International Mineral Processing Congress, Sydney, 23-28 May, pp. 999-1005.

Kelebek, S., 1996. Effect of polyamines on mineral separation of nickel-coppper ores: chelation equilibria in collectorless flotation with DETA. Trans. Instn. Min. Metall. (Sect. C: Mineral Process. Extr. Metall.), 105, pp. C75-C81.

Kelebek, S., Wells, P.F. and Fekete, S.O., 1996. Differential flotation of chalcopyrite, pentlandite and pyrrhotite in Ni-Cu sulphide ores. Canadian Metallurgical Quarterly, Vol. 35, No.4, pp. 329-336.

Kirjavainen, V., Schreithofer, N. and Heiskanen, K., 2002. Effect of calcium and thiosulfate ions on flotation selectivity of nickel-copper ores. Minerals Engineering, 15, pp. 1-5.

Klein, C. and Hurlbut, Jr. C.S., 1985. Manual of mineralogy (after J. D. Dana), 20th Edition, John Wiley & Sons, Inc.

Legrand, D.L., Bancroft, G.M. and Nesbitt, H.W., 1997. Surface characterization of pentlandite, $(Fe,Ni)_9S_8$, by X-ray photoelectron spectroscopy. International Journal of Mineral Processing, 51, pp. 217-228.

Lindsay, W.L., 1979. Chemical equilibria in solids, John Wiley and Sons, New York.

Liu, L., Rao, S.R. and Finch, J.A., 1993. Laboratory study of effect of recycle water on flotation of a Cu/Zn sulphide ore. Minerals Engineering, Vol. 6, No.11, pp. 1183-1190.

Mackenzie, J.M.W. and O'Brien, R.T., 1969. Zeta potential of quartz in the presence of nickel (II) and cobalt (II). Society of Mining Engineers, Vol. 244, pp. 168-173.

Malvern Instruments, 1996. PCS Training Manual, Issue 1.3.

Marticorena, M.A., Liechti, D. and Kerr, A.N., 1995. The role of diethylenetriamine as a gangue sulphide depressant. Proc. Copper 95-Cobre 95 International Conference, Volume II – Mineral Processing and Environment, (Eds.) A. Casali, G.S. Dobby, M. Molina and W.J. Thoburn, The Metallurgical Society of CIM.

McNeil, M. Rao, S.R. and Finch, J.A., 1994. Technical Note, Oxidation of amyl xanthate by pentlandite. Canadian Metallurgical Quarterly, Vol. 33, No.2, pp. 165-167.

Michelmore, A., Gong, W., Jenkins, P., Schumann, R. and Ralston, J., 1999. The influence of polyphosphates in modifying the surface behaviour and interactions of metal oxide particles. Polymers in Mineral Processing, Edited by J.S. Laskowski, Quebec City, pp. 231-245.

Nagaraj, D.R. and Brinen, J., 1995. SIMS study of metal ion activation in gangue flotation. Proceedings XIX International Mineral Processing Congress, SME, Chapter 43, pp. 253-257.

Nagaraj, D.R. and Brinen, J., 1996. SIMS and XPS study of the adsorption of sulphide collectors on pyroxene: a case for inadvert metal in activation. Colloids and Surfaces, A: Physicochemical and Engineering Aspects 116, pp. 241-249.

Perry, D.L., Tsao, L. and Taylor, J.A., 1984. Surface studies of the interaction of copper ions with sulphide minerals. In Electrochemistry in Minerals and Metal Processing, Electrochemical Society, Pennington, pp. 169-184.

Prestidge, C.A., Thiel, A.G., Ralston, J. and Smart, R.St.C., 1994. The interaction of ethyl xanthate with copper (II)-activated zinc sulphide: Kinetic effects. Colloids Surface, A. Physicochem. Eng. Aspects, 85, pp. 51-68.

Prestidge, C.A., Skinner, W.M., Ralston, J. and Smart, R.St.C., 1997. Copper (II) activation and cyanide de-activation of zinc sulphide under mildly alkaline conditions. Appl. Surf. Sci., 108, pp. 333-344.

Ralston, J. 1991. E_h and its consequences in sulphide mineral flotation. Minerals Engineering, Vol. 4, Nos. 7-11, pp. 859-878.

Ralston, J., Alabaster, P. and Healy, T.W., 1981. Activation of zinc sulphide with Cu (II), Cd (II), and Pb (II): III. The mass spectrometric determination of elemental sulphur. International Journal of Mineral Processing, 7, pp. 279-310.

Rao, S.R. and Finch, J.A., 1991. Adsorption of amyl xanthate at pyrrhotite in the presence of nitrogen and implications in flotation. Canadian Metallurgical Quarterly, Vol. 30, No. 1, pp. 1-6.

Rao, S.R., Xu, Z. and Finch, J.A., 1995. Selective solubilization of Zn (II), Cu (II), Ni (II) and Fe (III) in metal hydroxide sludges by diethylenetriamine. Waste processing and recycling in mineral and metallurgical industries II. Rao S.R. et al. (Eds.) (Montreal: CIM), pp. 69-77.

Rashchi, F. and Finch, J.A., 2000. Polyphosphates: A Review. Their chemistry and application with particular reference to mineral processing. Minerals Engineering, Vol. 13, No.10-11, pp. 1019-1035.

Rashchi, F. and Finch, J.A., 2002. Lead-polyphosphate complexes. Canadian Metallurgical Quarterly, Vol.41, No. 1, pp. 1-6.

Reich, F., 1997. The operators Guide for the 2100 TRIFT II ToF SIMS", Physical Electronics.

Ribbe, P.H., 1975. Feldspar Mineralogy. Mineralogical Society of America, Short Course Notes, Volume 2, Edited by P.H. Ribbe.

Richardson, S. and Vaughan, D.J., 1989. Surface alteration of pentlandite and spectroscopic evidence for secondary violarite formation. Mineralogical Magazine, Vol. 53, pp. 213-22.

Schueler, B.W., 1992. Microscope imaging by time of flight secondary ion mass spectrometry. Microsc. Microanal. Microstruct. 3, pp. 119-139.

Shehu, N. and Spaziani, E., 1999. Separation of feldspar from quartz using EDTA as modifier. Minerals Engineering, Vol. 12, No. 11, pp. 1393-1997.

Shimoiizaka, J., Nakatsuka, K., and Katayanagi, T., 1978. In Weiss, A. (Ed.): World Mining and Metals Technology. Baltimore, Port City Press, pp. 423-428.

Smart, R.St.C., 1994. Chemical and structural alteration in the surface layers of oxides. In Science of ceramic interfaces II, Ed. J. Nowotny, Elsevier Science, pp. 311-339.

Thornber, M.R., 1983. Mineralogical and electrochemical stability of the nickel-iron sulphides-pentlandite and violarite. Journal of Applied Electrochemistry, 13, pp. 253-267.
Trahar, W.J., 1983. In Principles of Flotation, The Wark Symposium.

Trahar, W.J., 1984. The influence of pulp potential in sulphide flotation. In M.H. Jones and J.T. Woodcock (Editors), Principles of Mineral Flotation, The Wark Symposium, Australasian Institute of Mining and Metallurgy, Symposia Series No. 40, Melbourne, pp. 117-135.

Tranter, M. and Raiswell, R., 1986. Electrophoretic mobility variations during feldspar dissolution. Materials Science Forum, Vol. 7, pp. 275-286.

Van Wazer, J.R. and Callis, C.F., 1958. Metal complexing by phosphates. Chemical Review, 58, pp. 1011-1046.

Vreughenhil, A., Markwell, R., Finch, J.A. and Butler, I., 1997. Formation and characterization of nickel-DETA complexes related to flotation systems. Met. Soc., CIM, Sudbury, pp. 283-289.

Wang, X., Forssberg, K.S.E. and Bolin, N.J., 1989a. Thermodynamic calculations on iron-containing sulphide mineral flotation systems, I. The stability of iron-xanthate. International Journal of Mineral Processing, 27, pp. 1-19.

Wang, X., Forssberg, E. and Bolin N.J., 1989b. Scand. J. Met. 18, pp. 243-272.

Wang, X., Forssberg, E. and Bolin N.J., 1989c. The aqueous surface chemistry of activation in the flotation of sulphide minerals – A review. Part II: A surface precipitation model. Miner. Process. Ext. Met. Rev. Vol. 4, pp. 167-199.

Wanxiong, C.J.C. and Zhenghe, X., 1986. Adsorption and flocculation behaviours of ilmenite and feldspar in the presence of sulphonated polyacrylamide. J. CSIMM, 12:86-93.

Warren, L.J. and Kitchener, J.A., 1972. Role of fluoride in the flotation of feldspar: 7adsorption on quartz, corundum and potassium feldspar. Instit. of Mining and Metallurgy, C137- C147.

Wesseldijk, Q.I., Reuter, M.A., Bradshaw, D.J. and Harris, P.J., 1999. The flotation behaviour of chromite with respect to the beneficiation of UG2 ore. Minerals Engineering, Vol. 12, No. 10, pp. 1177-1184.

Xu, Z., Rao, S.R., Finch, J.A., Kelebek, S. and Wells, P., 1997. Role of diethylene triamine (DETA) in pentlandite-pyrrhotite separation-Part 1: Complexation of metals with DETA. Trans. Instn Min. Metall. (Sect.C: Mineral Process. Extr. Metall.), 106, pp. C15-C20.

Yoon, R.H., Basilio, C.I., Marticorena, M.A., Kerr, A.N. and Stratton-Crawley, R., 1995. A study of the pyrrhotite depression mechanism by diethylenetriamine. Minerals Engineering, Vol. 8, No. 7, pp. 807-816.

APPENDIX A: Xanthate and Copper Surface Coverage Calculations

It is instructive to carry out semi-quantitative exploratory calculations of estimates of the particle surface coverage by various reagents. The case of copper sulphate and xanthate used during the study is shown below as an example. The calculations are based on a surface area required per copper and xanthate atoms for possible uptake.

Mineral Surface Area Determined Using BET Method:

Pyroxene:	$0.59\ m^2/g = 0.59 \times 10^{20}\ Å^2/g$
Feldspar:	$0.85\ m^2/g = 0.85 \times 10^{20}\ Å^2/g$
Pentlandite:	$0.30\ m^2/g = 0.30 \times 10^{20}\ Å^2/g$
1:1 Pentlandite-Pyroxene Mixture:	$0.89\ m^2/2g = 0.89 \times 10^{20}\ Å^2/2g = 0.45 \times 10^{20}\ Å^2/g$
1:1 Pentlandite-Feldspar Mixture:	$1.15\ m^2/2g = 1.15 \times 10^{20}\ Å^2/2g = 0.58 \times 10^{20}\ Å^2/g$

Copper Surface Coverage:

Cu Concentration:	$5 \times 10^{-5}\ mol.dm^{-3}$
Grams of Cu in 250 cm^3 (cell volume):	8×10^{-4}
Number of Cu Moles:	$8 \times 10^{-4}/63.5 = 1.2598 \times 10^{-5}$
Number of Cu Atoms:	$1.2598 \times 10^{-5} \times 6.023 \times 10^{23} = 7.5878 \times 10^{18}$

Gaudin et al. (1959) assumed that the possible copper uptake for sphalerite was one atom for each 20.8 $Å^2$. Assuming that the same copper surface area is relevant for the pentlandite-pyroxene and pentlandite-feldspar mixture uptake, the required surface area for pseudo-monolayer coverage would be:

$$7.5878 \times 10^{18} \times 20.8\ Å^2 = 1.5783 \times 10^{20}\ Å^2/g$$

This implies that 3.5 and 2.7 pseudo-monolayers of copper could be formed on pentlandite-pyroxene and pentlandite feldspar mixtures, respectively.

Xanthate Surface Coverage:

Xanthate Concentration:	$5 \times 10^{-5}\ mol.dm^{-3}$
Grams of Xanthate in 250 cm^3:	1.9×10^{-3}
Number of Xanthate Moles:	$1.9 \times 10^{-3}/149 = 1.2752 \times 10^{-5}$
Number of Xanthate Atoms:	$1.2752 \times 10^{-5} \times 6.023 \times 10^{23} = 7.6805 \times 10^{18}$

Bradshaw (1997) assumed that the possible thiol collector uptake for pyrite is one atom for each 37 $Å^2$. Assuming that the same xanthate surface area is relevant for the pentlandite-pyroxene and pentlandite-feldspar mixture uptake, the required surface area for pseudo-monolayer coverage would be:

$$7.6805 \times 10^{18} \times 37\ Å^2 = 2.8418 \times 10^{20}\ Å^2/g$$

This implies that 6.3 and 4.9 pseudo-monolayers of xanthate could be formed on pentlandite-pyroxene and pentlandite feldspar mixtures, respectively.

APPENDIX B: Zeta Potential Determination Procedure

A detailed zeta potential determination procedure used throughout the study is shown below. This procedure was used to ensure accuracy and repeatability of zeta potential data.

- Crush 0.3 g of a mineral sample to 100% -25µm in an agate mortar and pestle.
- Add 240 cm^3 of $Na_2B_4O_7$ solution (0.001M) and/or synthetic water.
- Stir well and split into 4 beakers (60 cm^3).
- Adjust pH to 4, 6, 8 and 10 with Na_2CO_3 or HCl.
- Condition for 20 minutes.
- Measure electrophoretic mobility, (volume used +/- 10 cm^3).
- Add reagent, e.g. copper sulphate (5×10^{-5}M), and condition for 5 minutes.
- Measure electrophoretic mobility.

APPENDIX C: Microflotation Test Procedure

The microflotation test procedure, given below, was followed during the study in order to obtain reproducible data.

- For a single mineral study, weigh 2 grams of a mineral sample after crushing and screening (38-106µm size fraction). For mineral mixtures study, weigh 1 gram of each mineral after crushing and screening (38-106µm size fraction).
- Add the mineral sample to 50 cm^3 of $Na_2B_4O_7$ solution and/or synthetic water adjusted to the desired pH.
- Transfer the solution to the microflotation cell and fill the cell to just below the overflow lip.
- Circulate pulp with peristaltic pump, set at 60 rpm / 1 min.
- Condition for 1 minute, add reagents as required and condition for the time required.
- Top up the cell volume to 250 cm^3, put cone in place and introduce the air (5 cm^3/min) through a syringe at the base of the cell.
- Remove the syringe and collect flotation products after:
  - 3 min - 1st Conc.
  - 20 min - 2nd Conc.
- Collect tailings sample.
- Filter each product on weighed filter paper and rinse with deionised water adjusted to the desired pH.
- Dry under argon if ToF-SIMS analysis is required.
- Conditioning times used during the study:
  - SIBX: 2 min
  - $CuSO_4$: 5 min
  - DETA: 5 min
  - Polyphosphate: 5 min

An example of microflotation test spreadsheet is shown below:

Pentlandite + Pyroxene, SIBX, Synthetic water, pH 9

Product	Mass (FP)	Mass (FP+S)	Mass (S)	Mass Pull	S		Pentlandite	Pentl. Rec.	Pyroxene	Pyrox.Rec.
	g	g	g	%	%		g	%	g	%
Concentrate 1	0.0000	0.0000	0.0000	0.00	0	0.0000	0.0000	0.00	0.0000	0.00
Concentrate 2	2.7470	3.1212	0.3742	18.80	26.21	82.8775	0.3101	30.95	0.0641	6.48
Tailings	1.3952	3.0112	1.6160	81.20	13.54	42.8142	0.6919	69.05	0.9241	93.52
			1.9902	100.00			1.0020	100.00	0.9882	100.00
Total Concentrate			0.3742	18.80				30.95		6.48

APPENDIX D: Example of ToF-SIMS Analysis Spreadsheet

A typical ToF-SIMS automated spectra evaluation report is shown below. The intensities obtained would be normalised for the elements of interest and presented as a relative percent surface coverage.

AUTOMATED SPECTRA EVALUATION REPORT

Grain Number	#Si	#Ni	#Ni+o	#Ni+o+h	#Na	#Ca	#Mg	#al	#fe	#fe+o	#fe+o+h	#cu	#cu+o+h	#cr	#c5+h9+o+	#s
02425p.tdc	3225	143	3	20	213	1178	4621	740	1837	38	15	20	3	65	0	573
02426p.tdc	3822	94	8	24	951	720	4903	759	1734	33	24	22	5	58	1	520
02427p.tdc	2668	315	4	7	110	411	3671	508	1049	18	5	15	4	35	0	55
02428p.tdc	14703	325	44	41	1127	2650	17779	3485	6084	118	78	76	12	218	0	80
02429p.tdc	2722	46	0	1	69	399	3006	443	997	9	0	6	1	40	0	2
02430p.tdc	4037	569	5	25	611	484	6022	731	1066	28	4	18	5	31	0	190
02431p.tdc	527	11	0	1	31	72	798	92	174	1	5	3	1	5	0	15
02432p.tdc	1597	211	0	0	37	70	2025	147	244	6	0	5	0	11	0	0
02433p.tdc	1482	55	1	0	52	59	1474	133	186	2	0	1	0	13	0	0
02434p.tdc	2698	74	4	10	145	1625	3728	367	1521	18	25	10	3	42	1	172
02435p.tdc	1598	35	0	0	69	184	1575	232	320	3	0	4	0	16	0	0
02436p.tdc	155	3	1	1	10	28	225	24	57	1	0	0	0	0	0	1
02437p.tdc	5111	187	14	43	408	1136	7429	1114	2439	49	49	29	10	86	0	225
02438p.tdc	36694	2774	65	113	1165	1406	49502	5516	11975	277	204	69	12	346	0	322
02439p.tdc	16867	236	18	21	1002	1327	22756	1822	3992	114	36	37	6	112	0	67
02440p.tdc	4058	263	4	4	206	145	5577	307	754	26	7	2	2	19	0	0
02441p.tdc	6387	52	4	3	477	790	8137	1627	1740	48	10	6	2	80	0	0
02442p.tdc	3518	231	1	4	330	188	4854	1004	2016	30	20	11	2	43	0	0
02443p.tdc	7865	219	5	8	234	116	9910	403	1121	32	12	2	0	19	1	1063
02444p.tdc	418	11	0	3	119	334	741	130	67	2	0	3	0	12	0	0
02445p.tdc	3548	19	0	1	90	118	4785	254	478	8	0	2	0	13	0	877
02446p.tdc	5300	37	0	2	453	478	7544	921	838	22	7	8	1	48	0	693
02447p.tdc	1589	24	2	0	186	240	2545	389	174	3	0	1	0	21	0	56
02448p.tdc	1811	168	2	2	192	360	2445	298	635	4	1	13	0	25	1	60
02449p.tdc	10023	1143	22	40	460	644	15042	2319	3929	71	65	33	3	110	1	384
02450p.tdc	15668	161	9	22	1091	1127	22583	1923	3458	97	33	27	5	80	0	144
02451p.tdc	21737	1146	33	62	1093	1073	31219	3082	7134	144	92	47	17	247	0	145
02452p.tdc	1988	85	5	6	192	363	3154	467	617	15	10	10	1	32	0	114
02453p.tdc	4062	1048	21	36	1825	778	6209	1113	3503	52	48	29	13	81	0	1
02454p.tdc	5458	183	9	12	296	574	7776	756	1480	32	8	13	4	47	0	8
02455p.tdc	814	12	5	4	45	117	1096	100	219	6	15	7	1	12	0	80
02456p.tdc	299	4	0	1	22	22	361	42	68	3	1	2	1	3	0	67
02457p.tdc	464	13	3	1	32	51	606	83	152	8	4	1	1	7	0	1
02458p.tdc	4552	138	9	8	281	205	6686	486	1454	27	18	11	6	26	0	129
02459p.tdc	2183	34	2	11	970	1099	2451	1670	365	7	4	7	1	14	0	417
02460p.tdc	6723	280	13	37	402	1135	11225	1348	2474	45	52	35	11	114	2	127
02461p.tdc	8563	266	11	20	1668	1254	13537	2027	2920	84	39	22	10	109	1	222
02462p.tdc	7386	764	3	14	223	311	10311	1190	2219	42	8	13	3	78	0	166
02463p.tdc	18177	1018	26	30	802	918	25317	2197	5071	131	71	34	6	201	0	214
02464p.tdc	11873	3079	50	105	8796	2616	18575	2967	8597	131	105	75	14	223	0	222
02465p.tdc	15580	441	25	39	1474	2293	22994	2896	4320	106	46	45	7	154	2	86
02466p.tdc	5728	103	7	11	268	890	8060	700	1282	53	16	10	4	65	0	89
02467p.tdc	142	1780	13	21	124	188	188	60	3875	26	35	61	3	12	3	1080
02468p.tdc	560	5905	30	132	356	2194	606	166	9085	101	82	115	8	27	87	9491
02469p.tdc	156	837	4	5	38	828	251	53	2350	10	4	20	3	6	57	3226
02470p.tdc	234	541	38	15	138	66	32	510	845	3	4	16	1	5	2	73
02471p.tdc	4	94	1	0	2	181	0	9	107	2	0	0	0	7	0	0
02472p.tdc	276	2595	18	45	225	442	94	40	3927	43	21	43	3	10	22	1376
02473p.tdc	1390	3671	29	32	60	1042	1122	267	9828	89	39	90	4	26	79	6864
02474p.tdc	810	6865	45	41	494	1636	533	149	9732	82	44	119	6	17	145	9091
02475p.tdc	822	4571	17	43	216	257	996	151	3061	38	7	26	0	10	71	2895
02476p.tdc	0	0	0	0	0	0	0	0	0	0	0	0	0	0	2	262
02477p.tdc	568	3441	18	24	55	3086	986	95	5983	58	5	59	3	22	49	3362
02478p.tdc	588	4899	13	35	71	1042	655	118	5620	50	13	145	0	18	44	4105
02479p.tdc	652	4781	21	18	81	309	579	165	7062	60	5	111	2	10	58	4101
02480p.tdc	1560	14463	116	163	294	1118	1332	533	27776	258	403	317	16	112	4	3195
02481p.tdc	1108	5210	37	71	329	2974	957	214	10031	90	96	156	10	35	1	1005
02482p.tdc	212	2632	25	44	87	681	208	60	4413	48	91	60	2	28	1	656
02483p.tdc	261	3702	24	35	135	878	304	90	5311	72	79	85	6	21	6	1062
02484p.tdc	72	1417	6	5	96	50	60	16	1258	12	0	24	2	5	15	3290
02485p.tdc	458	2641	26	32	78	675	310	77	5310	56	143	57	5	20	11	1102
02486p.tdc	198	2310	26	18	44	566	177	55	4272	34	29	60	1	8	8	1097
02487p.tdc	67	48	2	2	105	103	11	228	121	17	32	3	3	26	0	18
02488p.tdc	1268	7174	41	71	267	552	1052	272	13237	117	160	141	5	27	24	2423
02489p.tdc	1470	10737	73	104	544	4837	1435	549	16764	160	77	171	8	43	27	2312
02490p.tdc	101	309	1	0	10	59	62	11	478	4	3	6	0	2	9	307
02491p.tdc	310	2027	9	10	115	648	354	63	2359	17	6	35	0	12	42	1755
02492p.tdc	409	2779	32	50	50	146	110	108	3880	83	85	59	5	28	120	6425
02493p.tdc	272	943	1	0	9	55	70	28	1389	6	0	32	0	5	130	6061
02494p.tdc	0	0	0	0	0	0	0	0	0	0	0	0	0	0	74	3169
02495p.tdc	0	0	0	0	0	0	0	0	0	0	0	0	0	0	54	1205